OUT-PHASE PATCH POWER DIVIDER AND FILTERING DIRECTIONAL COUPLER

NGOI KAH FEI

A project report submitted in partial fulfillment of the
requirements for the award of the degree of
Bachelor (Hons) of Electrical and Electronic Engineering

Faculty of Engineering and Science
Universiti Tunku Abdul Rahman

APRIL 2012

DECLARATION

I hereby declare that this project report is based on my original work except for citations and quotations which have been duly acknowledged. I also declare that it has not been previously and concurrently submitted for any other degree or award at UTAR or other institutions.

Signature : _____

Name : Ngoi Kah Fei

ID No. : 09UEB00659

Date : 18th April 2012

APPROVAL FOR SUBMISSION

I certify that this project report entitled **"Out-Phase Patch Power Divider and Filtering Directional Coupler"** was prepared by **Ngoi Kah Fei** has met the required standard for submission in partial fulfillment of the requirements for the award of Bachelor of Electrical and Electronic Engineering (Hons.) at Universiti Tunku Abdul Rahman.

Approved by,

Signature : _____

Supervisor : Dr. Lim Eng Hock

Date : 18th April 2012

Specially dedicated to
my beloved parents and friends.

ACKNOWLEDGEMENTS

I would like to thank everyone who had contributed to the successful completion of this project. I would like to thank my supervisor, Dr Lim Eng Hock, for his valuable ideas and guidance throughout the development of the research.

In addition, I would also like to express my gratitude to my loving family for giving me encouragement and support in research. Besides that, I would like to thank senior and friends who have been doing their research under my project supervisor, Dr. Lim Eng Hock. They have shared their ideas and knowledge with me and provided me with help whenever I faced a problem.

.

OUT-PHASE PATCH POWER DIVIDER AND FILTERING DIRECTIONAL COUPLER

ABSTRACT

In the recent years, microstrip line technology is used widely in microwave circuits because it is cheap and easy to fabricate. Power divider is used extensively in microwave applications, where it is used to divide and combine microwave power. However the directional coupler is used to couple power flowing in one direction. Power dividers and direction coupler have been used widely in microwave circuits such as the feeding network for an antenna array, power amplifiers, and phase shifters. A new design of power divider and direction couple that is fabricated with the substrate thickness of 1.57 mm and relative permittivity of 2.33 is introduced. There are four main stages to this project, known as the simulation, modeling, fabrication and experiment stage. In the simulation stage, High Frequency Structure Simulator (HFSS) has been used to simulate and optimized the frequency responses of the power divider and direction coupler design. Modeling is the process of generating abstract by using Microwave Office. After get the best frequency responses, the proposed power divider and direction coupler design will be fabricated. In the experiment stages, Vector Network Analyzer (VNA) is used to measured the result and compare with the simulated results. After that, parametric analyze are necessary for the discussions on the case studies and for future application.

TABLE OF CONTENTS

LIST OF TABLES

LIST OF FIGURES

LIST OF SYMBOLS / ABBREVIATIONS

λ	wavelength, m
f	frequency, Hz
c	speed of light, m/s
ε_r	dielectric constant
ε_{eff}	effective dielectric constant
h	thickness of substrate, mm
w	width of striplines, mm
Z_o	characteristic impedance, Ω
Z_{in}	input impedance, Ω
S_{11}	reflection loss, dB
S_{21}	insertion loss, dB

CHAPTER 1

INTRODUCTION

1.1 Background

Microwaves are radio wave with wavelength ranged from 300 MHz to 30 GHz with a corresponding wavelength from 100cm to 1cm.In the recent years, microstrip are getting more popular and used to convey microwave-frequency signals. Microstrip is easy to fabricate, high performance, multi-frequency and much less expensive than traditional waveguide technology.

The most common and widely power divider know as Wilkinson power divider and published by Ernest J. Wilkinson. Wilkinson power divider can be made using Microstrip or stripline as illustrated in Figure 1.1. The Wilkinson power divider can be made to give arbitrary power division.

The Wilkinson power divider can splits the signal into equal-amplitude, equal-phase output signals at ports 2 and 3. The two identical signals at ports 2 and port 3 can combine by Wilkinson power divider in the port 1.

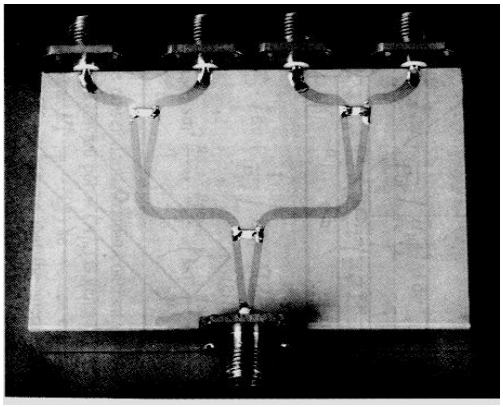

Figure1.1: Wilkinson Power Divider

The most common directional couplers constructed from two unshielded transmission lines set close enough together such that power can be coupled between the lines due to the interaction of the electromagnetic fields of each line. Coupler transmission line only operates in TEM mode and valid in microstrip .The port1 power will appears at the output port except for the portion intended to be sampled. (M.Pozar, 1998)

1.2 Aims and Objectives

The goal with this project is to design and construct a new microstrip power divider and direction coupler. Understanding the knowledge of microwave is very important to design the microstrip power divider and a directional coupler. Besides that, authors had study few related journals and articles in IEEE Xplore database under the UTAR OPAC system. This journals and articles are very important in the designing of power divider and direction-coupler.

The first design is Out-Phase Patch Power Divider. The power divider resonates at frequency of 2.22 GHz to 2.55 GHz and divides the signal into equal-amplitude, 180 °-phase output signals at ports 2 and 3. The second design is Filtering Directional Coupler. The filtering directional coupler can filters the signal at frequency of 2.07 GHz to 2.39 GHz with the coupling effect.

1.3 Project Motivation

The motivation of the project is to design high performances Out-Phase Patch Power Divider and Filtering Directional Coupler. Return loss, insertion loss and voltage stand wave ratio was the parameters affect the performance of the power divider and directional coupler. Return loss is a convenient way to measure the matching between input and output. Usually the insertion loss is contributed by mismatch loss at the input port, attenuation loss through the device and mismatch loss at the output. However, VSWR is a measure of the impedance mismatch.

To achieve best performance, the power divider and directional coupler should have the low return loss and insertion loss. A lot of power divider and coupler are very complicated and this encourages authors to design the power divider at the simplest design and with good performance.

1.4 Thesis Overview

The thesis is organized into 5 chapters. Chapter 1 describes the project background, issues, research aim and objectives. Chapter 2 discusses the literature review and theoretical background for project. It includes the background and the theory of the power divider and directional coupler. Besides that, description of simulation tools and research mythology are presented in this chapter.

Chapter 3 summarizes the author's first design of the Out-Phase Patch Power Divider. The filtering directional coupler will present in Chapter 4. The configuration, transmission model, result and parametric analysis of the design will review in Chapter 3 and Chapter 4.In the last chapter, authors concludes the thesis with future works and recommends

CHAPTER 2

LITERATURE REVIEW

2.1 Background

The term microwave refers to alternating current signal with frequencies 300 MHz to 300 GHz (M.Pozar, 1998).In the microwave engineering, transmission-line theory was used instead of low frequency circuit analysis techniques. In transmission-line theory, voltage and current along a transmission line can vary in magnitude and phase as a function of position (Neuman, 2000).

Microstrip was developed by ITT Ferearl Telecommunications Laboratories in Nutley New Jersey, as a competitor to stripline. Before 1960s, the microstrip used fat substrates, which allowed non-TEM waves to propagate which makes results unpredictable. With the rapid growth of commercial microwave technology, the thin version of microstrip became popular (microwaves101, 2012) and many design has been published in the IEEE Xplore.

The general structure of a microstrip is shown in Figure 2.1. The microstrip consists of consists of a signal line on the surface of a board of dielectric constant ε_r , a thickness h and referenced to a power or ground plane. The value of ε_r, the dielectric constant of the board material, will be a significant component of the value of the characteristic impedance of the line. (Hong, 2001)

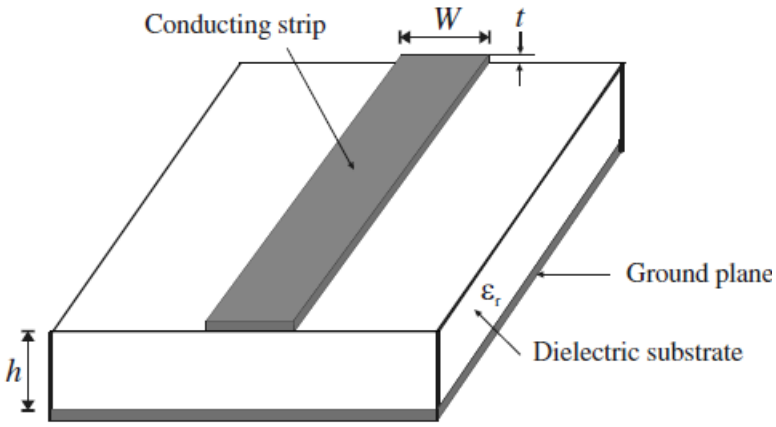

Figure 2.1: Microstrip line cross section.

2.2 Power Divider

Power dividers are passive microwave components used for divides an RF signal into two or more signals while maintaining good impedance match at all ports. In our design, we consider the general design of power division. The simplest power divider is three ports network which is composed of single input and two outputs .In additional, the other types of power divider can be carried out in similar way. To simplify complexity, discussion in the others sub chapter is focused on three ports and four-port power dividers.

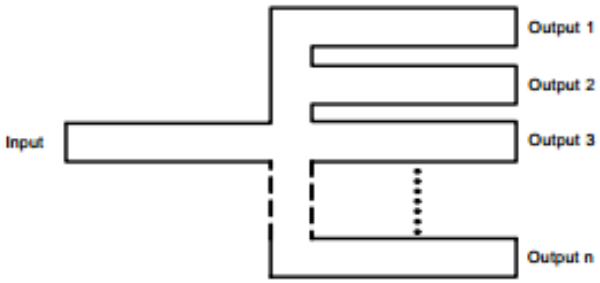

Figure 2.2 : Power divider

2.2.1 Side-Coupled Bandpass Filter

Parallel-coupled microstrip bandpass filters also know as edge-coupled bandpass filters using the half-wavelength line resonators and show in Figure 2.3.This bandpass filters are designed so that adjacent resonators are parallel to each other along half of their length. Hence, the spacing between resonators wills gives relatively large coupling and prove a wider bandwidth bandpass filter. The bandpass filter design are given by

$$\frac{J_{01}}{Y_0} = \sqrt{\frac{\pi}{2}\frac{FBW}{g_0 g_1}} \quad (2.1a)$$

$$\frac{J_{j,j+1}}{Y_0} = \frac{\pi FBW}{2}\frac{1}{\sqrt{g_j g_{j+1}}} \qquad j = 1 \ to \ n-1 \ (2.1b)$$

$$\frac{J_{n,n+1}}{Y_0} = \sqrt{\frac{\pi}{2}\frac{FBW}{g_n g_{n+1}}} \ (2.1c)$$

where $g_0, g_1 \ldots g_n$ are the element of a ladder-type lowpass prototype with a normalized cutoff $\Omega c = 1$,J j,j+1are the characteristic admittances of J-inverters and Y_0 is the characteristic admittance of the terminating lines (Hong, 2001).

From equation 2.1, it shows that parallel-coupled microstrip bandpass filter have the same network representation with lowpass filter. However, both of the filer have the implementation. Besides that, coupled microstrip line resonators even-mode and odd-mode characteristic impedances can determined by

$$(Z_{0e})_{j,j+1=}\frac{1}{Y_0}\left[1+\frac{J_{j,j+1}}{Y_0}+\left(\frac{J_{j,j+1}}{Y_0}\right)^2\right] \qquad j = 0 \ to \ n(2.2a)$$

$$(Z_{0e})_{j,j+1=}\frac{1}{Y_0}\left[1-\frac{J_{j,j+1}}{Y_0}+\left(\frac{J_{j,j+1}}{Y_0}\right)^2\right] \qquad j = 0 \ to \ n(2.2a)$$

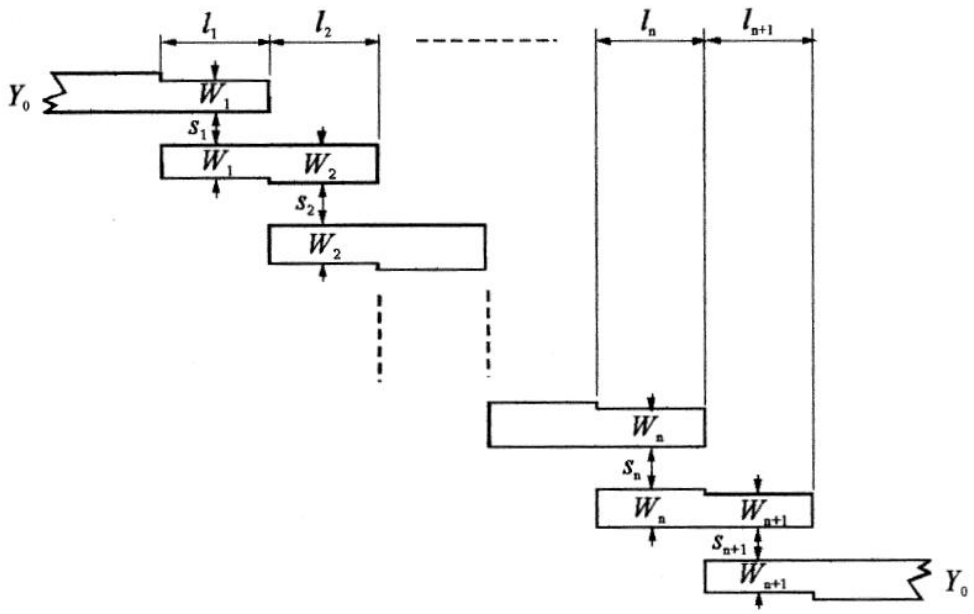

Figure 2.3 : General structure of parallel (edge)-coupled microstrip bandpass filter.

2.2.2 2-way and 3-way Power Dividers

T-junction power divider is a simple three-port network in the absence of transmission line loss, lossless junction (Pozar, 1998).It can spilt the power evenly into the arms of the T with each arm having half the original power shown in Figure 2.4.The T-junction power divider suffer from very poor isolation between the output ports which a large part of the power reflected back from port 2 finds its way into port 3.

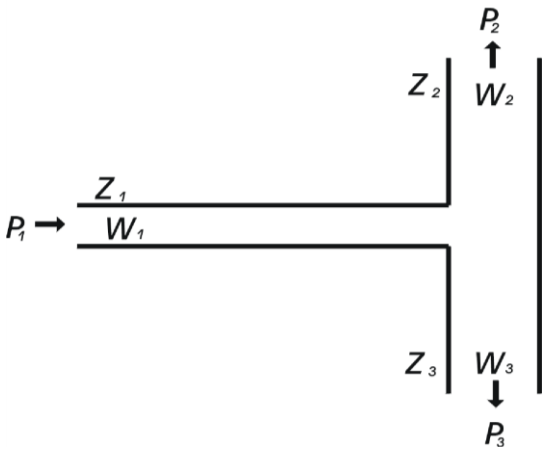

Figure 2.4 : T-junction Power Divider

In the T-junction power divider, the input power P_1 is delivered to the intersection on a microstrip of width W_1 and impedanceZ_1. The line then branches into two arms with power, width and impedance given by $Z_2P_2W_2$ and $P_3W_3Z_3$respectively. The design equations for this divider are

$$Z_2 = \frac{Z_2 \times Z_3}{Z_2 + Z_3}, P_2 = \left(\frac{Z_1}{Z_2}\right) P_1, P_3 = \left(\frac{Z_1}{Z_3}\right) P_1$$

In order to get equal split T-junction power divider, the equations above must $Z_2 = Z_3 = 2Z_1$.

Wilkinson known is the most commonly used device to achieve N-way power division. The simplest Wilkinson 2-way power divider consists of two parallel uncoupled λ/4 transmission lines shown in figure 2.5. The input is fed to both

lines in parallel and the outputs are terminated with twice the system impedance bridged between them (Dib, 2010).

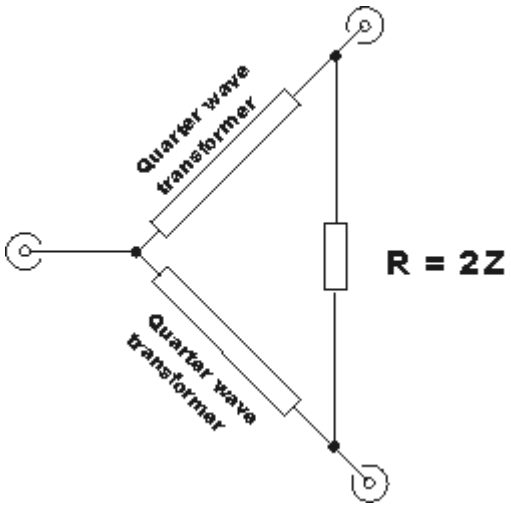

Figure 2.5 : Two-way Wilkinson power splitter

In order to get better matching between the two output ports, the values within the two-way Wilkinson divider must be twice of the system impedance:

$R = 2 \times Z_0$

$Z_{match} = \sqrt{2} \times Z_0$

$= 1.414 \times Z_0$

Where:

R = the value of the terminating resistor connected between the two ports

Z_o = the characteristic impedance of the overall system

Z_{match} = the impedance of the quarter wave transformers in the legs of the power divider combiner.

2.2.3 Theory

There are nine independent variables of scattering matrix describe the behavior of the simplest power three ports divider circuit written as:

$$[S] = \begin{bmatrix} S_{11} & S_{12} & S_{13} \\ S_{21} & S_{22} & S_{23} \\ S_{31} & S_{32} & S_{33} \end{bmatrix}$$

In order to get maximum impedance matched and minimum reflection occurred at each port, the three port network must reciprocal and its scattering matrix will be symmetric. For a network to be well-matched, it should have reflection coefficients Sij = 0 for i = j and the matrix rewritten as:

$$[S] = \begin{bmatrix} 0 & S_{12} & S_{13} \\ S_{12} & 0 & S_{23} \\ S_{13} & S_{23} & 0 \end{bmatrix}$$

Reciprocal property was very important to ensure two ports suffer similar power losses despite having different propagation directions. Reciprocal networks have symmetrical scattering matrix across the diagonal from up left to the bottom right and written as:

$$[S] = \begin{bmatrix} S_{11} & S_{12} & S_{13} \\ S_{12} & S_{22} & S_{23} \\ S_{13} & S_{23} & S_{33} \end{bmatrix}$$

However, it is impossible to construct a three port lossless reciprocal network that is matched at all ports.

An ideal passive network is said to be lossless, where the network energy is converted to heat when the wave is propagate. However, active network is different.

In a lossless network, incident energy at one port equals the sum of total energy leaving other ports. Reflected energy occurred at the incident port, and no energy is converted into other form. From the scattering matrix, when a matched network is completely lossless, the following conditions must be satisfied: For an ideal case, the sum of square of each component in a row equals unity. In reality, that sum never achieve 1 but is usually less than 1. This indicates that the energy is somehow converted into other forms. In general, it is quite difficult or almost impossible to achieve an ideal lossless network. Moreover, ideal conditions would make $S_{ij} \neq S_{ji}$, which means the network is nonreciprocal. It can be concluded that a matched reciprocal lossless network is unachievable with a simple power divider (M.Pozar, 1998).

$$S_{12}^{*} S_{13} = 0$$

$$S_{21}^{*} S_{23} = 0$$

$$S_{31}^{*} S_{32} = 0$$

$$|S_{12}|^2 + |S_{13}|^2 = 1$$

$$|S_{21}|^2 + |S_{23}|^2 = 1$$

$$|S_{31}|^2 + |S_{32}|^2 = 1$$

2.2.4 Recent Developments

2.2.4.1 Dividing and filtering function integration for the development of a band-pass filtering power amplifier

Dual-band bandpass filtering power amplifier (0.9GHz and 1.94GHz) has published in IEEE by Stephane Avrillon, Arine Chousseaud and Serge Toutain. The filter composed of two looped Steeped Impedance Resonator and power is split equally by the coupling effects. The design has greater power divider characteristics which is matched impedance input, three power-balanced mismatched outputs and dual-pass-hand filtering transfer responses to switch on different telecommunication standards.

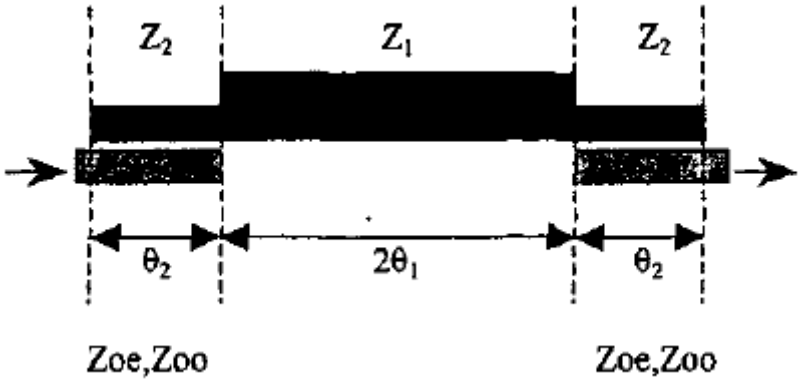

Figure 2.6: One S.I.R Filter

A general S.I.R non-conventional filter was shown in Figure 2.6. The filtering power divider modified from the S.I.R non-conventional filter. The size of S.I.R. non-conventional filter was reduced and simplified with three degrees of freedom on frequencies ($K=Z_2/Z_1$, θ_{10} and θ_{20} where Z, and Z, are lines impedances and θ_{10} and θ_{20} electric lengths at center frequency) and four on bandwidth (K, θ_{10} and θ_{20} and Zoe that is even mode characteristic impedance).From the equation 1 and 2, the first and second resonant frequency (f_0 and f_{S1}) are fixed. Beside, few properties of this structure are given:

I. Coupling areas must be equivalent to match the global filter,

II. The number of the resonator is coupled (length and distance), affect the bandwidth.

III. If K<I, then $f_{s1}>2f_0$ (for K=l, $f_{s1}=2f_0$ and for K<I, $f_{s1},> 2f_0$)

IV. The resonator electrical length is close to 180 ℃(K=l).

$$K = \tan\theta_{10} \,.\, \tan\theta_{20}$$

$$K.\tan\left(\frac{f_{s1}}{f_0}\theta_{10}\right) + \tan\left(\frac{f_{s1}}{f_0}\theta_{20}\right) = 0$$

From the S.I.R non-conventional filter, 4-way power divider has been designed and shown in Figure 2.7. In comparison, coupled length on port 3, which have two-side coupled lines, be shorter than port 2 and 4 ones. Shown in Figure 2.8, S21, S31, and S41 are closed to -4.8dB.

Figure 2.7: Three port S.I.R power divider.

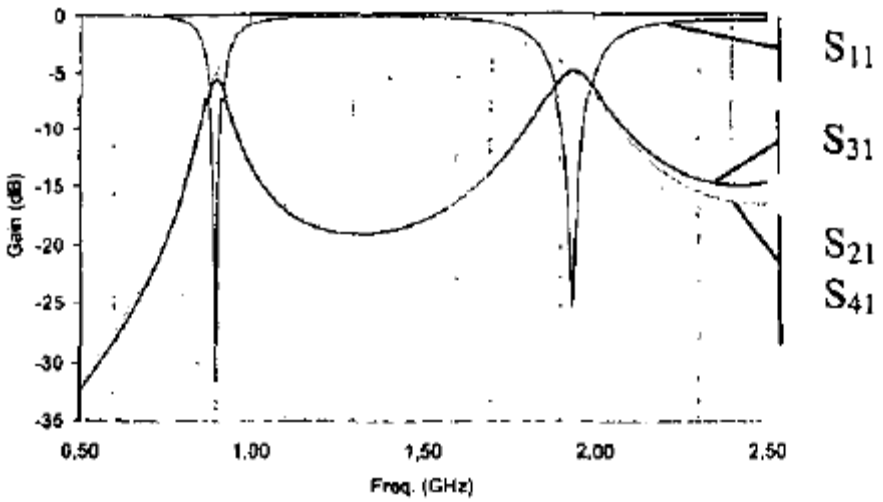

Figure 2.8: Simulated S.I.R power divider response.

Loop resonator was using to reduce the previous structure length. As comparison, the resonator have different coupling path. Besides that, the loop-filter imposes conditions on lengths that lead to a maximum coupling length Lm which is equivalent to a Lm/2 coupling length on S.I.R. filters. The loop-filter bandwidth is much smaller than S.I.R. filter since the length coupling is linked to bandwidth.

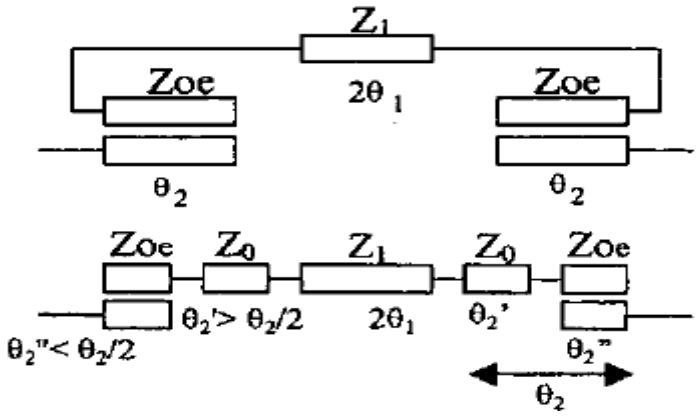

Figure 2.9: Correspondence between loop and S.I.R filters.

S.I.R filter, semi-loop filter and loop filter were considered to evaluate how geometry influences bandwidth.

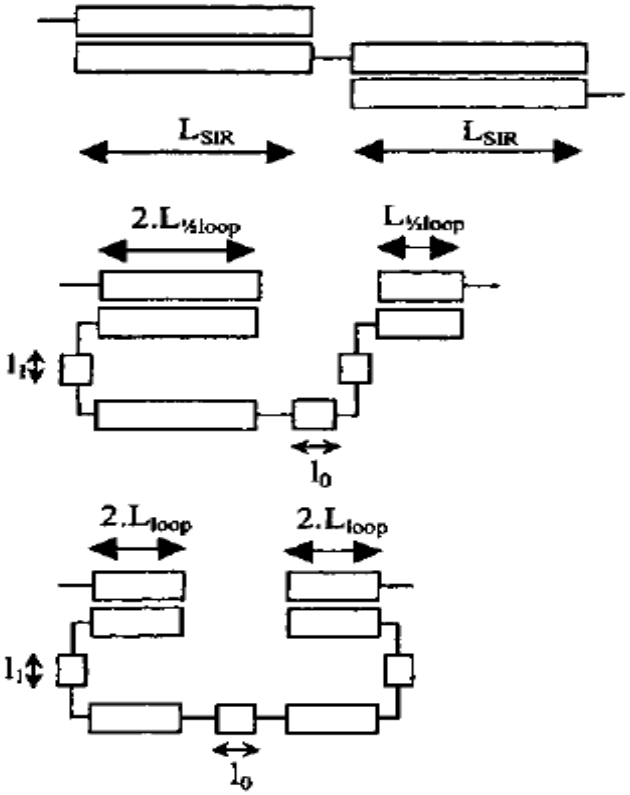

Figure 2.10 :Different filter configurations

The coupling effects can limit by I_0 and I_1. The resonator has length closed to squares to a 180 ° electric length at f_0.Besides that was assume constant along the resonator, where $\beta=2\pi/\lambda$ is the propagation constant and λ the guided wavelength. Few equations were using to build a 0.9GHz filter in FR4 substrate and with 0.2mm spacing between coupled lines.

$$L_{SIR} = \frac{L_R}{2} \qquad B_{max} = 14\%$$

$$L_{\frac{1}{2}loop} = \frac{L_R}{5} - \frac{2l_1 + l_0}{5} \qquad B_{max} = 2.5\%$$

$$L_{loop} = \frac{L_R}{8} - \frac{2l_1 + l_0}{8} \qquad B_{max} = 1\%$$

The loop filters have the reverse problem .Besides that, filter bandwidth was reduced when the geometry is compact. However, a semi-loop filter does not have this issue and it is easier to couple three ports in this structure. The general configuration 3-way semi-loop resonator power divider show in below.

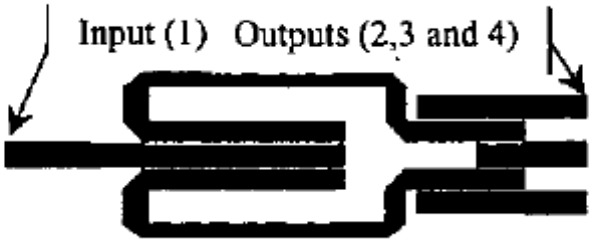

Figure 2.11: Layout of the three-port semi-loop-resonator power divider.

FR4 substrate with dielectric permittivity of 4.5 is using and the result show in Figure 2.12 and Figure 2.13. The experiment result shows two resonant frequencies (0.91GHz and 1.96GHz) with reduced bandwidths. Moreover, the result show that high return loss (-7db) at 0.9 GHz. From Figure 2.13, three outputs have the same isolation loss and identical with the theoretical cases. Few improvement has been suggest which is reduce coupling lengths and then device size, by inserting interdigited structure into resonator input and output (Stephane Avrillon, 2002).

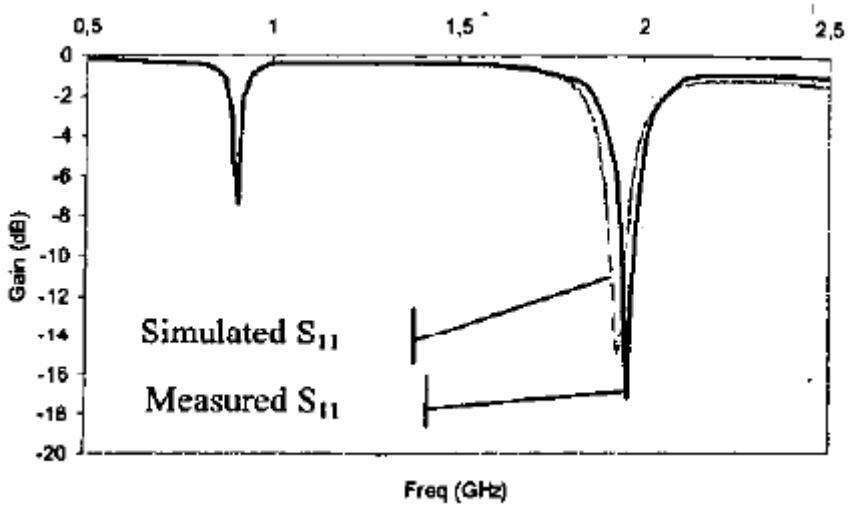

Figure 2.12: Simulated and measured return loss.

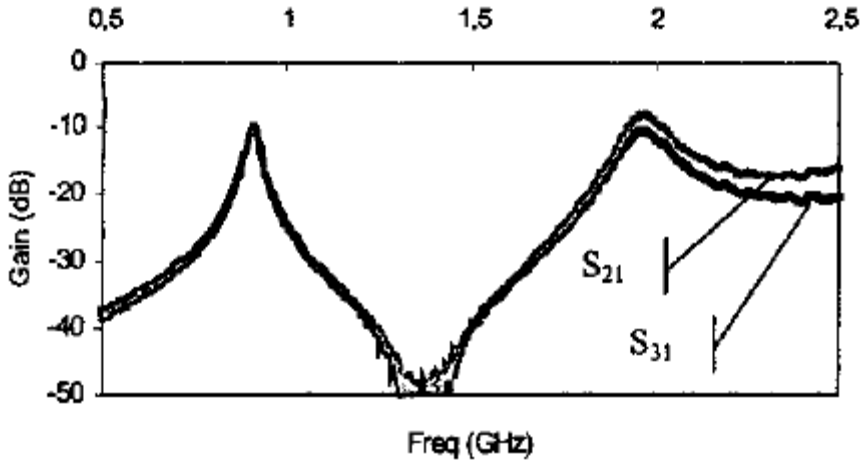

Figure 2.13: Measured isolation loss.

2.2.4.2 A Novel Microstrip Line Three-way Power Divider

A novel three-way power divider structure using branch directional coupler is proposed by Kejia Ding .The structure of the divider is simple and compact without degrade the performance of the power divider. The general structure of power divider proposed shown in Figure 2.15. It consists of two branch directional couplers with the parallel connection. Each length of the transmission line is 1/4 wavelength at central operation frequency. The output power ratios were tunable by adjusting the transmission lines impedances and isolation resistors value.

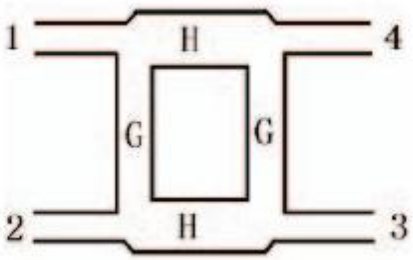

Figure 2.14: The typical two-branch directional coupler.

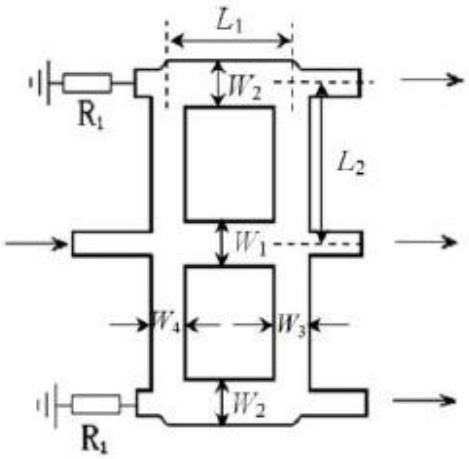

Figure 2.15 : The three-way power divider

The main analyzing results are presented in this paper. When there was no reflection on port 1, the power divider condition is:

$$\frac{G^2}{H} + \frac{1}{H} - H = 0$$

$$or\ G^2 = H^2 - 1$$

Define the couple degree of the branch directional coupler is

$$c = \left|\frac{u_3}{u_1}\right|$$

,then

$$c = \frac{G^2 + 1}{G.H}$$

Equation (3) can be expressed logarithmically.

$$c(dB) = 20lg\frac{G^2 + 1}{G.H}$$

From the analysis, the branch directional coupler can attain various couple degree.

The power divider power output ratio is 1:2:1 was proposed. Hence the power division design target is:

$$|S21| = |S41| = \frac{\sqrt[2]{2}}{2}|S31|$$

The design target of the equivalent paralleled branch directional couplers, D2 and D3, is:

$$|S3'1'| = |S2'1'|$$

In order to match the impedances of the paralleled ports, nonsymmetrical branch directional coupler structure was adopted. The three-way power divider has been optimized numerically by software Ansoft HFSS and the result shown in Figure 2.16 and Figure 2.17.

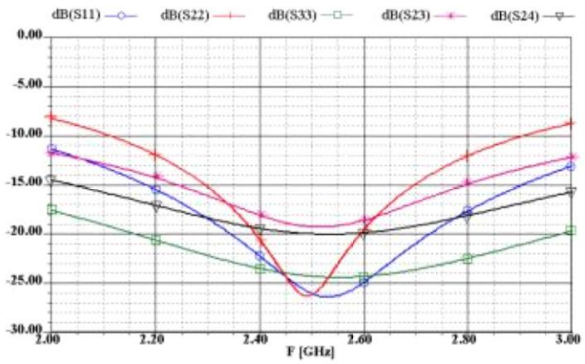

Figure 2.16 : The simulation results of impedance matching and isolation.

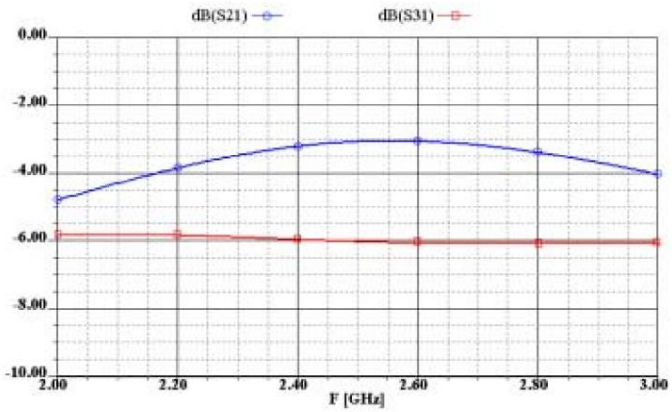

Figure 2.17: The simulation results of output ratio of the divider.

Figure 2.17 illustrated the power divider has working frequency of 2.45-2.65Ghz.The reflection loss is less than -22dB.In addition, the isolation degree between port 2 and port 3, port 2 and port 4 are both higher than 20dB (Kejia Ding, 2011).

2.3 Direction Coupler

Directional couplers are general purpose tools used in microwave systems for isolating, separating or combining signals. The high performance characteristics of directional coupler to measure incident and reflected power to determine voltage standing wave ratio (VSWR), signal sampling, signal injection, signal generator and power flow monitoring.

2.3.1 Edge-coupled Directional Coupler

Figure 2.18 illustrated the basic configuration of the directional coupler. Directional coupler composed of two unshielded transmission line over a length of ¼ λ .This transmission lines are separated by a gap. Hence, the power can be coupled between the lines due to the interaction of the electromagnetic field of each line. The term coupling defines as total power was sampled to coupled part which is 10 time ratio of incident power and forward power:

$$C = 10 \log 10(Pf/Pi)$$

In practical, coupling values found was 3, 6, 10, 20, 30, 40 & 50 dB. Usually, the directional coupler operate in TEM mode and valid for stripline or microstrip structure (MECA Electronic,INC).

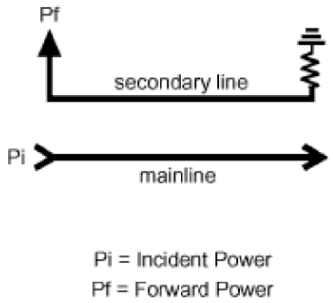

Figure 2.18 : Single Directional Coupler

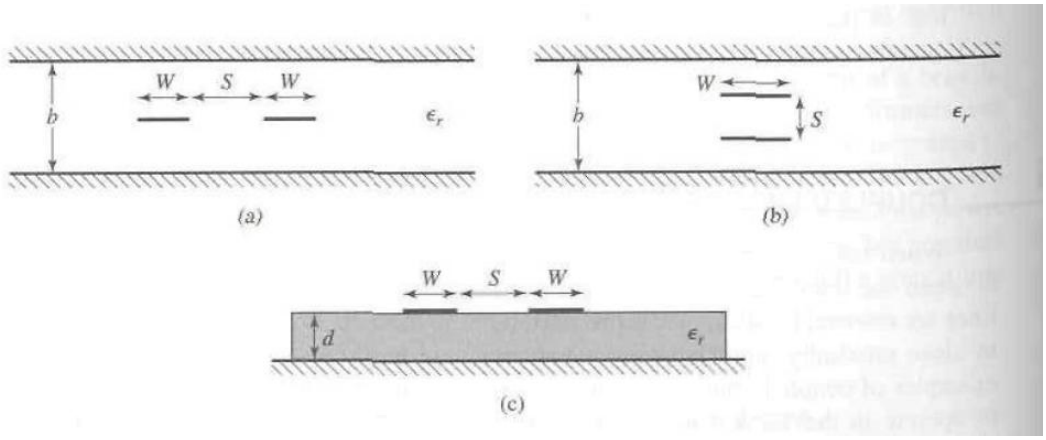

Figure 2.19 : Various coupled transmission line geometries (a) Coupled stripline (planar, or edge-coupled). (b) Coupled stripline (stacked, or broadside-coupled).(c) Coupled microstrip.

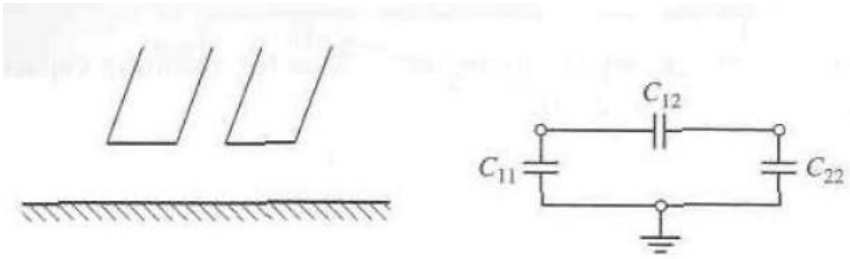

Figure 2.20 : A three-wire coupled transmission line and its equivalent capacitance network.

From the Figure 2.19, the coupled lines can be represented by the structure shown in Figure 2.20. The electrical characteristic of coupled lines can be completely determined from the effective capacitances between the line and velocity propagation on the line when TEM propagation was assumed. With the absence of the ground conductor, C_{12} represent the capacitance of the transmission lines. In addition, the C_{11} and C_{22} represent the capacitance between the transmission lines. If the two transmission lines are identical, then

$$C_{11} = C_{22}$$

Hence, the circuit can using odd or even mode to analyze. In even mode, the incident wave along the two transmission lines has the equal magnitude and phase. However, the odd mode have equal amplitude butt opposite direction transmission line.

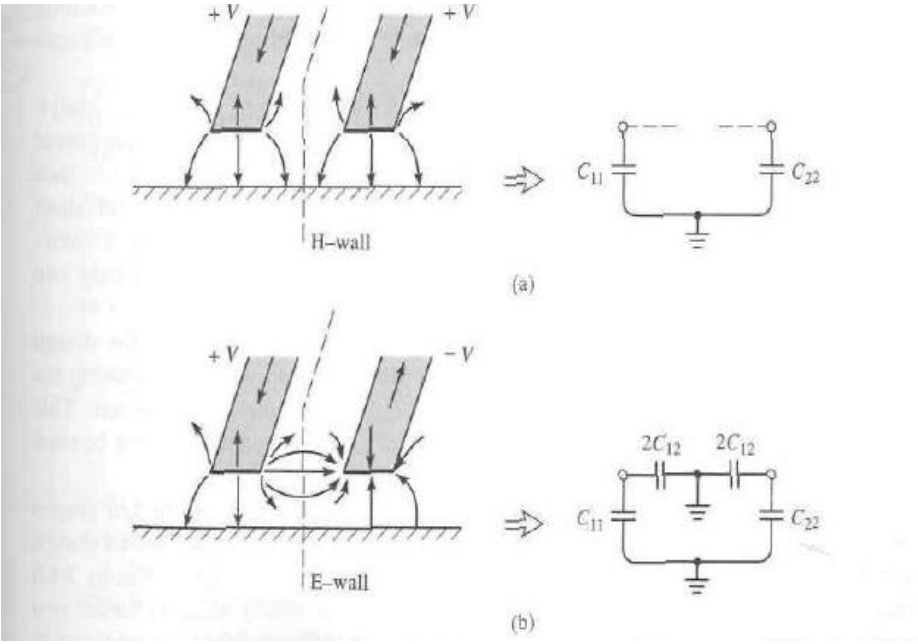

Figure 2.21 : Even and odd-mode excitations for a coupled line, and the resulting equivalent capacitance networks (a) Even-mode excitation (b) Odd-mode excitation

From Figure 2.21(a), it show that the C_{12} is open-circuited in even mode whereby the electric field has even symmetry about the center line and no current flows between the transmission lines .Thus, the capacitance of either line to ground for the even mode is

$$C_e=C_{11}=C_{12}$$

The characteristic impedance for the even mode is

$$Z_{0E} = \sqrt{\frac{L}{C_e}} = \frac{\sqrt{LC_e}}{C_e} = \frac{1}{vC_e}$$

where v is the velocity of propagation on the transmission line.

Figure 2.21(b) illustrated a ground plane through the middle of C_{12} in odd mode, which the electric lines have an symmetry about the center line, and a voltage null exists between the two transmission line .Thus, the effective capacitance and characteristic impedance are

$$C_0 = C_{11} + 2C_{12} = C_{22} + 2C_{12}$$

$$Z_{0o} = \frac{1}{vZC_0}$$

An arbitrary excitation of a coupled line can always be treated as a superposition of appropriate amplitudes of even and odd modes (M.Pozar, 1998).

2.3.2 Theory

There are nine independent variables of scattering matrix describe the behavior of the directional couplers written as:

$$[S]=\begin{bmatrix} S_{11} & S_{12} & S_{13} & S_{14} \\ S_{21} & S_{22} & S_{23} & S_{24} \\ S_{31} & S_{32} & S_{33} & S_{34} \\ S_{41} & S_{42} & S_{43} & S_{44} \end{bmatrix}$$

When the directional couplers are match with all ports, the scattering matrix of the form is:

$$[S]=\begin{bmatrix} 0 & S_{12} & S_{13} & S_{14} \\ S_{12} & 0 & S_{23} & S_{24} \\ S_{31} & S_{23} & 0 & S_{34} \\ S_{14} & S_{24} & S_{34} & 0 \end{bmatrix}$$

If the network is lossless, the symmetrical coupler will have a scattering matrix of the form:

$$[S]=\begin{bmatrix} 0 & \alpha & j\beta & 0 \\ \alpha & 0 & 0 & j\beta \\ j\beta & 0 & 0 & \alpha \\ 0 & j\beta & \alpha & 0 \end{bmatrix}$$

However, the antisymmetrical coupler will have a scattering matrix of the form:

$$[S]=\begin{bmatrix} 0 & \alpha & \beta & 0 \\ \alpha & 0 & 0 & -\beta \\ \beta & 0 & 0 & \alpha \\ 0 & -\beta & \alpha & 0 \end{bmatrix}$$

Note that the two couplers differ only in the choice of reference planes .Besides that, the amplitudes α and β are not independent. Hence, $\alpha^2 + \beta^2 = 1$ (M.Pozar, 1998).

2.3.3 Recent Developments

2.3.3.1 New broad-band 5 section microstrip-line directional coupler

New broad-band 5 section microstrip-line directional coupler has proposed by Masayuki Nakajima. 3 semi-re-entrant tight-coupling was using to design the 2 to 18 GHz 6dB microstrip-line directional coupler. There are few advantages of the 3 semi-re-entrant tight-coupling, it provide broad-band coupler without bonding wires or air bridges. Besides that, the structure is easy connecting to ordinary edge coupling section and even-mode and odd mode field and of multi section coupler are available.

Figure 2.22 and figure 2.23 show the plan schematic and cross-sectional view of a semi-re-entrant tight-coupling section respectively. The ordinary edge-coupling mechanism allows the strip conductor 2 and 3 coupled each other. Strip conductor 1 was using to enhance the coupling strength between two strip conductors, 2 and 3.

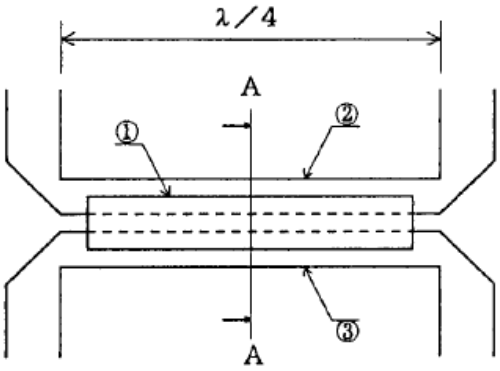

Figure 2.22 : A plan schematic view of a single section semi-re-entrant coupler.

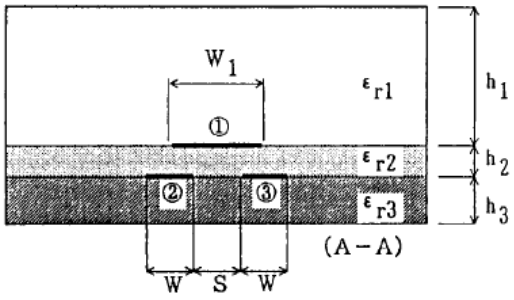

Figure 2.23 : A Cross-sectional view of a semi-re-entrant coupled section.

Quasi-TEM wave analysis was using in the capacitance matrix per unit length of the three strip conductor system and defined as:

$$\begin{bmatrix} Q_1 \\ Q_2 \\ Q_3 \end{bmatrix} = \begin{bmatrix} C_{11} & C_{12} & C_{13} \\ C_{12} & C_{22} & C_{23} \\ C_{113} & C_{23} & C_{33} \end{bmatrix} \begin{bmatrix} V_1 \\ V_2 \\ V_3 \end{bmatrix}$$

Q_1,Q_2.and Q_3 denote the line charge per unit length of each strip conductor and V_1,V_2, and V_3 the line potential of each strip conductor. From capacitance matrix $C_{odd}$and C_{even} defined as:

$$C_{odd} = C_{22} - C_{23}$$

$$C_{even} = C_{22} + C_{23} - \frac{2C_{12}^2}{C_{11}}$$

The impedance for each mode and the coupling coefficient are obtained with the above mode capacitances. Figure 2.24 illustrated the general structure of the microstrip-line directional coupler. The first three sections was semi-re-entrant symmetrical structure and two other sections was edge-coupled section.

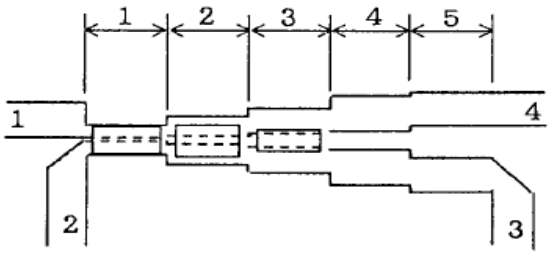

Figure 2.24 : The plan schematic view of the designed 5-section directional coupler.

The 5-section directional coupler was formed on Teflon substrate. The measurement result and experiment result shown in Figure 2.25 and Figure 2.26. As comparison, coupling coefficient |S21| obtains -6.5+0.5dB in experiment, but the simulation value was -6+0.36dB. From Figure 2.26, |S31| was affected by the phase velocity difference between the even- and odd-mode field, and by the discontinuities between sections. In additional, author proposed equalizing the phase velocity with the wiggly line technique to improve the characteristics of |S31| (Nakajima, Yamashita, & Asa, 1990)

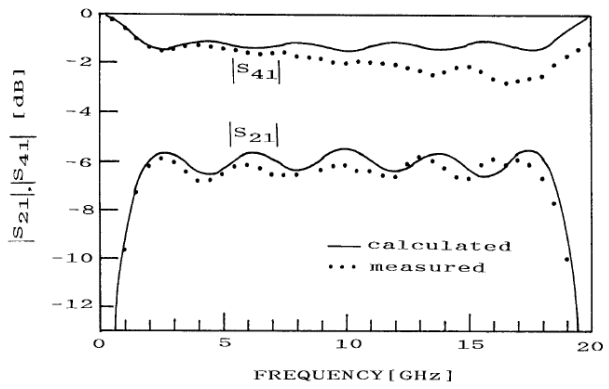

Figure 2.25 : Comparison of measure and calculated coupling characteristic, |S21| and |S41| of the designed directional coupler.

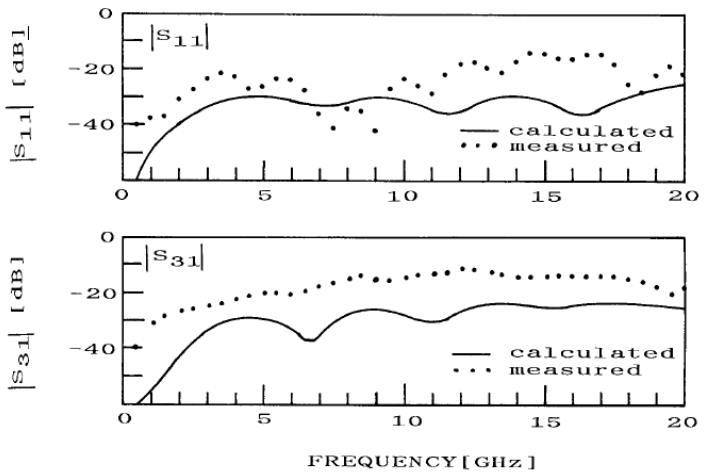

Figure 2.26 : Comparison of measured and calculated coupling characteristic,|S11| and |S31| of the designed directional coupler.

2.3.3.2 Sharp-Rejection Microwave Planar Filters Using the Branch-Line Directional Coupler

Bandpass filtering topologies using branch-line coupler as a transversal filtering section has been propose in this paper. Perceptible stopband and sharp cutoff slopes can be obtained by using the branch–line coupler as a transversal filtering section. Figure 2.27 illustrated the transversal section is made up of a conventional branch-line coupler .The proposed transversal filtering section consists on obtaining the overall frequency selective transfer function from the feed forward combination of the two signal components . The two signal are derived from the input signal, and propagating among the different paths of the branch-line coupler in the transversal configuration .Hence ,the bandpass filter profile can achieved by producing a transmission zero.

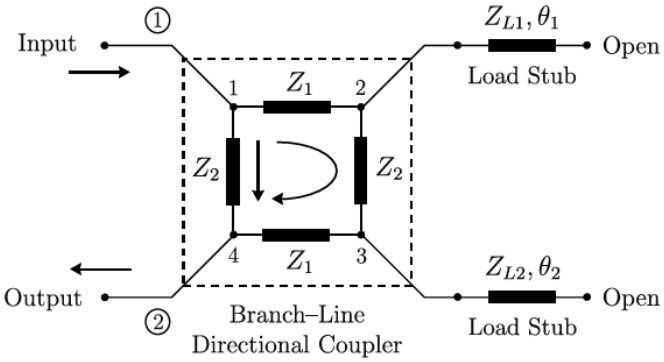

Figure 2.27 : Circuit scheme of the transversal filtering section based on the branch line directional coupler.

In order to generate appropriate amplitude and phase relationships between the signal components to be combined, the action of the load stubs is needed. Hence, high-selective filtering responses must be achieve by changing of the electrical lengths θ_1, θ_2.Besides, the branch-line coupler must exhibit a symmetrical bandpass transfer function with a power transmission maximum at the center frequency f_0.The effect of the electrical lengths θ_1, θ_2 and best transfer function regarding close to-passband selectivity and stopband rejection is achieved and shown in Figure 2.28.

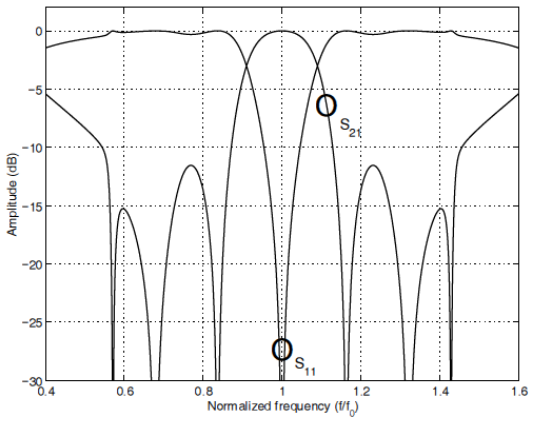

Figure 2.28 : Power reflection and transmission responses of the transversal filtering section based on the branch-line directional coupler.

Characteristic-impedance design parameters are very important to the passband behavior and the out-of-band performance of the transversal filtering section. The bandwidth of the transversal filtering section response can adjust by the characteristic impedances Z_{L1} , Z_{L2} of the load stubs. However, out-of-band

performance of the transversal filtering section is control by the characteristic impedance Z 1.

The filter is formed by cascading two equal filtering sections based on the branch-line coupler and shown in figure 2.29. The measured results show that the filter exactly centered at 3.05 GHz, has a 3-dB fractional bandwidth equal to 12.5%.At center frequency, the filter have 1.46 dB insertion loss and 21.6 dB return loss at 3.05GHz. The stopband situated in both sides of the filter passband at 1.99–2.62 GHz and 3.51–4.12 GHz respectively (Gomez-Garcia, Alonso, & Amor-Martin, 2005).

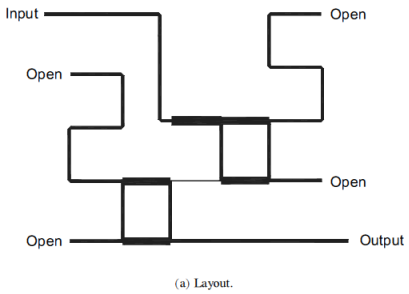

(a) Layout.

Figure 2.29 : Layout of the constructed microstrip filter prototype.

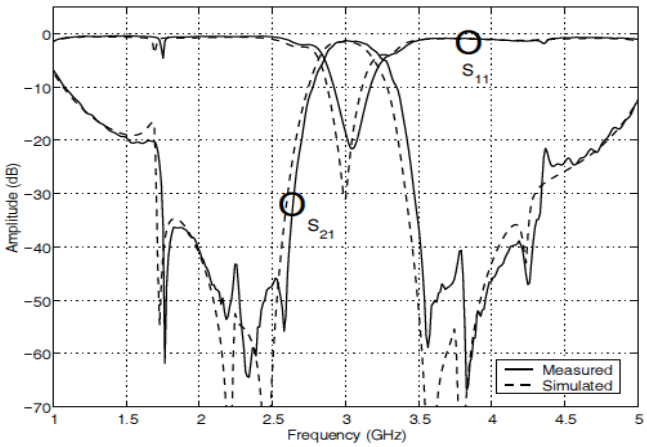

Figure 2.30 : Power reflection and transmission responses.

2.4 Introduction of Simulation Tools

There are two software tools using in this project which is Ansoft HFSS (High Frequency Structure Simulator) and Microwave office. Ansoft HFSS was using to simulated and optimized the design numerically .However, Microwave office use to reflect the real situation of the model.

2.4.1 High Frequency Structure Simulator

Ansoft HFSS (High Frequency Structure Simulator) enables the fast and accurate analysis of high frequency devices such as antennas, filters, couplers, planar and multi-layer structure and SI and EMC effects. It was the industry-standard simulation tool for 3D full-wave electromagnetic field simulation. Moreover, it was user friendly where the users only required specifying geometry, material properties and the simulation settings to generate the simulation. Besides that, proven finite elemental method was using to generate the appropriate solution and accurate mesh for solving the problem. The software can complete the complex simulation in hours. The Ansoft High Frequency Structure Simulator (HFSS) is a full-wave electromagnetic (EM) software package for calculating the electromagnetic behavior of a 3-D structure.

2.4.2 Microwave Office

Microwave Office enables the design of circuits either in schematics or its layout configuration. It can perform simulations using several simulation engines and display the output in a wide variety of graphical forms. It can also tune or optimize the designs. The changes are automatic and immediately reflected in the layout.

2.5 Research Methodology

The out-phase microstrip power divider and filtering directional coupler design procedures will be discussed in this section. There are three main stage, which is simulation stage, fabrication stage and experimental stage.

In the simulation stage, few High Frequency Structure Simulator (HFSS) tutorials have been gone through by the author .Next, a journal had been chosen by the supervisor and the author is required to repeat the journal by using High Frequency Structure Simulator (HFSS) software. After a design had been given by supervisor and the author is required to optimize until the design meet the desired results.

The design is fabricated by using RO4003C with the dielectric constant of ε_r = 2.33 and with thickness of h = 1.57mm.Next, the circuit design was printed to the transparency paper to covered the substrate and expose in the UV light. Chemical was using to remove unwanted metal and wash in running demonized water. After that, all port was soldered on the board.

Lastly, Vector Network Analyzer (VNA) is used to measure the result from the fabricated board. Calibration is needed before the measurement. After that, the result was saving into the USB flash drive and compare with the simulated results.

CHAPTER 3

OUT-PHASE MICROSTRIP POWER DIVIDER

3.1 Background

In this chapter, out-phase microstrip power divider will be discussed in details Three "C" shape patch was proposed as a resonator for this design. There are three feeding line was connected to one input and two output port .The signals from feeding line will coupling with the patch and splitting the signal equally to the feeding line and subsequently to the output ports. The out-phase power divider was designed to resonate from 1.5 GHz to 3.5 GHz with a wide band-passing bandwidth from 2.22 GHz to 2.55 GHz. The out-phase power divider is fabricated by using RO4003C with the dielectric constant of $\varepsilon_r = 2.33$ and with thickness of $h = 1.57$mm.

3.1.1 Configuration

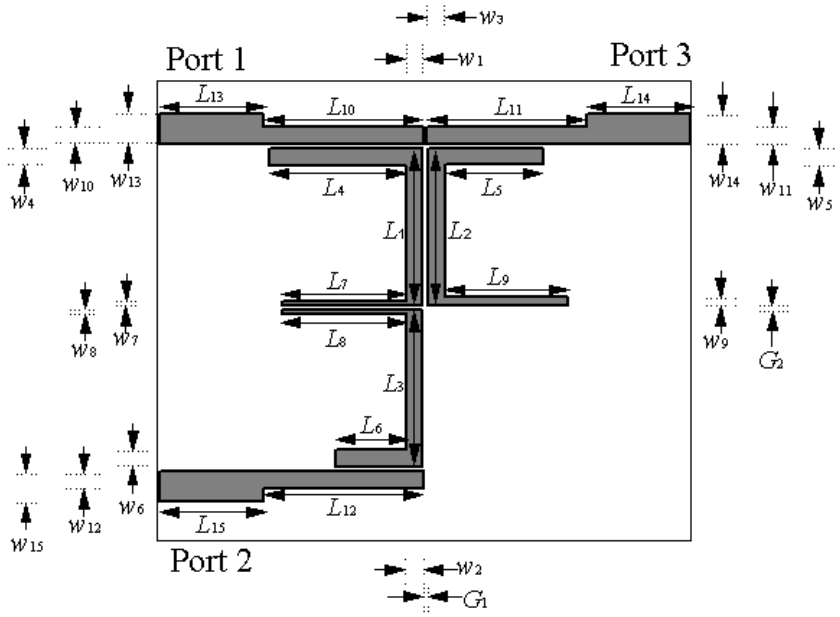

Figure 3.1:Dimension of proposed out-phase patch power divider: L1=L2=20.7mm,L3=21.0mm,L4=17.8mm,L5=14.5mm,L6=13.5mm,L7=L8=16.7mm, L9 =17.0mm, L10 =L11=L12=23.1mm, L13 =L14=L15= 16.4mm, W1= W2= 4.9mm,W3=4.6mm,W4=W5=W6=2.0mm,W7=W8=0.9mm,W9=1.5mm,W10=W11=W12=1.5mm,W13=W14=W15=4.2mm,G1=G2=0.2mm.

The general configuration of the power divider is shown in Fig3.1.When the thickness and dielectric constant of the substrate are 1.57mm and 2.33, respectively the microstrip size is 70mm x 79.2mm.The ground plane is fully consists of thin film at the bottom of substrate. The proposed power divider is not symmetric in structure but able to split an input signal to two equal amplitude signals with 180 ° phase different. The input signal from the port1 to the feeding line will couple to the patch, respectively the patch will split the signal equally and couple to port2 and port3 feeding line.

3.1.2 Transmission Line Model

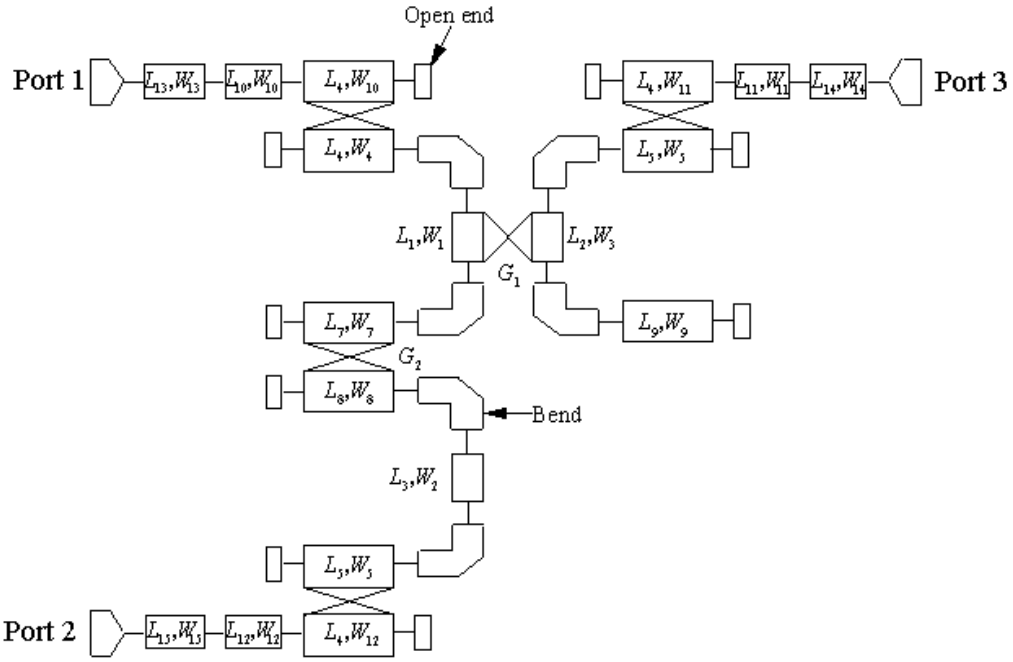

Figure 3.2: Out-phase microstrip power divider model.

Symbols are used for circuit representation of the power divider. Behind each symbol there is a model, the input parameters for the model are specified under each symbol. In this case the power divider is composed of microstrip coupled lines, microstrip open circuit with end effect, microstrip bend and port. Component microstrip coupled lines is used when two coupled lines was closed each other. Moreover, microstrip opens circuit with end effect using at the end of coupled line. Microstrip bend was using when there are bend at the coupled line .However, this model does not include the effects of dielectric losses. Once the power divider is specified we can generate the layout from the circuit representation.

3.1.3 Result

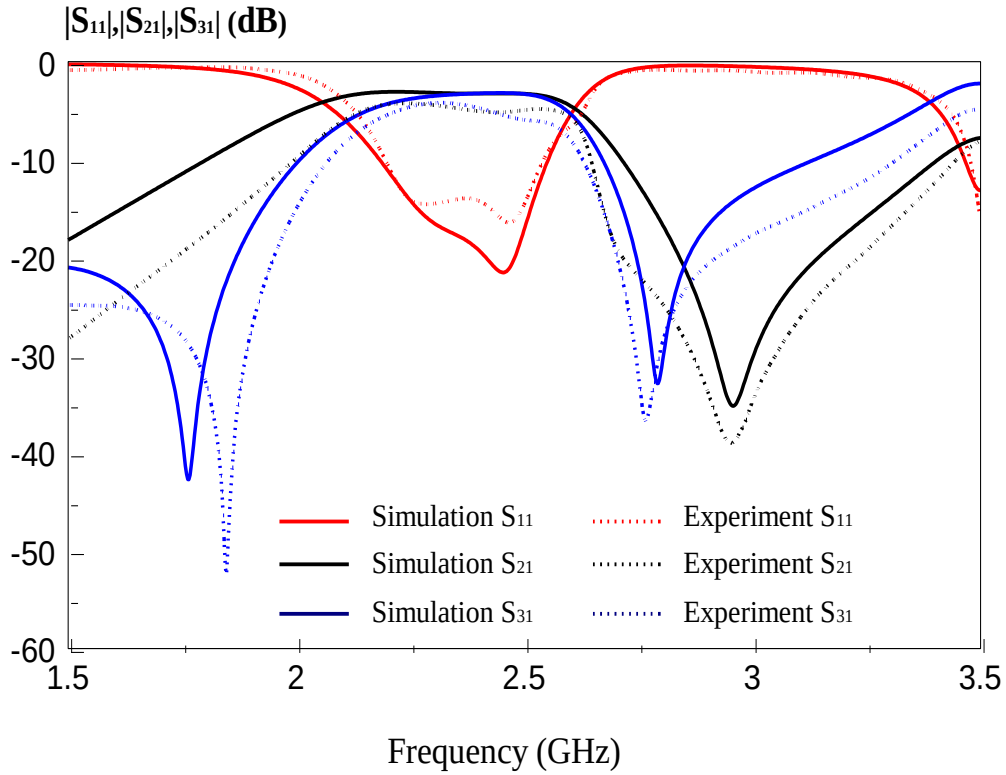

Figure 3.3 : Simulation and measurement results.

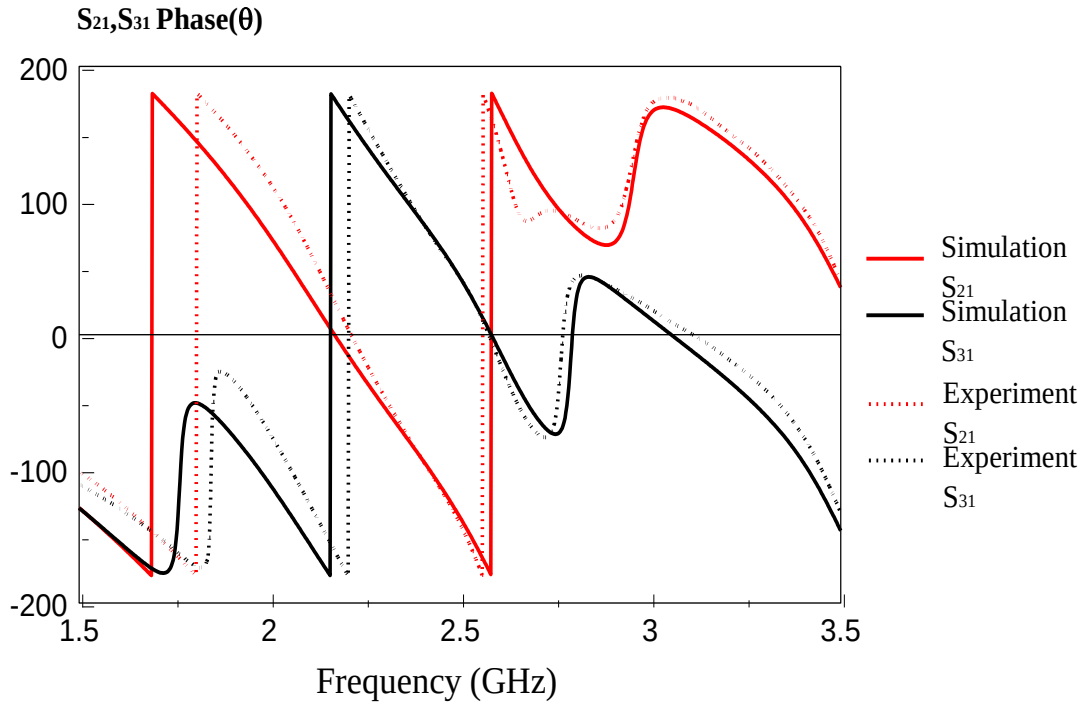

Figure 3.4 : Phase angle of simulated and measure S21 and S31 parameters.

Figure 3.3 and figure 3.4 show the results of simulation and measurement proposed power divider. Figure 3.2 and figure 3.3 illustrated that the measurement results verified the simulated results. From the simulation result, S21 has a transmission zero at 2.95GHz and S31 has two transmissions zero at 1.76 GHz and 2.79 GHz. This transmission zeros can provide better skirt rejection. Besides, the result showing proposed design was a balun which have a precise 180 ° phase shift, with equal amplitude.

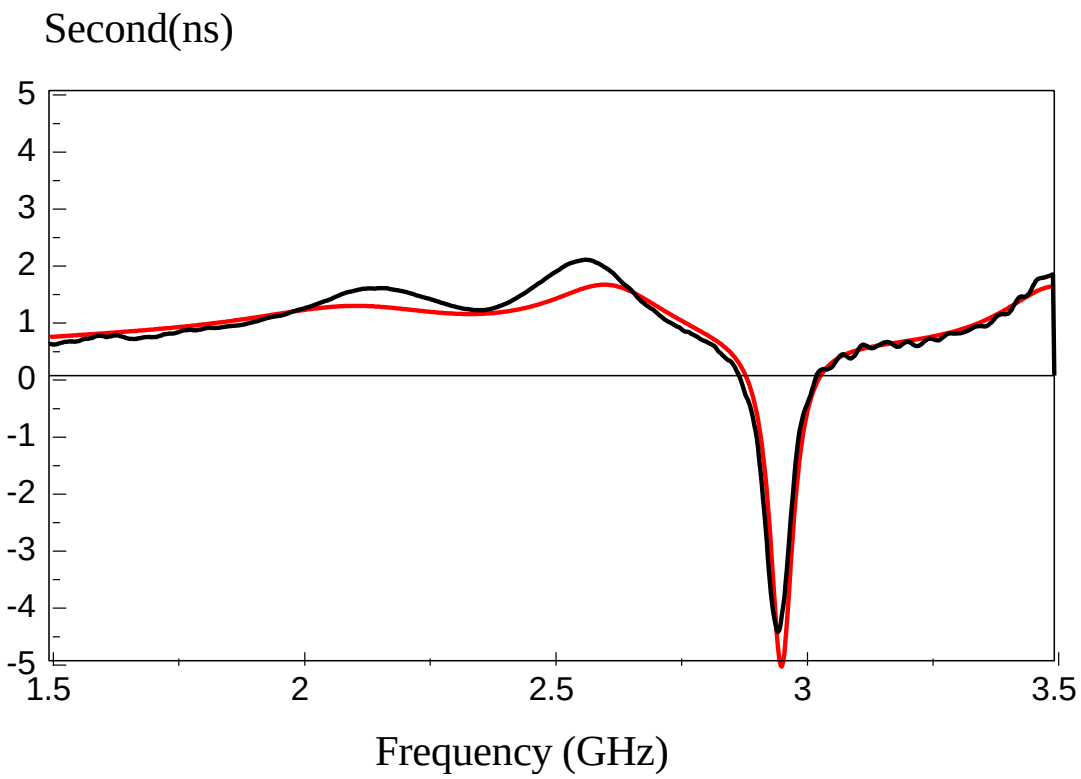

Figure 3.5 : Group delays of simulation and measure S21 parameters.

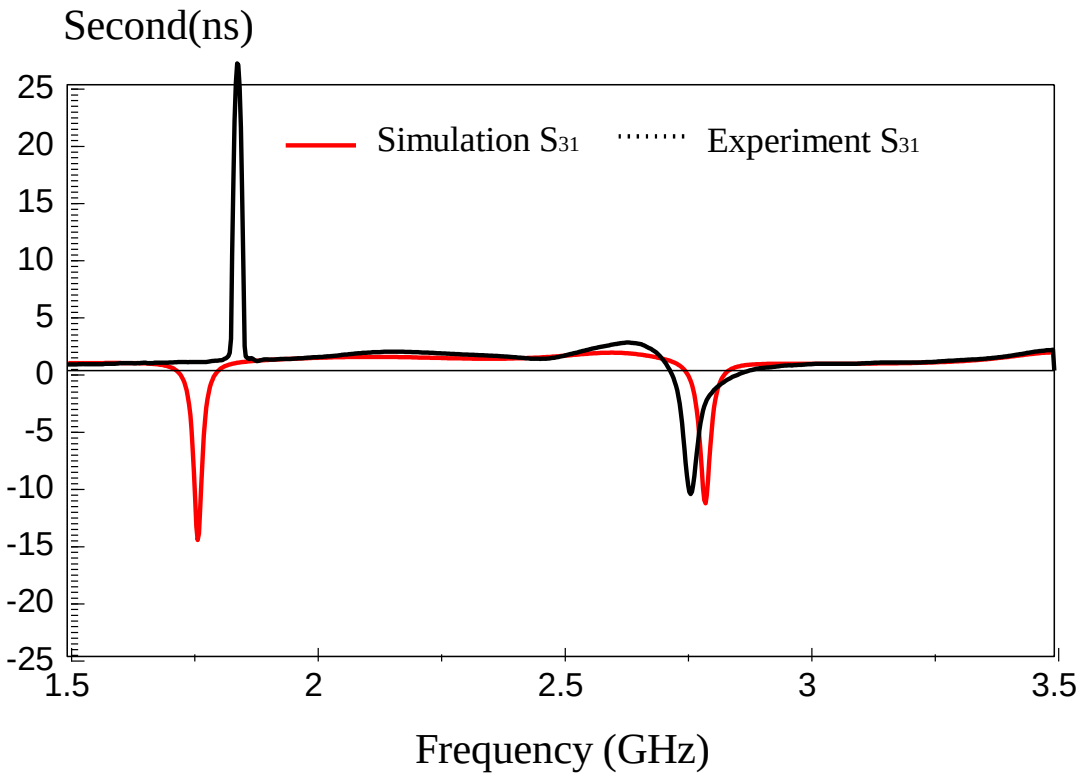

Figure 3.6 : Group delays of simulated and measured S21 parameters.

Figure 3.5 illustrates the group delays in the passband between port 1 and port2.However, Figure 3.6 shows that the group delays in the passband between port 1 and port3.The group delay in the passband remand constant, and is about 2ns .This showing the proposed power divider has a very good linearity within passband.

3.2 Parametric Analysis

Parametric analysis is very important for the future development. We can much more understand each parameter and how affect the result. In this part, the propose power divider analysis result can achieve with a variation of parameter individually. The patch parameter will be analysis and discuses are length, width and gap.

3.2.1 Patch Length

Analysis Parameter: L_1 and L_2.

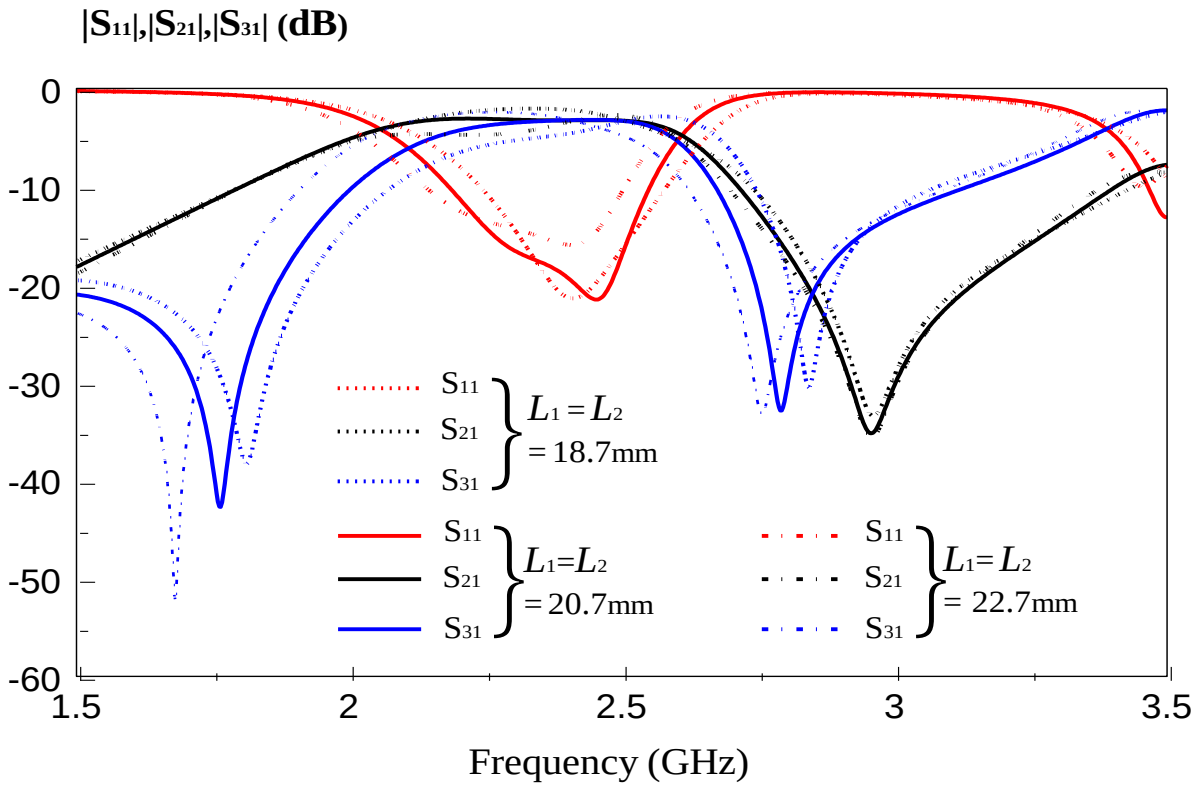

Figure 3.7 : Effect of Patch Length, L_1 and L_2 (Magnitude)

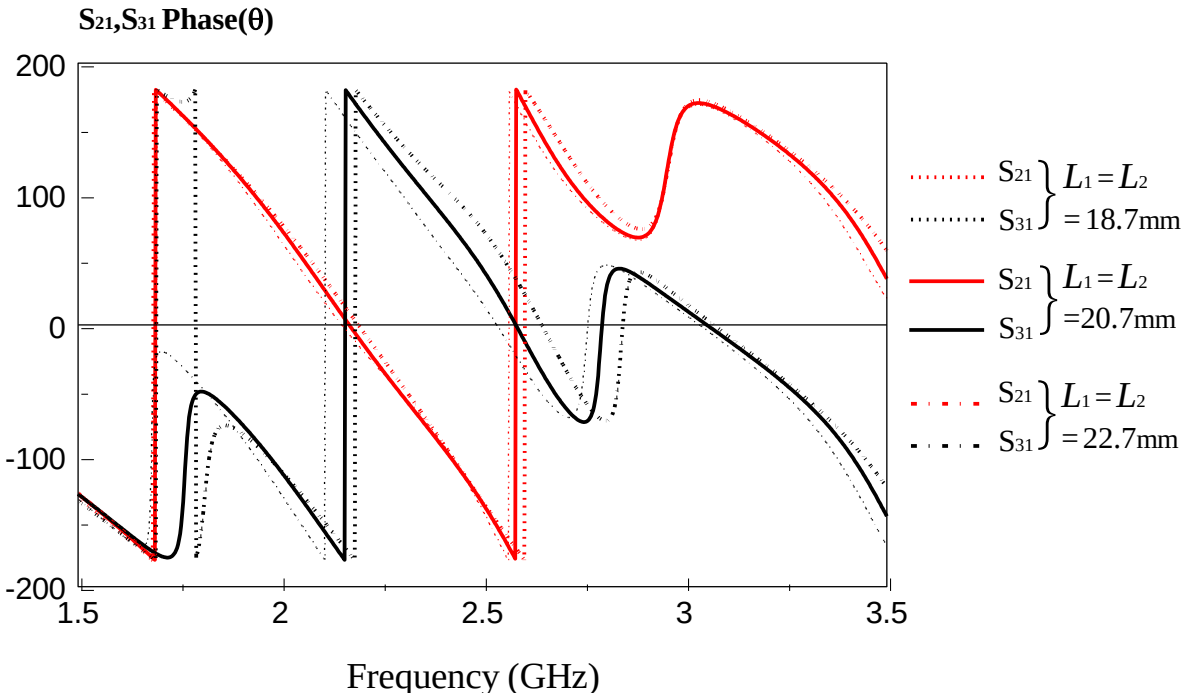

Figure 3.8 : Effect of Patch Length, L_1 and L_2 (Phase)

The values of L_1 and L_2 that are used in this power divider are 20.7mm. From the Figure 3.7, two modes of S11 are merged into one mode by reducing L_1 to 18.7mm. It also shows that the two transmission zeros are shifted to a higher frequency. In comparison, simulation results show that phase angle has increased. When L_1 and L_2 are increased by 2.0mm, the S31 transmission zeros are shifted to a lower frequency. Besides that, the phases of S21 and S31 are slightly decreased.

Analysis Parameter: L_3.

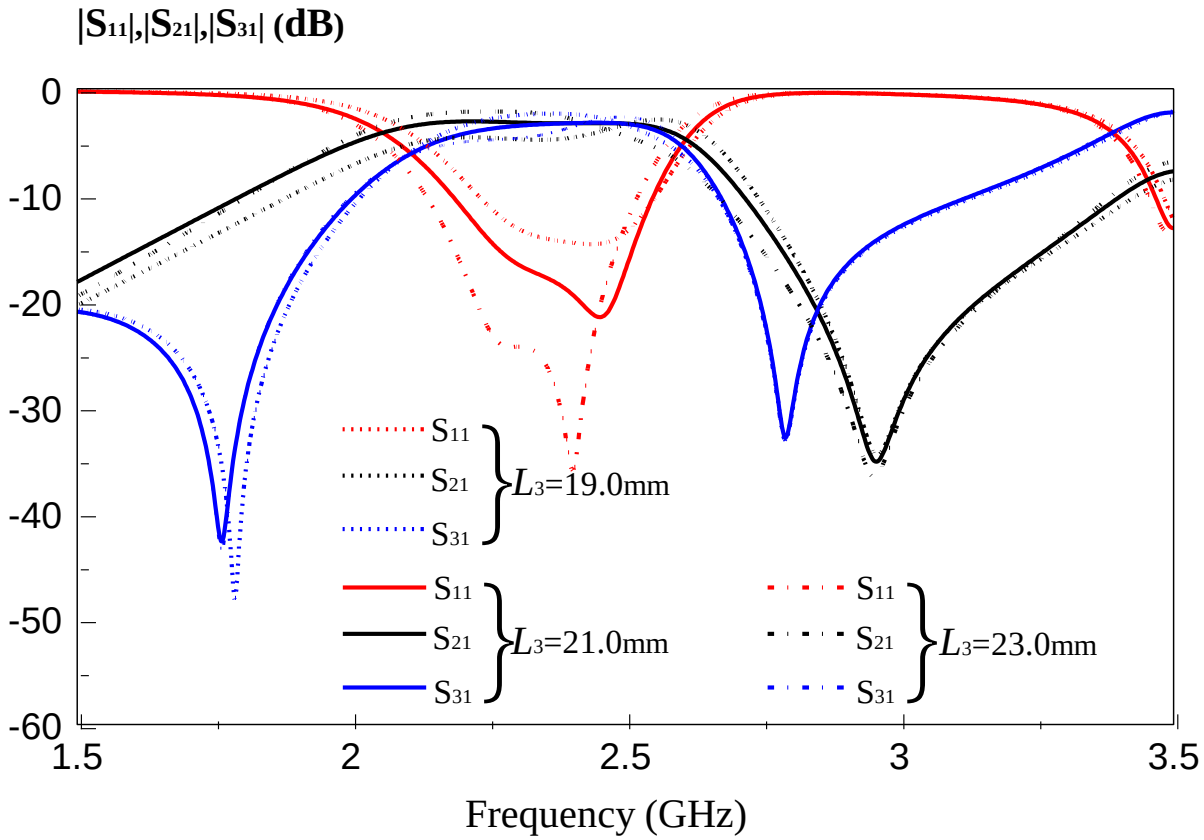

Figure 3.9 : Effect of Patch Length L_3 (Magnitude)

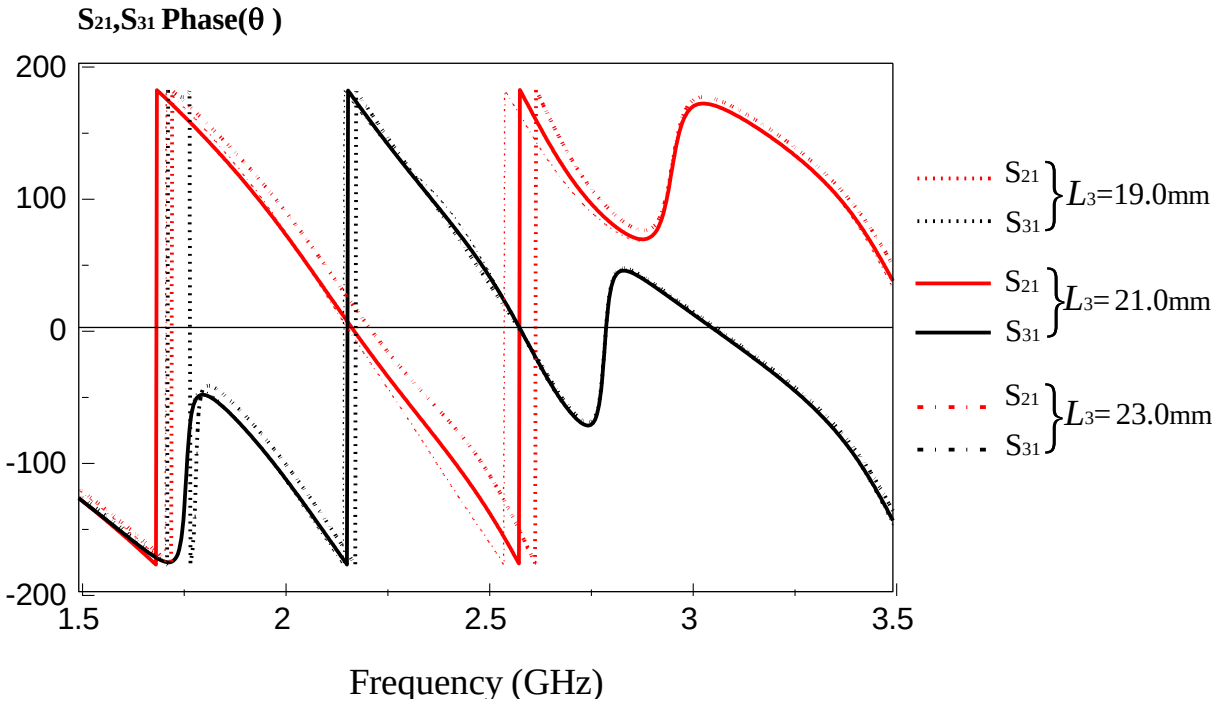

Figure 3.10 : Effect of Patch Length L_3 (Phase)

21.0mm L_3 is using in the proposed power divider. The parameter values are 19.0mm and 23.0mm.The S21 amplitude are slightly reduced via reducing the L_3 to 19.00mm.It was also increase the reflection loss. At the same time, phase angle is reduced. When the length is increased to 23.0mm, the return loss is more than -20dB. However, it does not provide good results since S21 amplitude and phase angle are become larger.

Analysis Parameter: L_4.

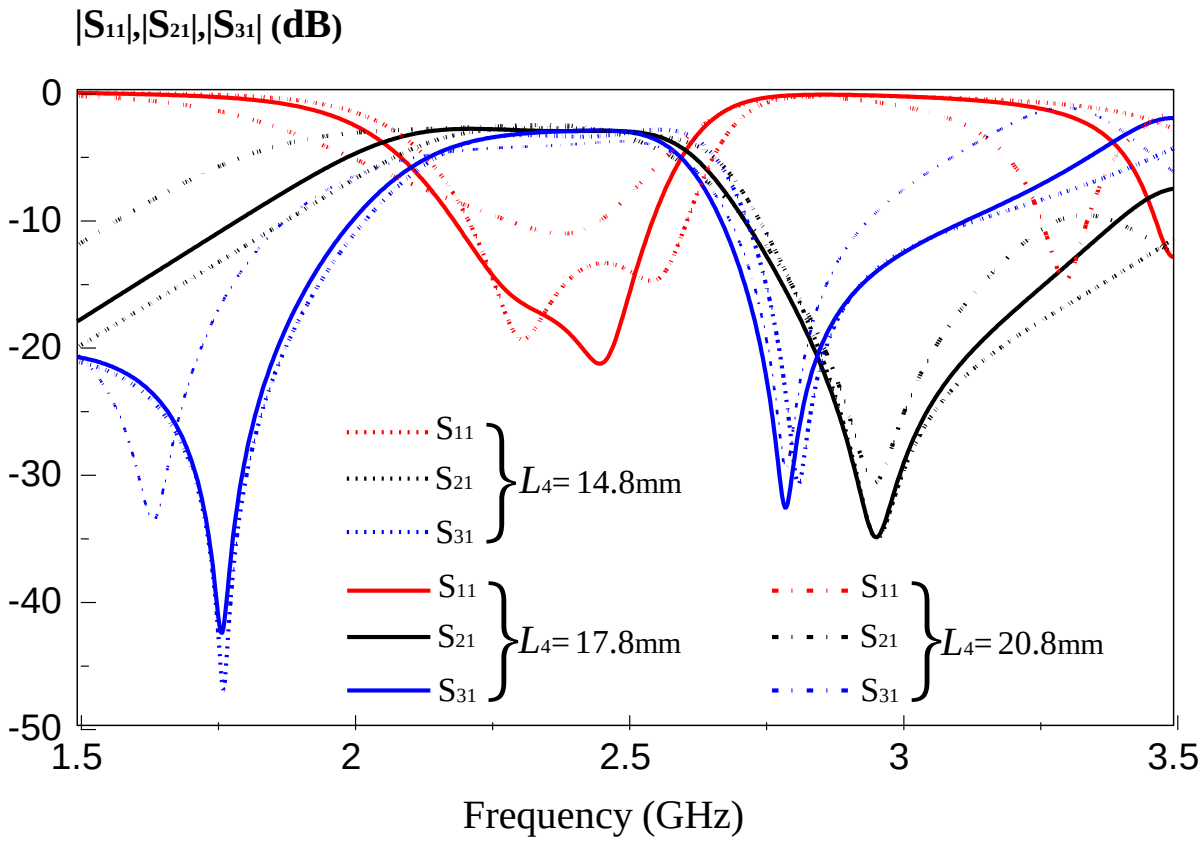

Figure 3.11: Effect of Patch Length L_4 (Magnitude)

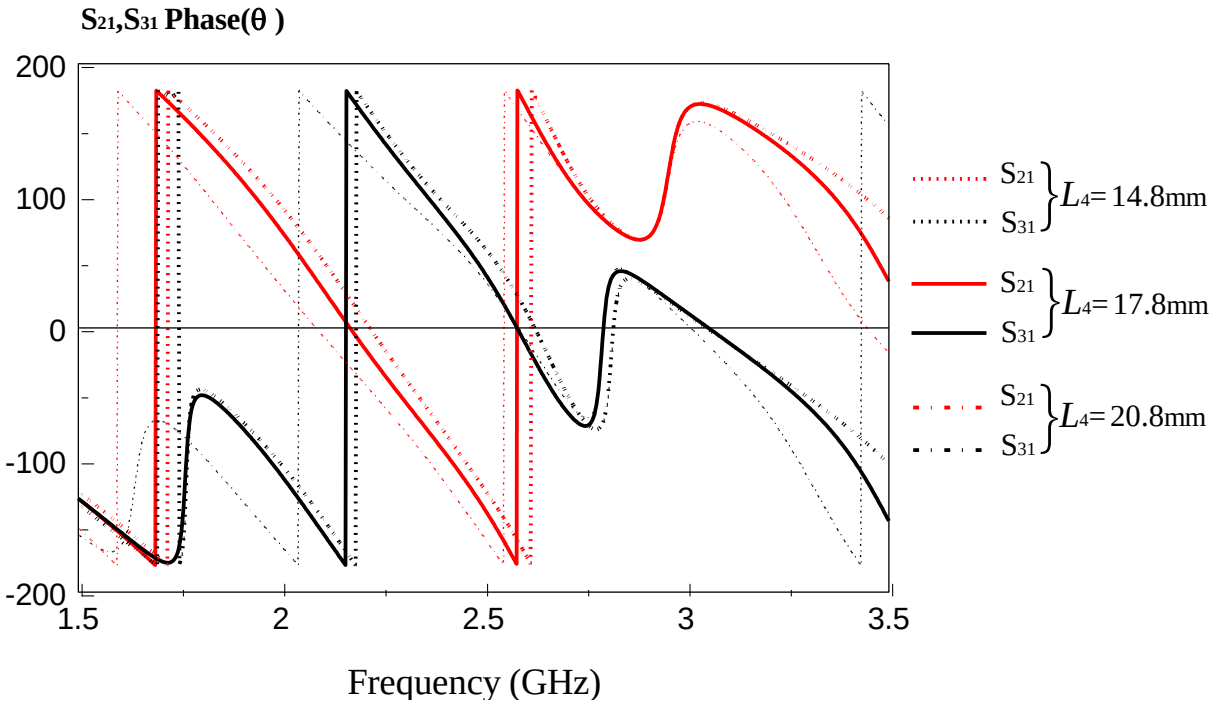

Figure 3.12 : Effect of Patch Length L_4 (Phase)

From the simulated result, as shown in Figure 3.11, the 14.88mm L_4 provides two modes S11. The simulated S31 slightly shift to higher frequency compare with the proposed result. When the L_4 increased to 20.8mm, the reflection loss was increase. Consequently, S31 first transmission zero shifts to lower frequency.

Analysis Parameter: L_5.

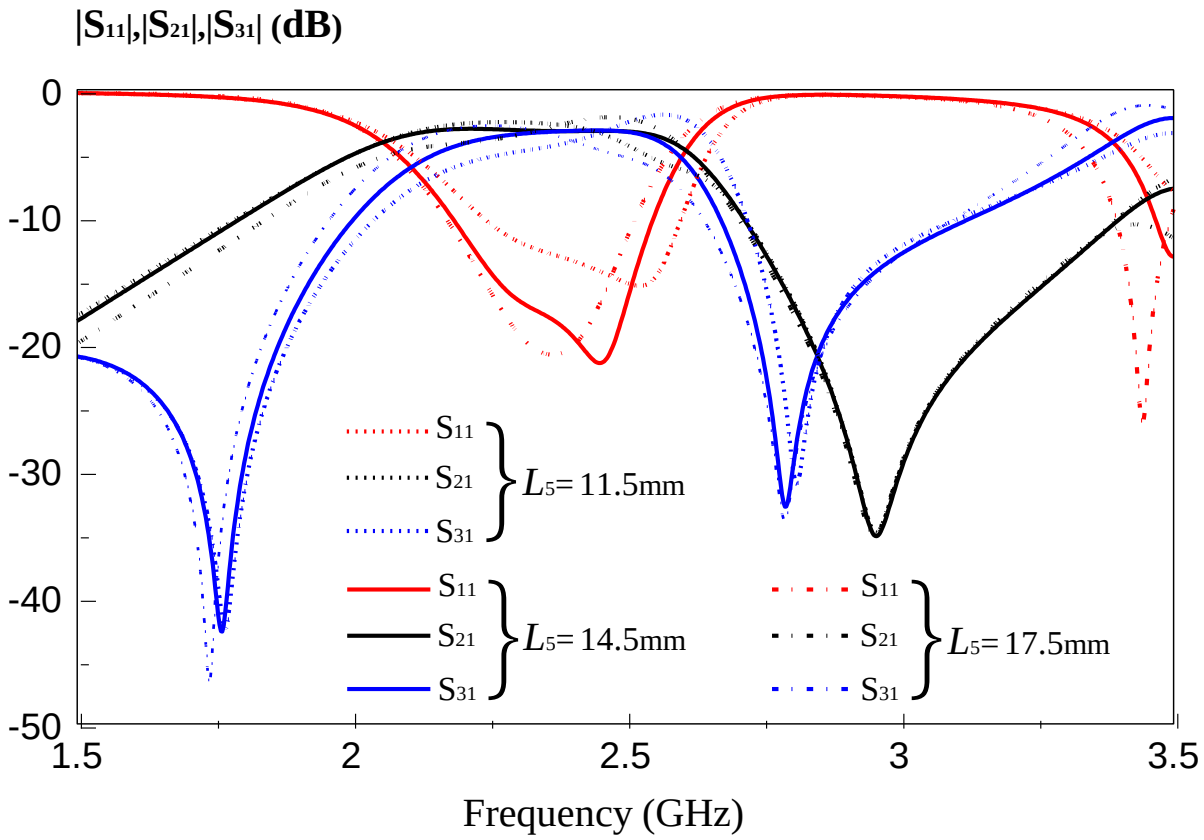

Figure 3.13 : Effect of Patch Length L_5 (Magnitude)

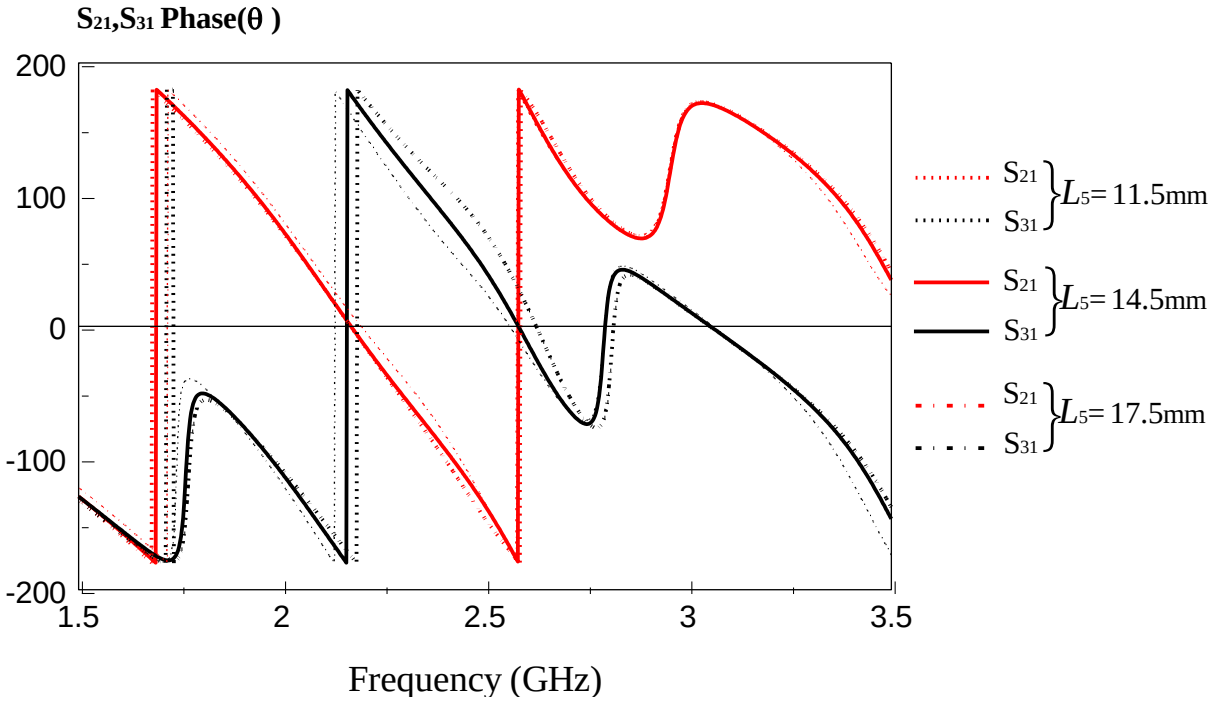

Figure 3.14 : Effect of Patch Length L_5 (Phase)

The simulated results of L_5 are shown in Figure 3.13. It shows that 11.5mm L_5 does not provide a good matching. Moreover, S31 have lower amplitude and is unable to provide equal amplitude. Besides that, it also provide larger phase angle. Reducing L_5 by 3.0mm can provide better matching but reduce the phase angle.

Analysis Parameter: L_6.

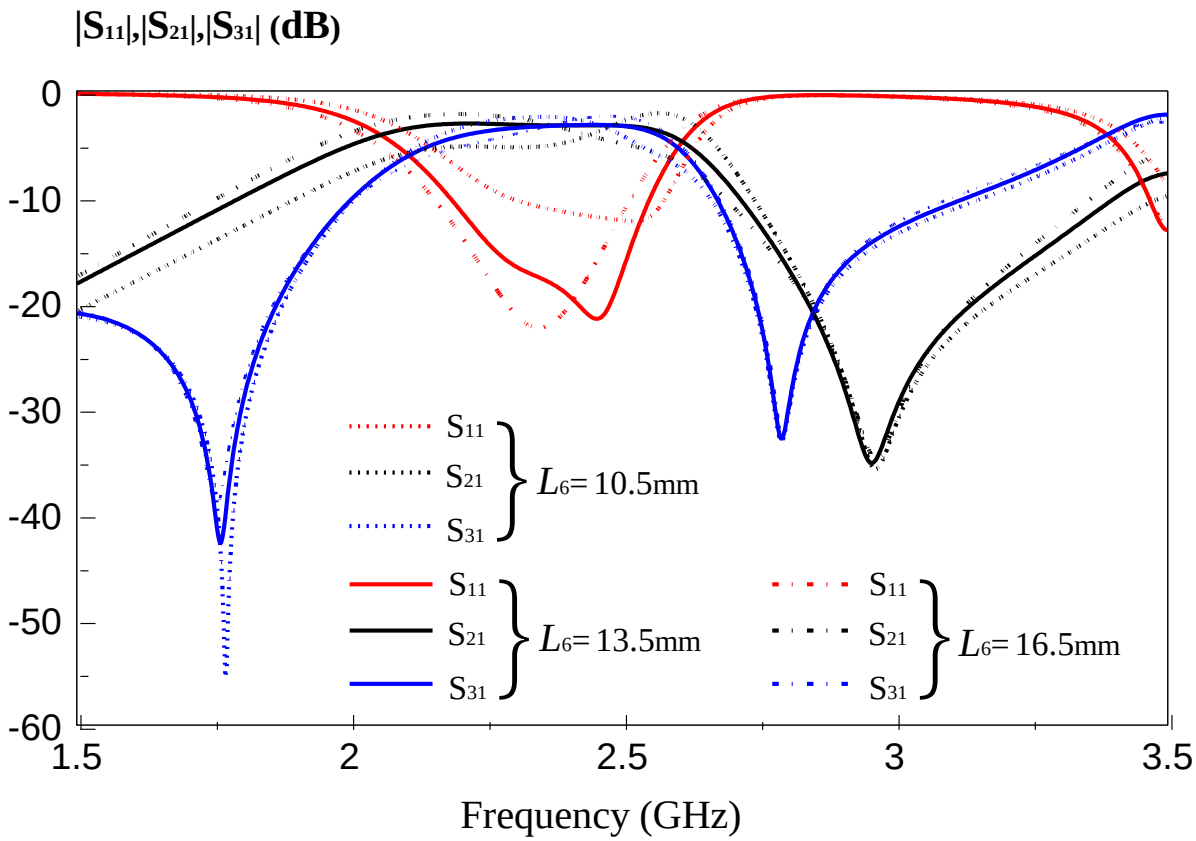

Figure 3.15 : Effect of Patch Length L_6 (Magnitude)

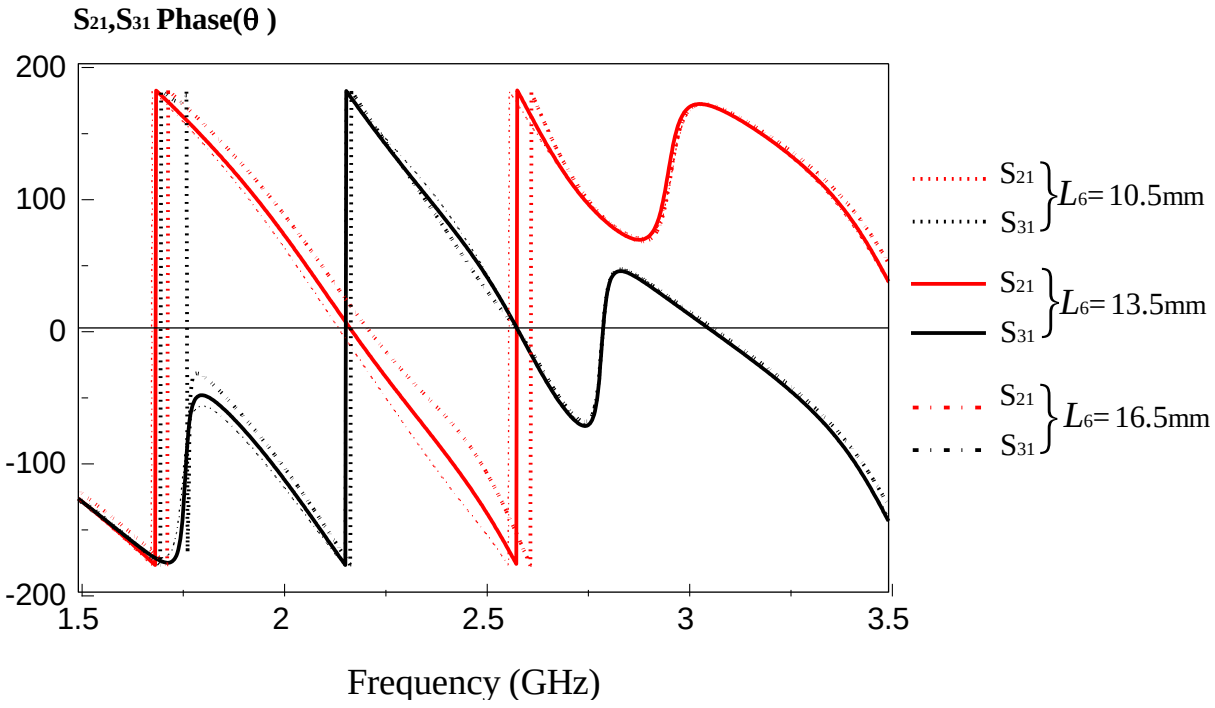

Figure 3.16 : Effect of Patch Length L_6 (Phase)

It is shown in Figure 3.15 that returns loss of power divider dependent on the L_6. Furthermore, the phase angle goes lower when L_6 is reduced to 10.5mm.However; the phase angle goes higher when L_6 is increased to 16.5mm.

Analysis Parameter: L_7 and L_8.

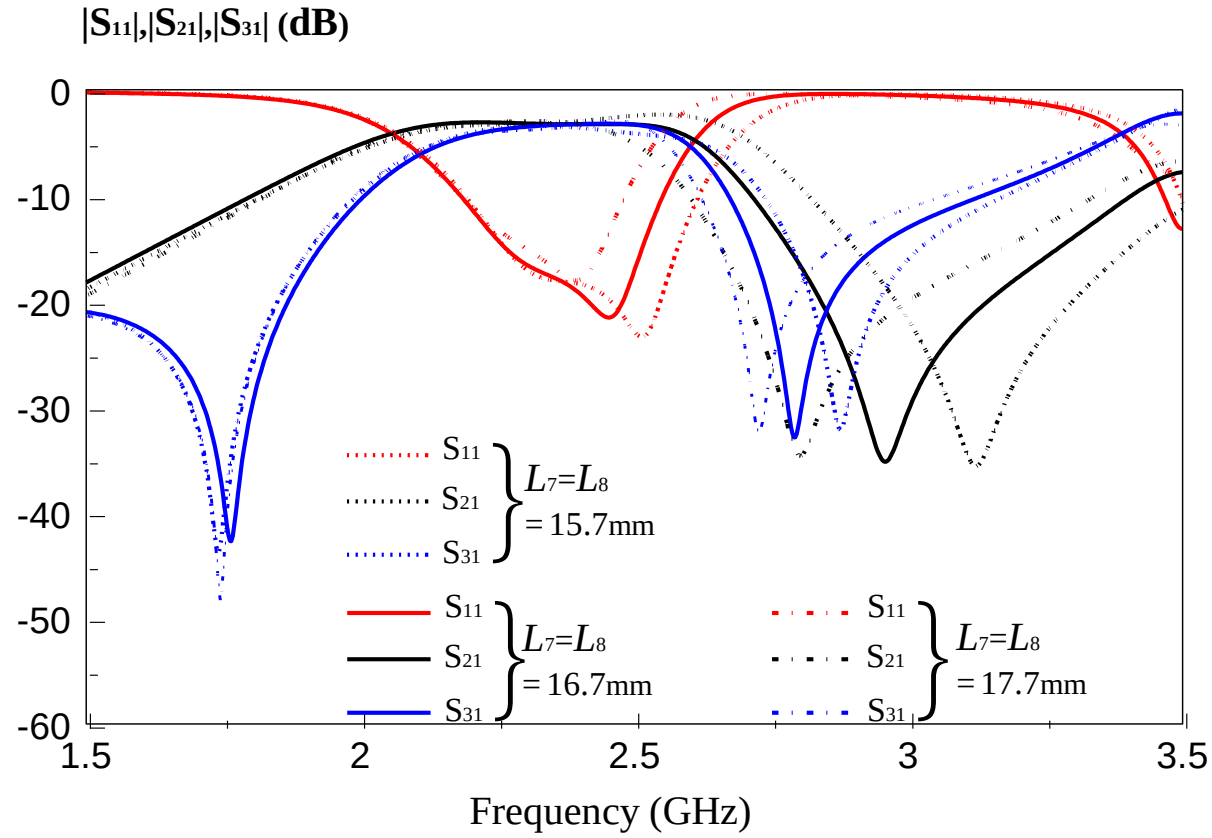

Figure 3.17 : Effect of Patch Length L_7 and L_8 (Magnitude)

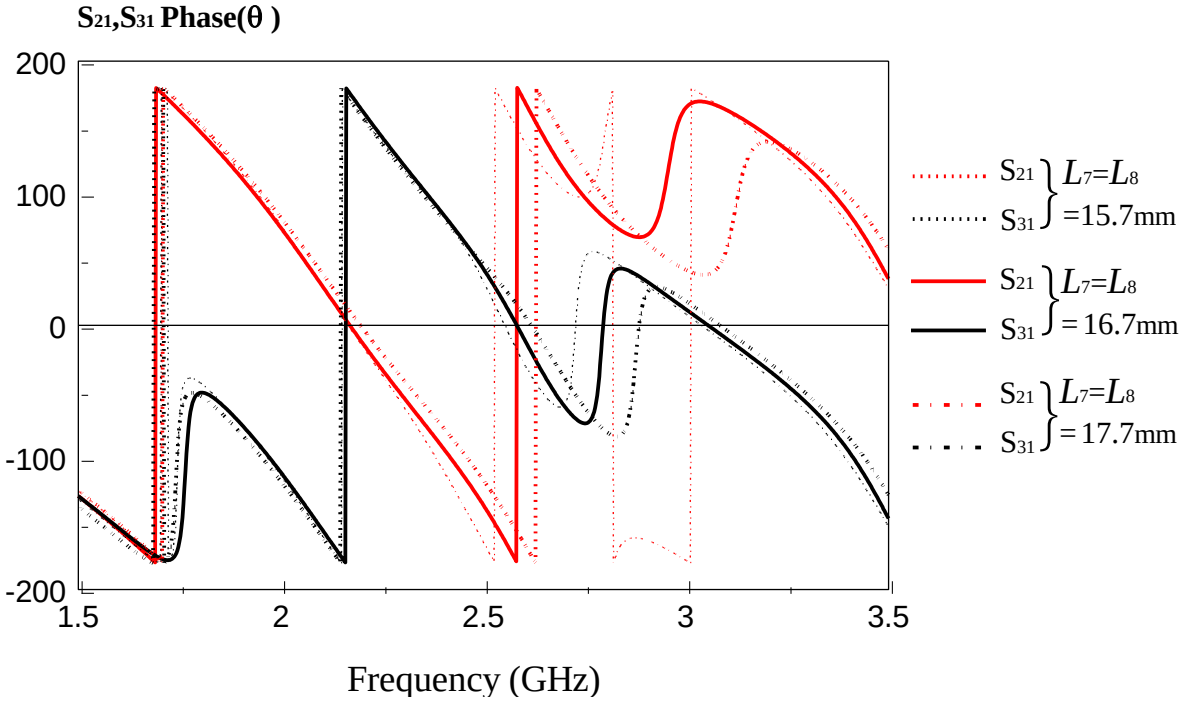

Figure 3.18 : Effect of Patch Length L_7 and L_8 (Phase)

Figure 3.17 and Figure 3.18 is analyzed with others L_7 and L_8 values. The simulation results of parametric analysis are compared with the proposed power divider result, second pole of S21 and S31 are shift to higher frequency when L_7 was reduced to 15.7mm.However, second pole of S21 and S31 are shift to lower frequency when L_7 was reduced to 15.7mm.It also reduce the phase angle between S21 and S31.

Analysis Parameter: L_9.

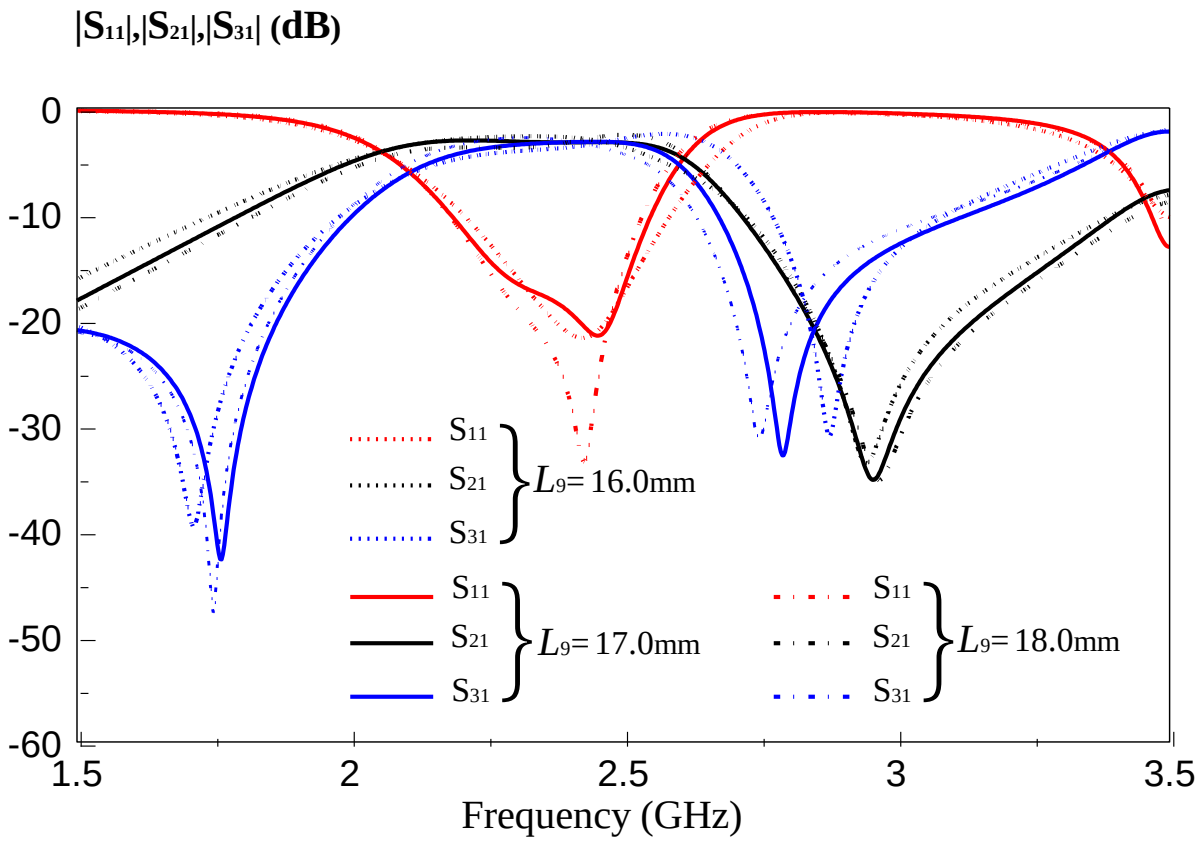

Figure 3.19 : Effect of Patch Length L_9 (Magnitude)

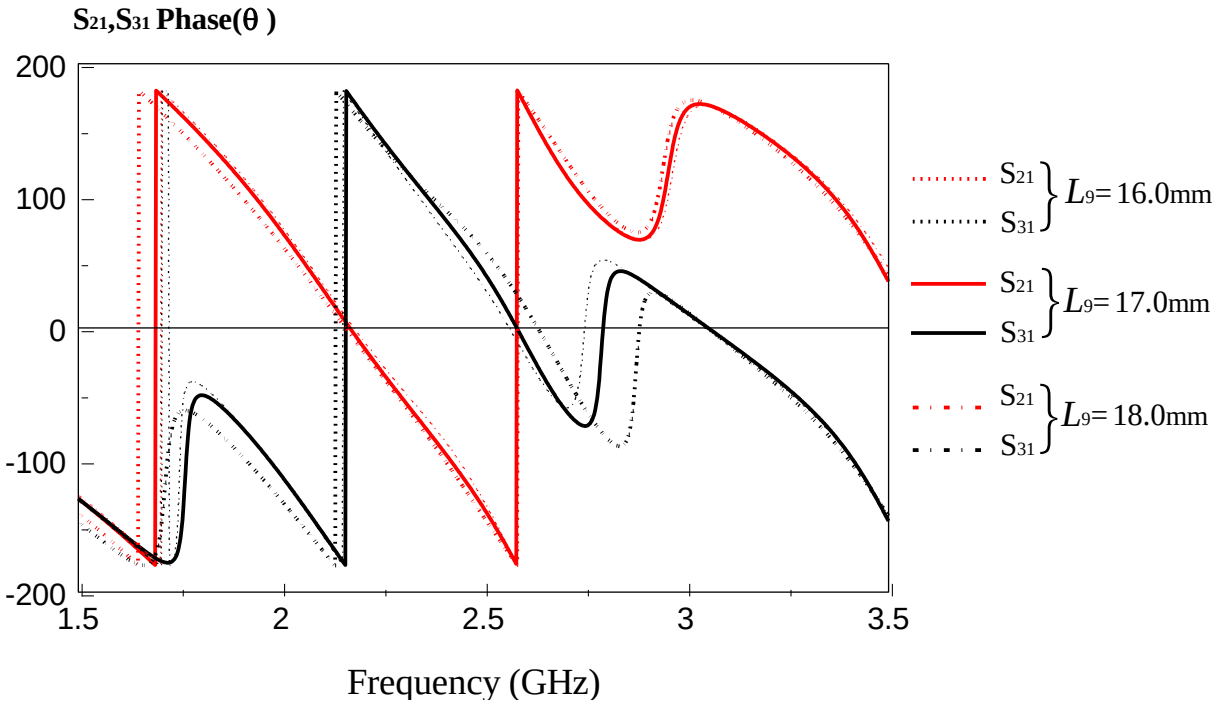

Figure 3.20 : Effect of Patch Length L_9 (Phase)

It was found that L_9 with 16.0mm, two poles in S11 are merged in the result .Meanwhile, the phase angle is increased. When the L_9 increased to 18.00, it provide better matching at S11 but unequal amplitude in S21 and S31.

3.2.2 Patch Width

Analysis Parameter: W_1 and W_2.

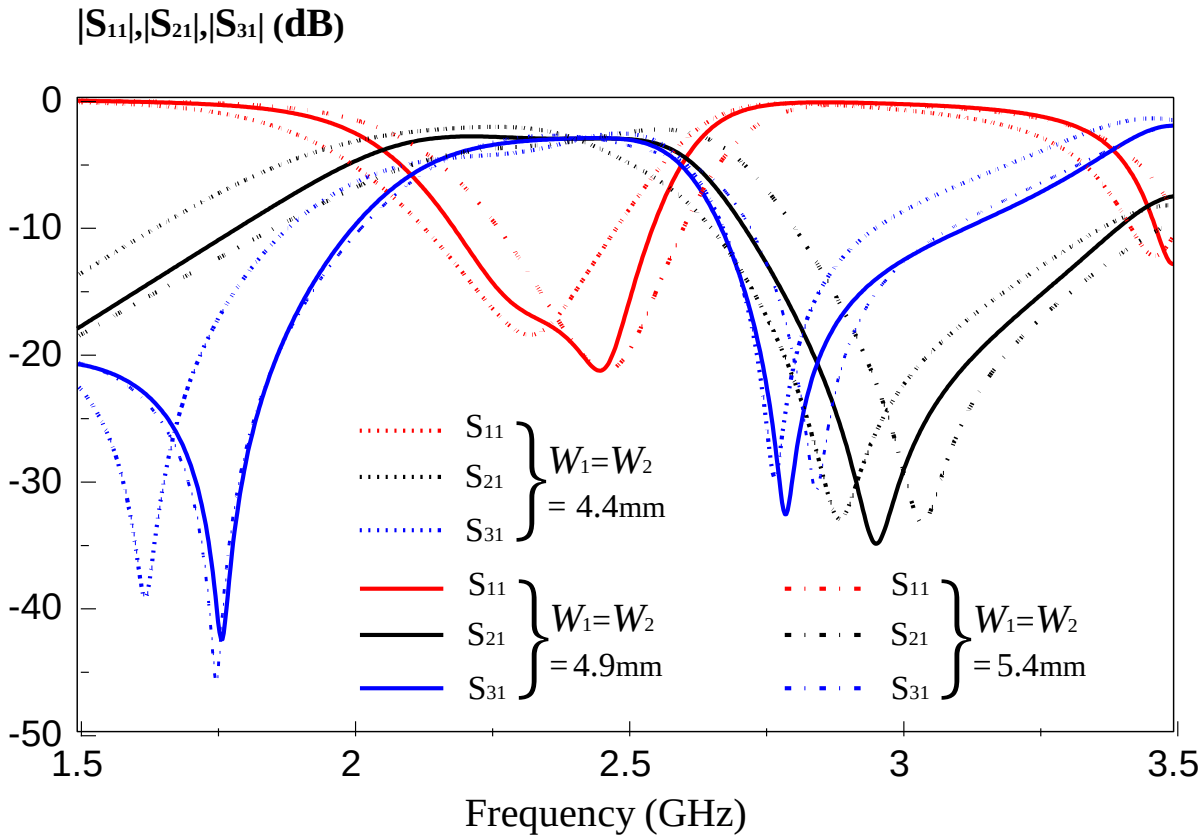

Figure 3.21: Effect of Patch Width W_1 and W_2 (Magnitude)

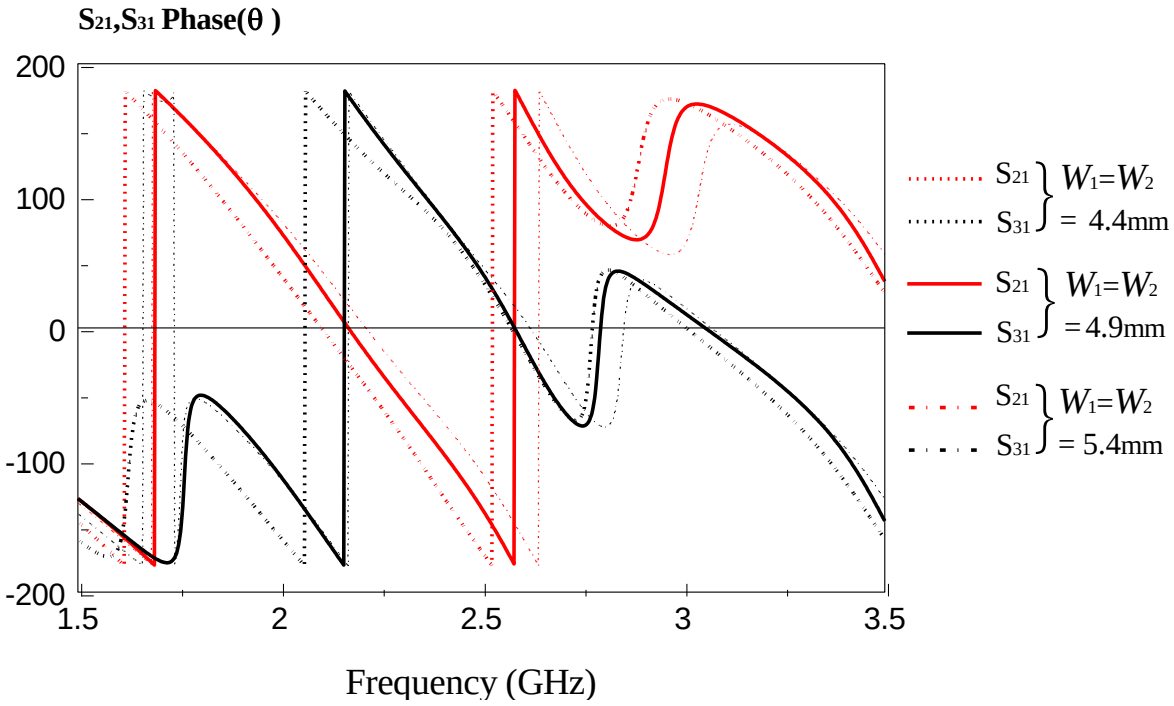

Figure 3.22 : Effect of Patch Width W_1 and W_2 (Phase)

In the effect of W_1 and W_2 of Figure 3.21, and Figure 3.22, it is shown that the S21 transmission zero is shifted to lower frequency when W_1 and W_2 reduce to 4.4mm.It also shows that S31 transmission zero is shift to lower frequency. Besides that, the phase angle between the S21 and S31 is increased. Both of the S21 and S31 second transmission zero will shift to higher frequency when reduce the width Furthermore, reducing the width of the W_1 and W_2 does not bring any benefit, but reduce the phase angle.

Analysis Parameter: W_3.

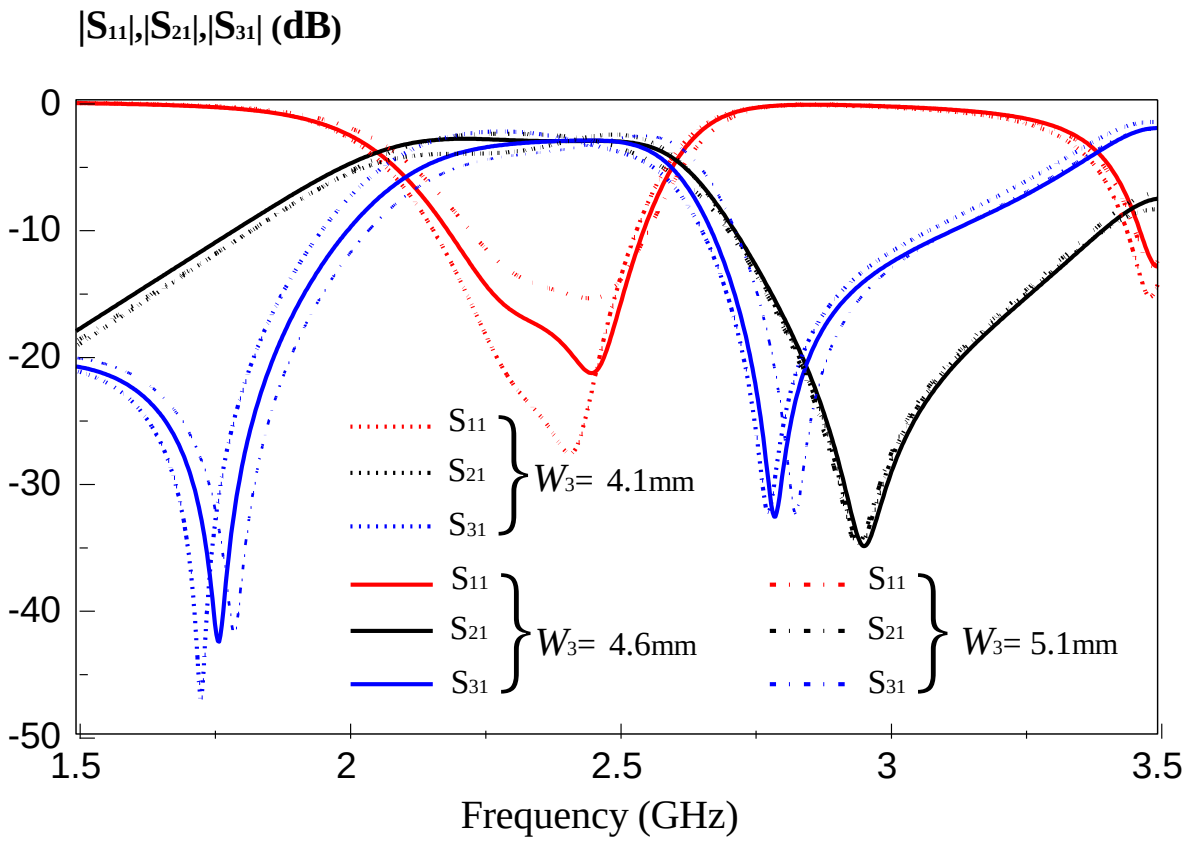

Figure 3.23: Effect of Patch Width W_3 (Magnitude)

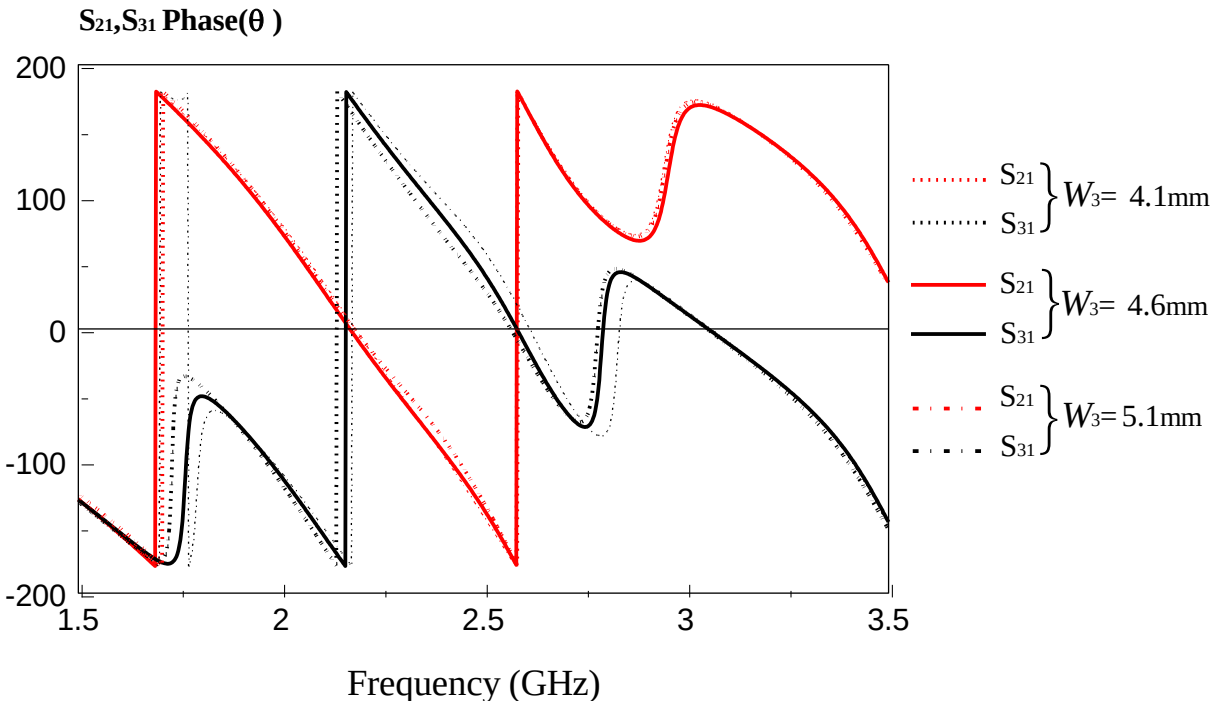

Figure 3.24 : Effect of Patch Width W_3 (Phase)

Shown in Figure 3.23 and Figure 3.24 are the affect W_3 which has the less significant change in S21 and S31.The reflection loss has decrease when W_3 is reduced. Meanwhile, the phase angle is slightly reduced. The figures also show that the reflection loss and phase angle is increase when W_3 is increased.

Analysis Parameter: W_4, $W5$ and W_6

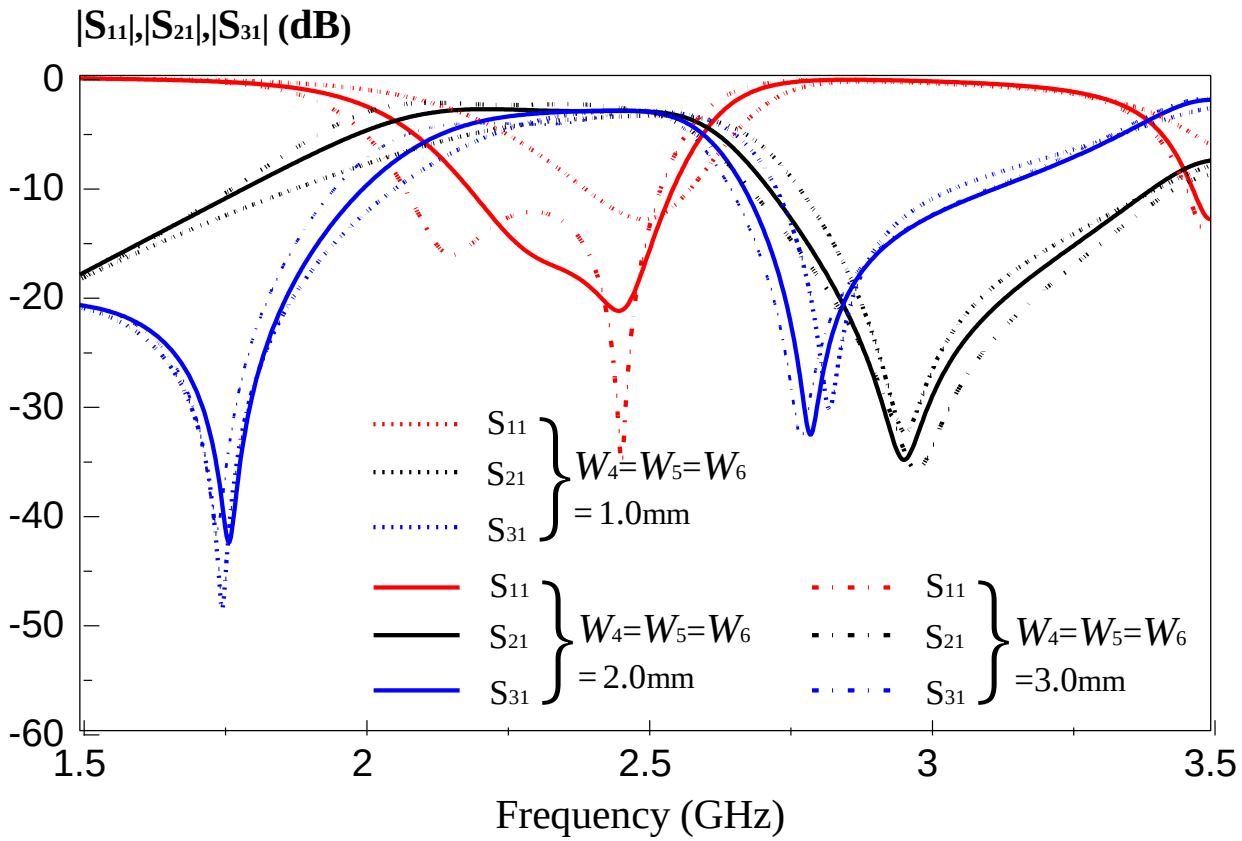

Figure 3.25 : Effect of Patch Width W_4, $W5$ and W_6 (Magnitude)

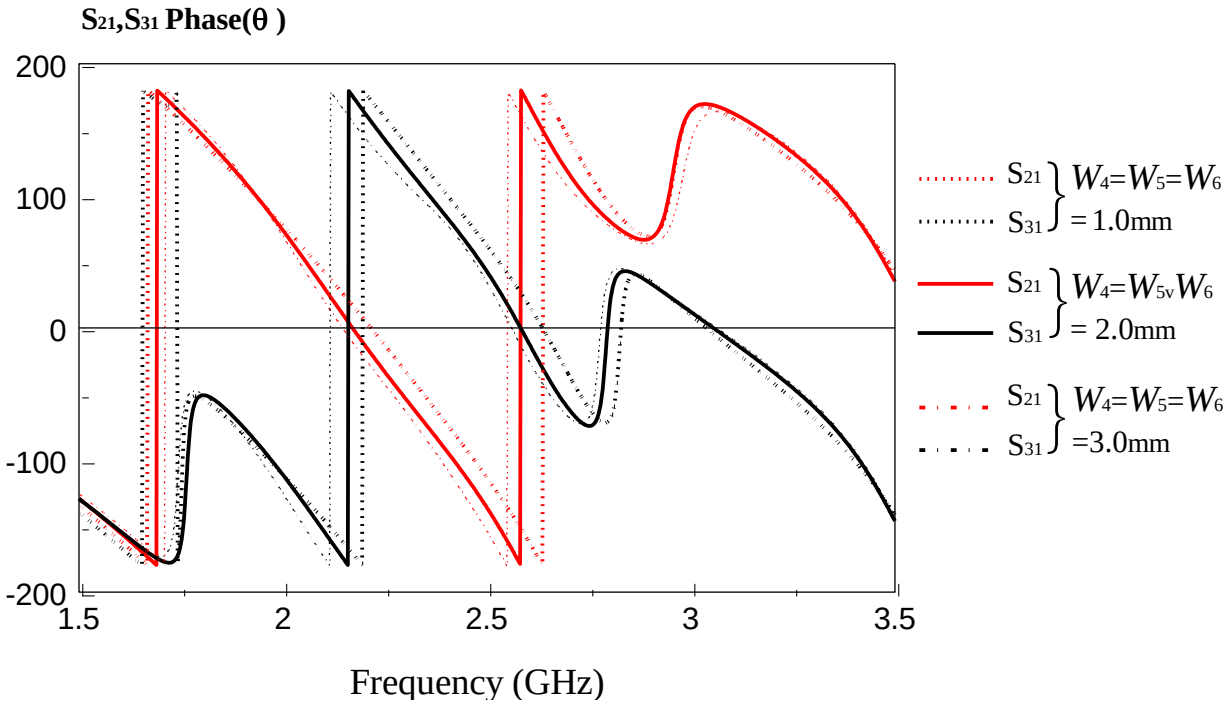

Figure 3.26 : Effect of Patch Width W_4, $W5$ and W_6 (Phase)

The simulation results are plotted as shown in Figure 3.25 and Figure 3.26. From Figure 3.24, the reflection loss getting higher when the width of the W_4, $W5$ and W_6 are changing. While, the phase angle results of simulation are getting worst when W_4, $W5$ and W_6 are increasing or decreasing.

Analysis Parameter: W_7 and W_8.

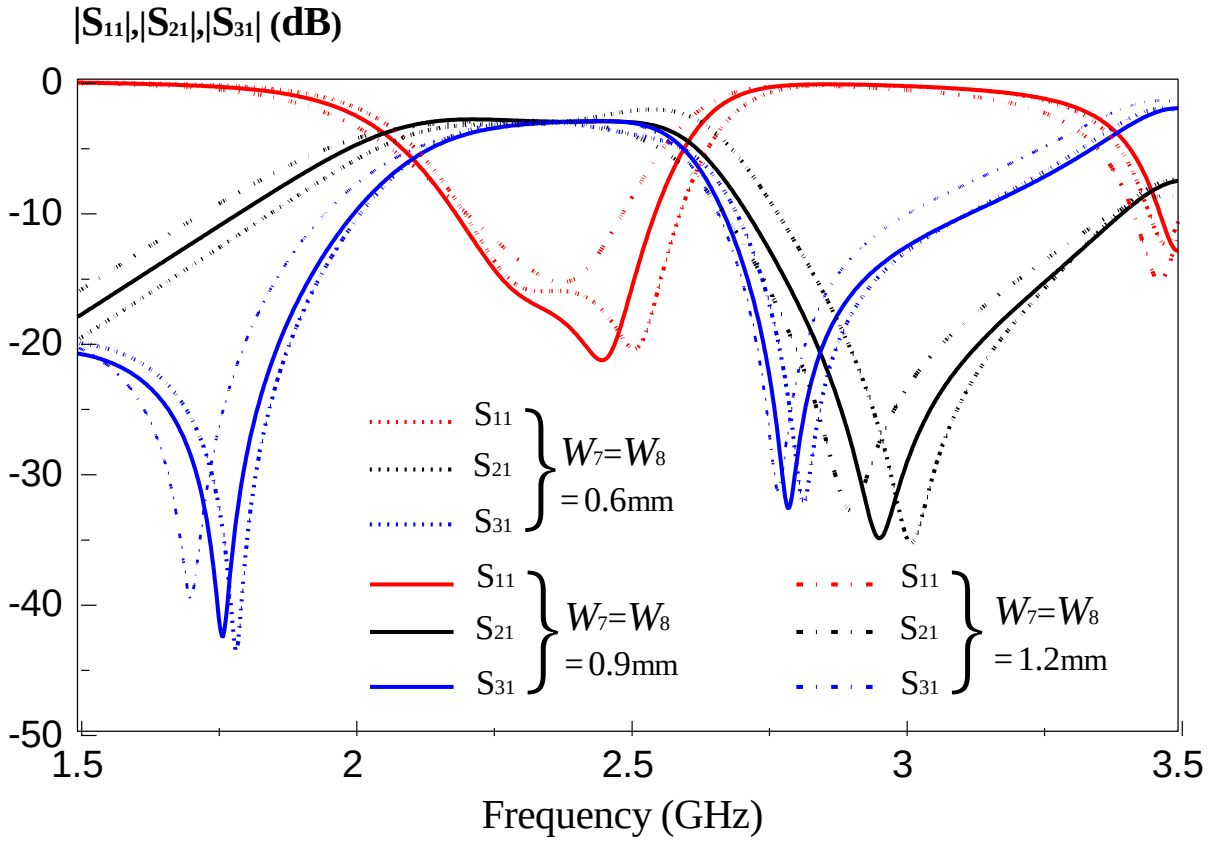

Figure 3.27 : Effect of Patch Width W_7 and W_8 (Magnitude)

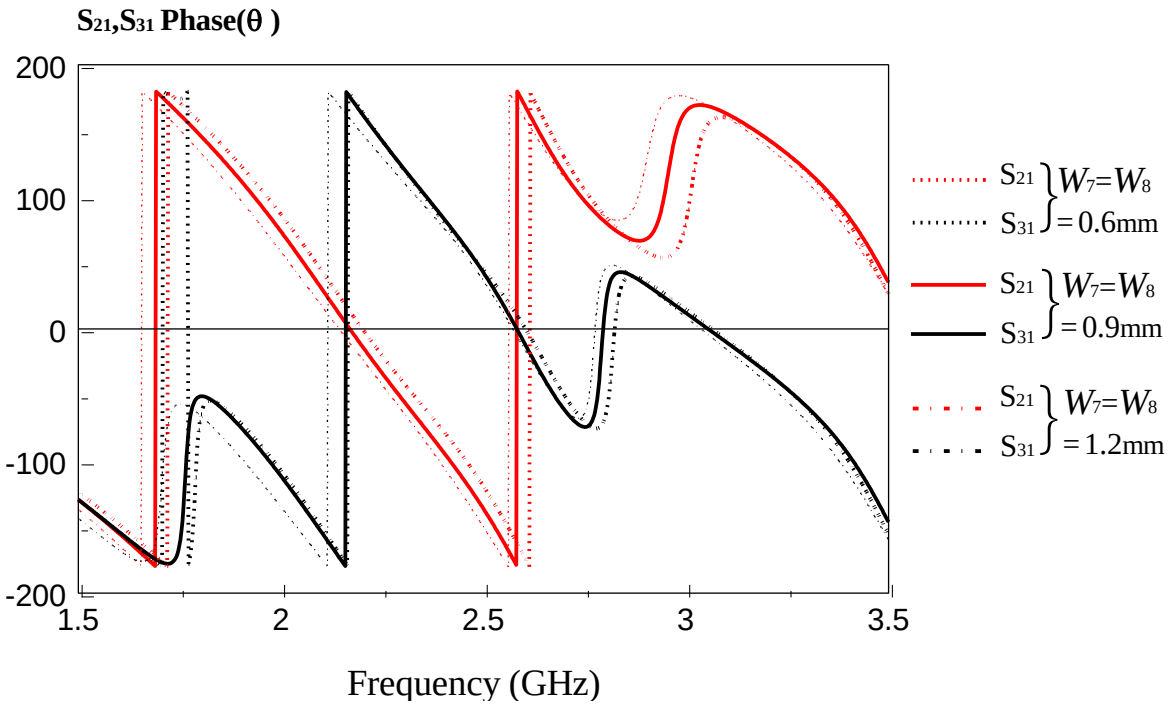

Figure 3.28 : Effect of Patch Width W_7 and W_8 (Phase)

As shown in Figure 3.27, S21 and S31 transmission zero are shifted to different frequency when W_7 and W_8 are adjusted. Besides that, phase angle between S21 and S31are changing with W_7 and W_8.

Analysis Parameter: W_9.

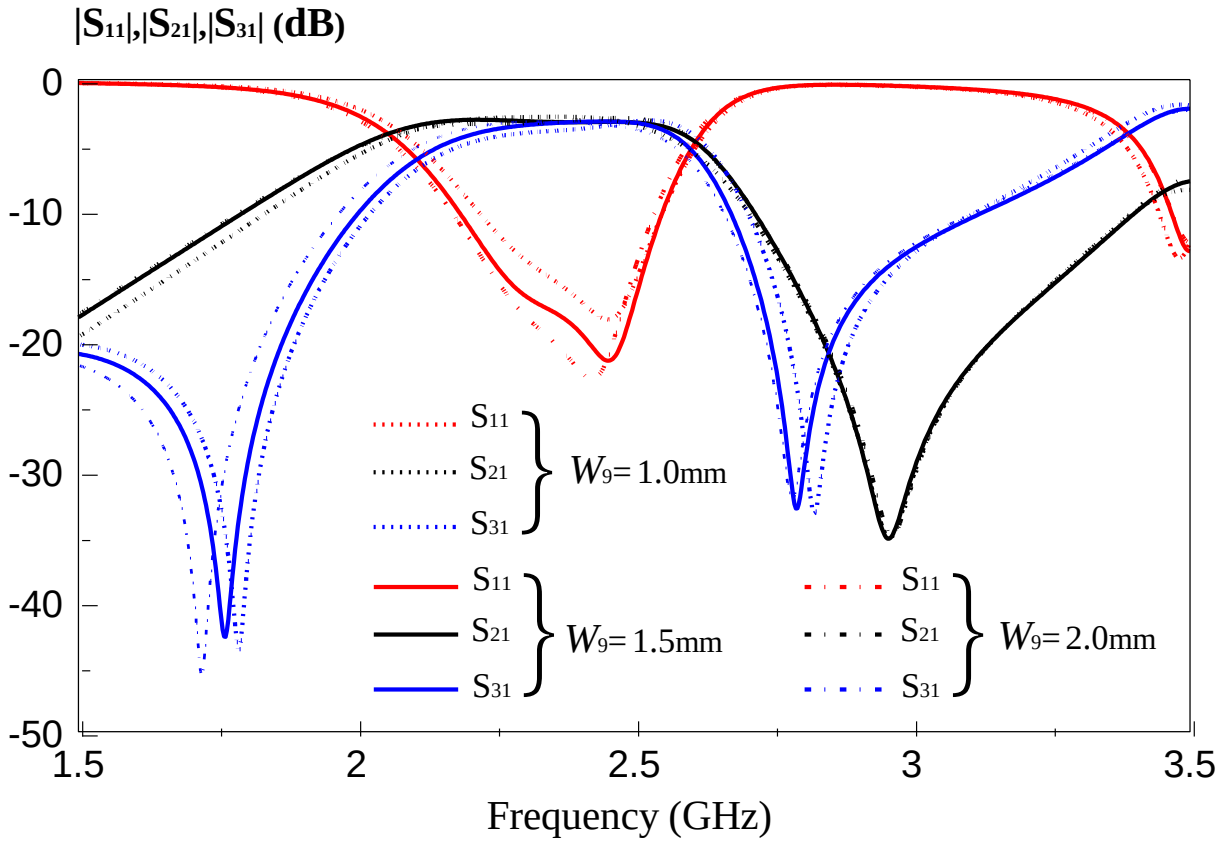

Figure 3.29 : Effect of Patch Width W_9 (Magnitude)

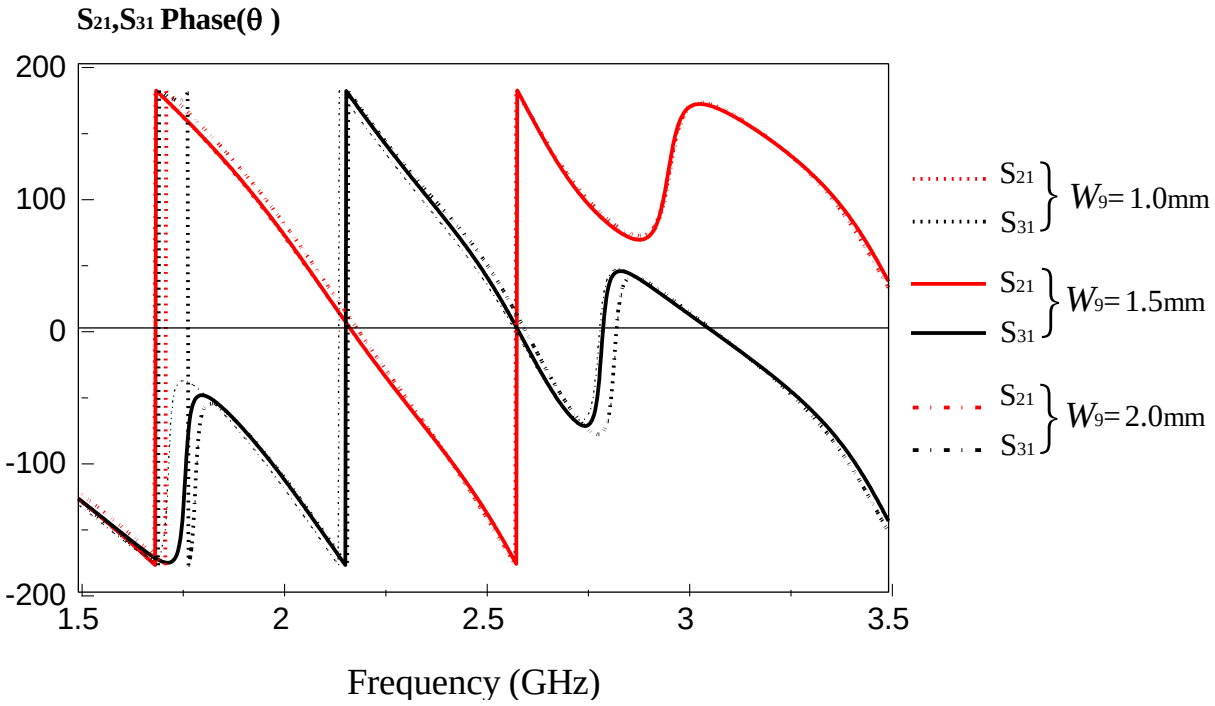

Figure 3.30 : Effect of Patch Width W_9 (Phase)

The simulation results plotted in Figure 3.29 are reasonably close to each other, although it has different width. However, 2.0mm W_9 provide better matching compare with the 1.5mm and 1.0mm.

3.2.3 Gap

Analysis Parameter: G_1

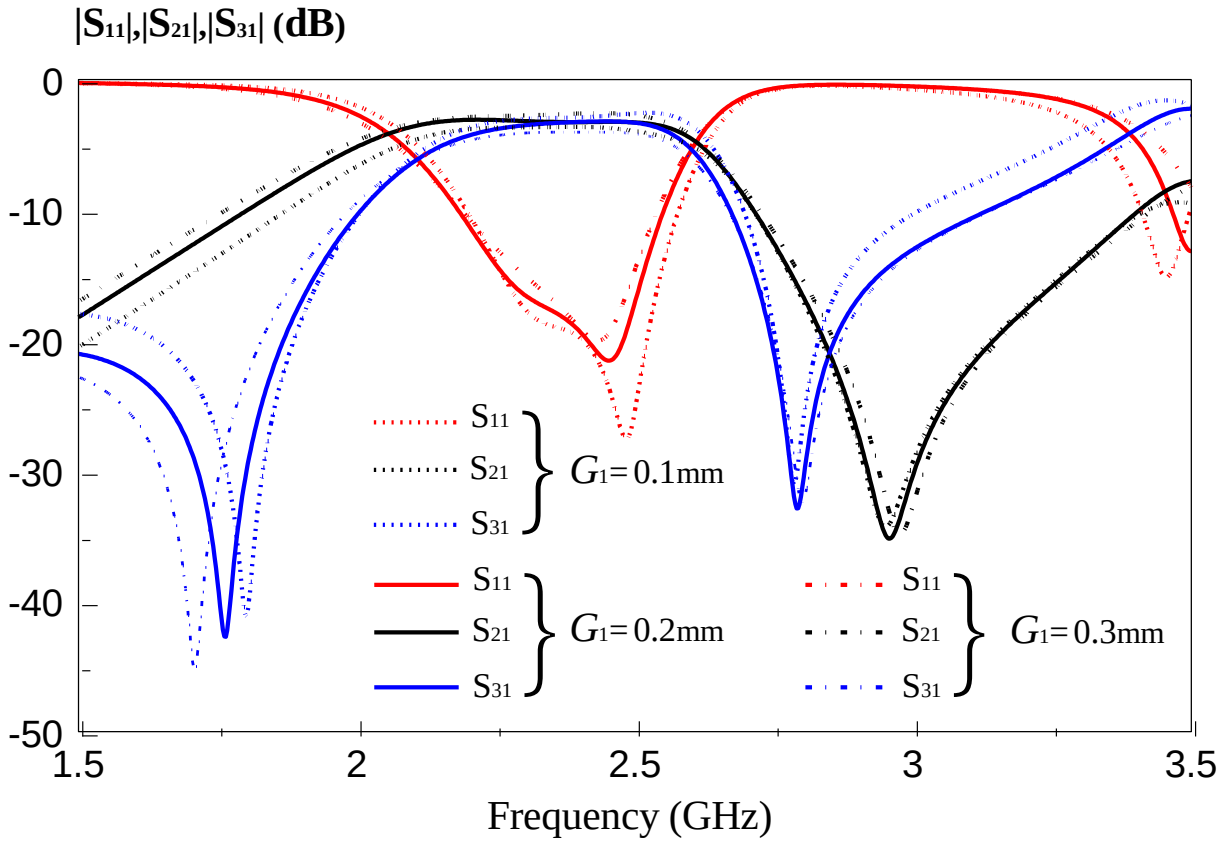

Figure 3.31 : Effect of Patch Gap G_1 (Magnitude)

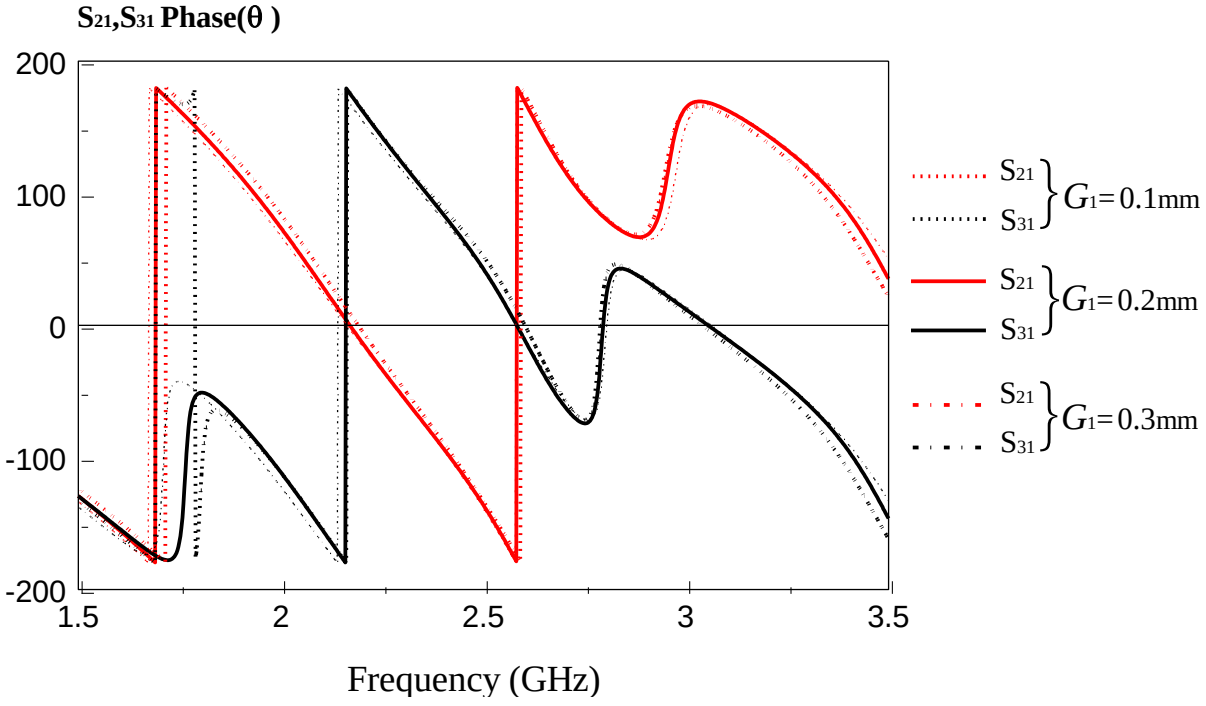

Figure 3.32 : Effect of Patch Gap G_1 (Phase)

The value of gap distance used in this proposed power divider is 0.2mm. It shows that the gap distance of 0.1mm produces better result. The S11 provide better matching after replacing the gap distance of 0.1mm with 0.2mm. These results prove that the smaller gap is able to create a stronger capacitive coupling between the resonators. However, the gap distance with 0.1mm shall not be used because other problem would arise during the fabrication stage and thus, 0.2mm gap distance is chosen.

3.3 Discussion

It can be summaries that the proposed out-phase microstrip power divider exhibit broadband characteristics, compared to the conventional power divider. Besides that, proposed out-phase microstrip have a greater advantage with very good linearity within passband The center frequency f_c , fractional bandwidth and error for both simulation and measurement result are calculated through the formulas shown below:

$$f_c = \frac{f_l + f_h}{2}$$

$$Fractional\ Bandwidth = \frac{f_h - f_l}{f_c} \times 100\%$$

$$Error = \frac{|fc\ (measured) - fc\ (simulated)|}{fc\ (measured)} \times 100\%$$

Center frequency f_c is the measurement of a central frequency between the upper and lower cutoff frequencies. Whereas the fractional bandwidth is the difference between the upper and lower frequencies in a contiguous set of frequencies divide by the center frequency. The measurement and simulation results was calculated and shown below.

	Result	
	Simulation	Experiment
f_l	2.221598	2.2141074
f_h	2.551186	2.4338327
fc	2.386392	2.3239700
BW	13.81%	9.45%
Error		2.68%

Table 3-1: Comparison between the measurement and simulation.

From the electric field, resonances are observed in the step impendence “C” shape microstrip line. Each of the “C” shape patches has one standing wave. Out-phase microstrip power divider have 180 ° phase difference in between port 2 and port 3.Hence, each “C” shapes microstrip line have different electric field.

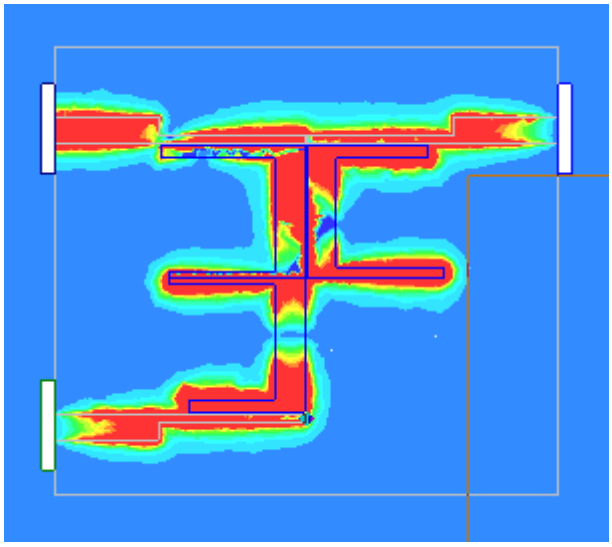

Figure 3.33 : Electric field on centre frequency.

CHAPTER 4

FILTERING DIRECTIONAL COUPLER

4.1 Background

2.07 GHz to 2.39GHz filtering directional coupler will discuss in this chapter. Four "C" shape patches was proposed as a resonator for this design. The signals from feeding line will couple with the patch and splitting the signal to the feeding line and subsequently to the output ports. The out-phase power divider was designed to resonate from 1.5 GHz to 3 GHz with a wide band-passing bandwidth from 2.07 GHz to 2.39 GHz. The filtering directional coupler is fabricated by using ro4003c with the dielectric constant of $\varepsilon_r = 2.33$ and with thickness of $h = 1.57$mm.

4.1.1 Configuration

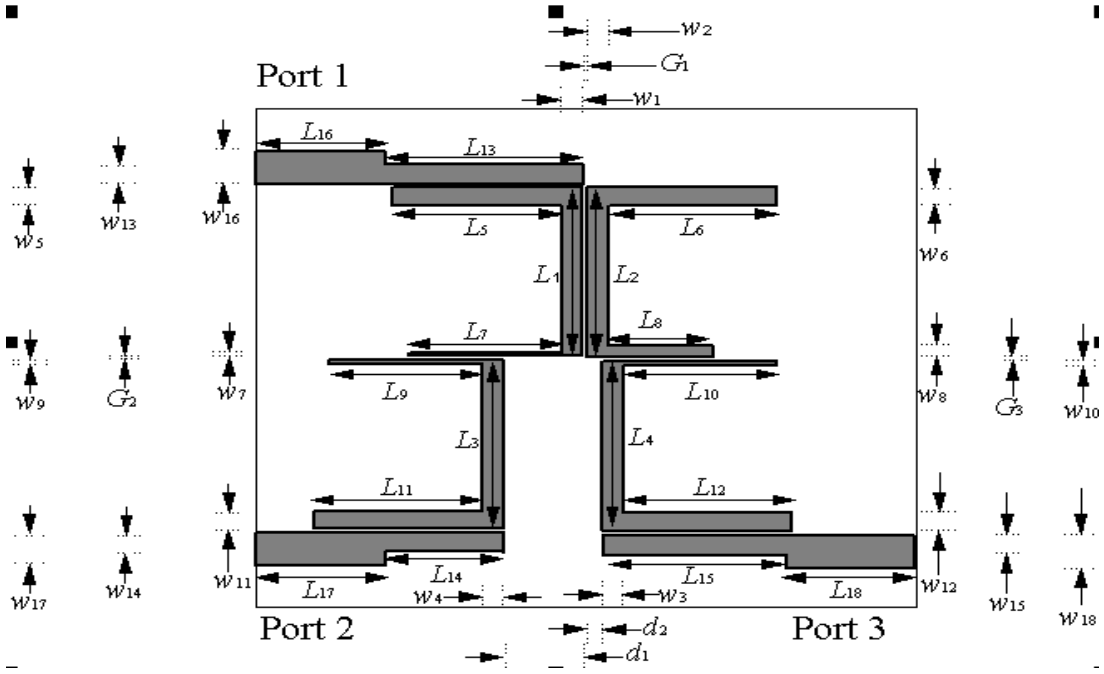

Figure 4.1: Dimension of proposed filtering directional coupler.

The parameters of the proposed circuit are L_1=L_2=L_3=L_4=24.7mm, L_5=L_6=16.8mm, L_7=13.2mm, L_8=12.0mm, L_9=12.7mm, L_{10}=13.2mm, L_{11}=16.3mm, L_{12}=17.1mm, L_{13}=23.1mm, L_{14}=16.8mm, L_{15} =23.4mm, L_{16}=22.2mm, L_{17}= 14.4mm , L_{18}=20.2mm, W_1= W_2=W_3=4.8mm, W_4=5.3mm, W_5=3.2mm, W_6=2.0mm, W_7=1.3mm, W_8=1.3mm, W_9=1.5mm, W_{10}=0.3mm, W_{11}=2.2mm, W_{12}=3.2mm, W_{13}= W_{14}=W_{15}=1.3mm, W_{16}= W_{17}=W_{18}=4.2mm, G_1=0.3mm, G_2= G_3=0.2mm, d_1=14.0mm and d_2=1.7mm.

The directional coupler was realized on a RO4003C substrate with thickness 1.57mm and dielectric constant 2.33. Besides that, the ground plane is fully consists of thin film at the bottom of substrate. From the figure, the designed directional coupler has been realized using four “C” shape patch. The input signal will feed to port1 and the feeding line will couple to the patch, respectively the patch will split the signal. Meanwhile, port 2 ratio can be controlled by adjust d_1.

4.1.2 Transmission Line Model

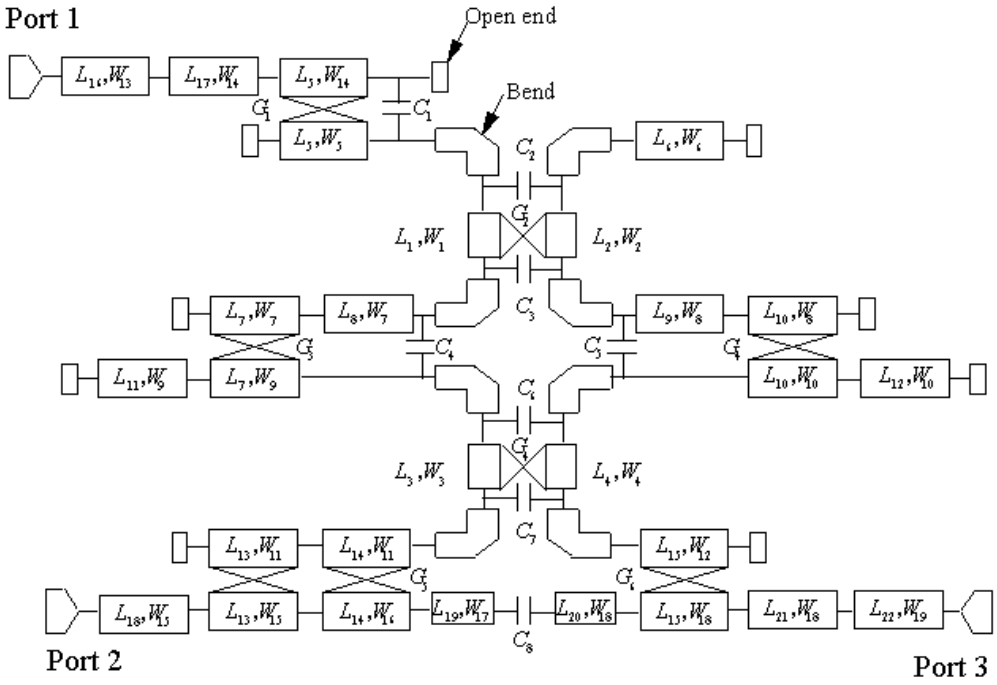

Figure 4.2 : Filtering directional coupler model.

In previous chapter transmission line model, each symbol has been mentioned. There are the different between the Ansoft HFSS (High Frequency Structure Simulator) and Microwave Office. The stray field or unwanted magnetic field was included in Ansoft HFSS simulation result .However, the Microwave office was unable to figure it out hence it cannot reflect the real situation. In order to solve the problem, few capacitors are using to represent the stray fields. The capacitor values chosen were relatively large, where the value is larger than$1 \times 10^{-15} H$.

4.1.3 Result

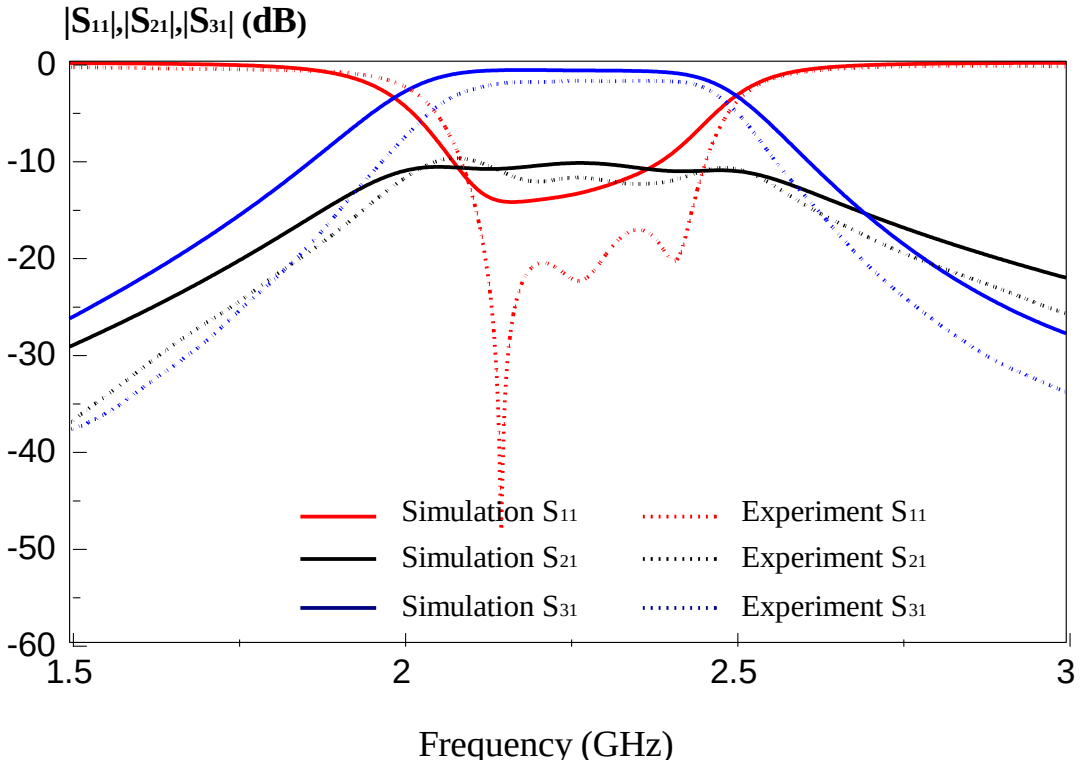

Figure 4.3 : Simulation and measurement results.

The results of the filtering directional coupler are depicted in Figure 4.3. From the simulation result, S21 and S31 have a wider bandwidth compare with the experiment result. As comparison, fabricated filtering directional coupler has high reflection loss compared with simulation result. Besides, the result showing proposed design has a flat within the passband.

4.2 Parametric Analysis

Parametric analysis is very useful enhance the performance characteristics of the filtering directional coupler. It is evident from the results that the gap between patch can provide different ratio of output. As has already been mentioned, the parametric analysis result can achieve with a variation of parameter individually. The patch parameter will be analysis and discuses are length, width and gap.

4.2.1 Patch Length

Analysis Parameter: L_1, L_2, L_3 and L_4.

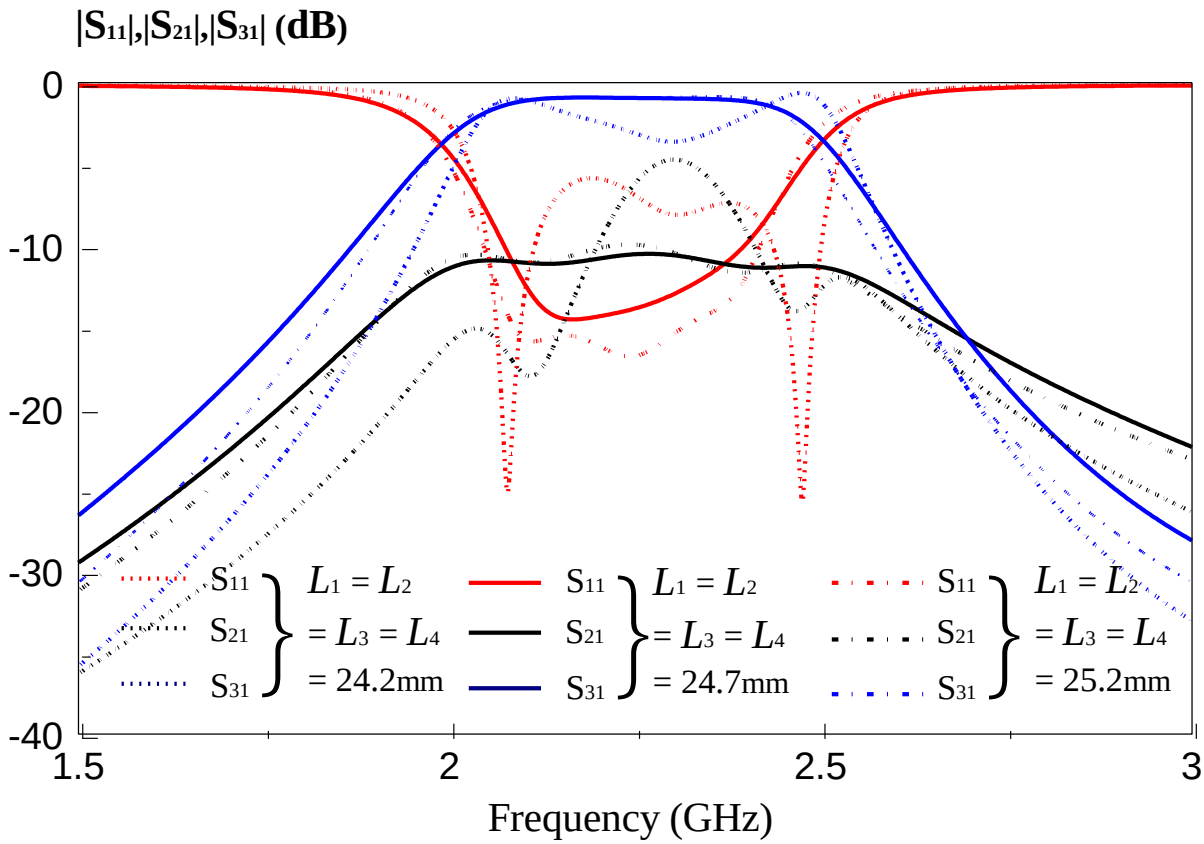

Figure 4.4 : Effect of Patch Length L_1, L_2, L_3 and L_4.

The return losses are greater than -8dB in operating frequency when L_1, L_2, L_3 and L_4 reduced to 24.2mm. It can be clearly observed the S21 and S31 is no flat between the passbands .However, 25.2mm L_1, L_2, L_3 and L_4 can provide low return loss.

Analysis Parameter: L_5 and L_6.

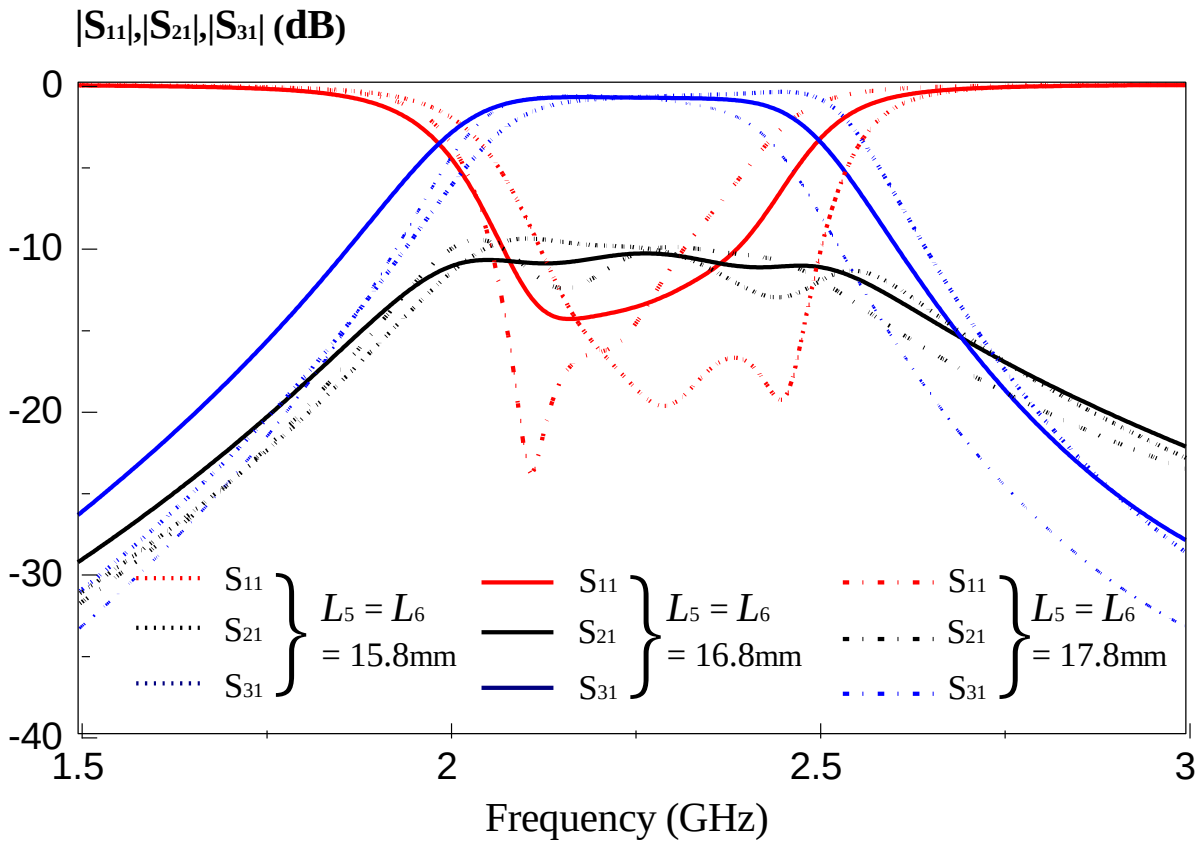

Figure 4.5 : Effect of Patch Length L_5 and L_6.

Figure 4.5 shows values of 15.8mm and 17.8mm are used to analysis. These values provide two poles to the S11 parameter. Meanwhile, it will affect the bandwidth of the directional coupler.

Analysis Parameter: L_7.

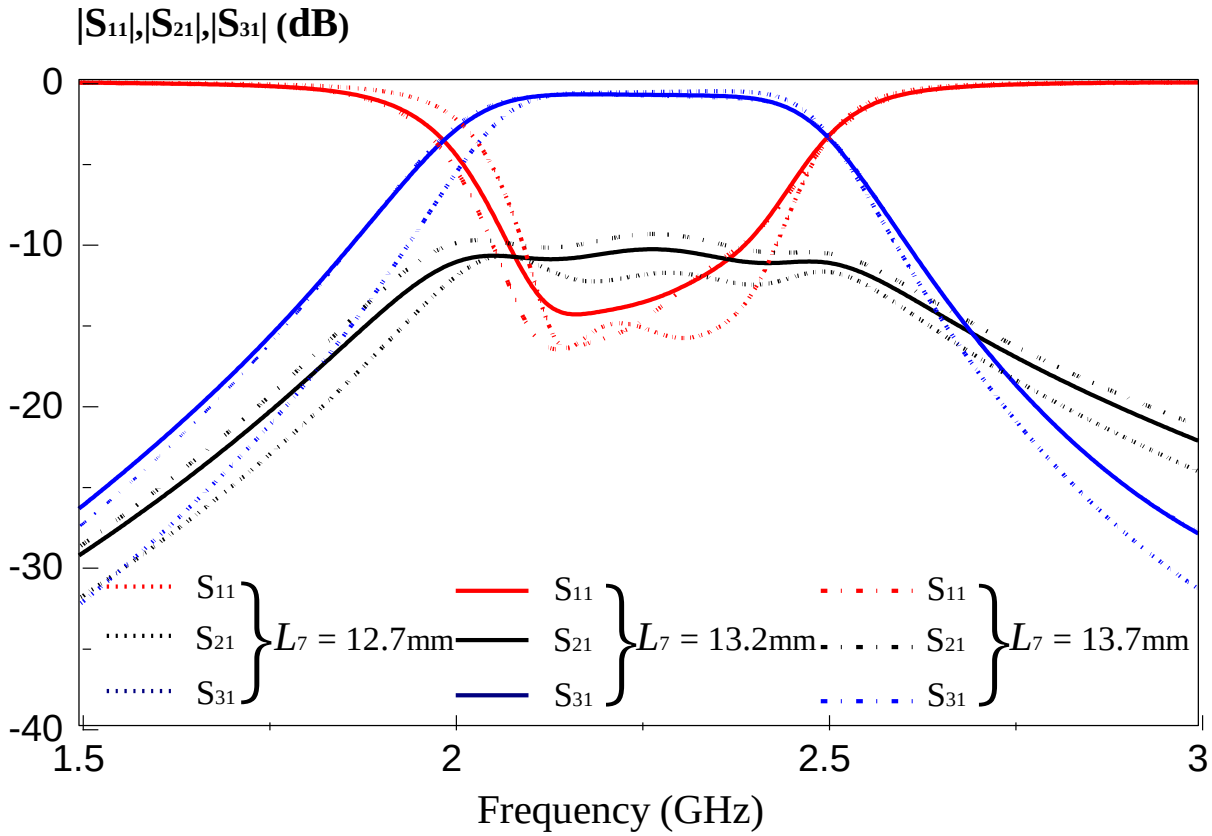

Figure 4.6 : Effect of Patch Length L_7.

From Figure 4.6, when the length $L_7$is changed to 12.7mm or 13.7mm, S21 is not flat across operating frequency. Additionally, the L_7 will slightly affect the s21 ratio.

Analysis Parameter: L_8.

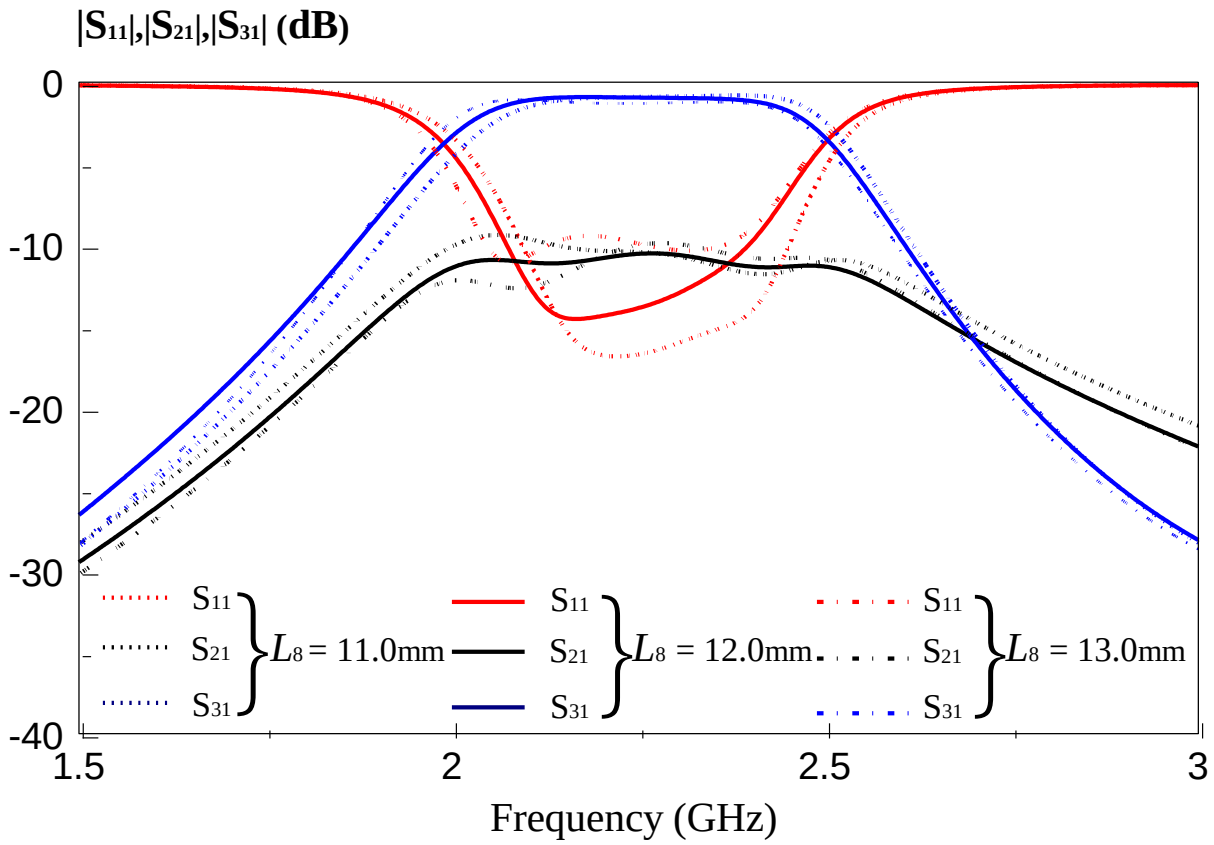

Figure 4.7 : Effect of Patch Length L_8

When the width L_8 is reduced to 11.0mm the return loss will reduce. Meanwhile, the S21 is not flat across operating frequency. In Figure 4.7, when the width L_8 is increased to 13.0mm, there is a large return loss and S21 is not flat across operating frequency.

Analysis Parameter: L_9.

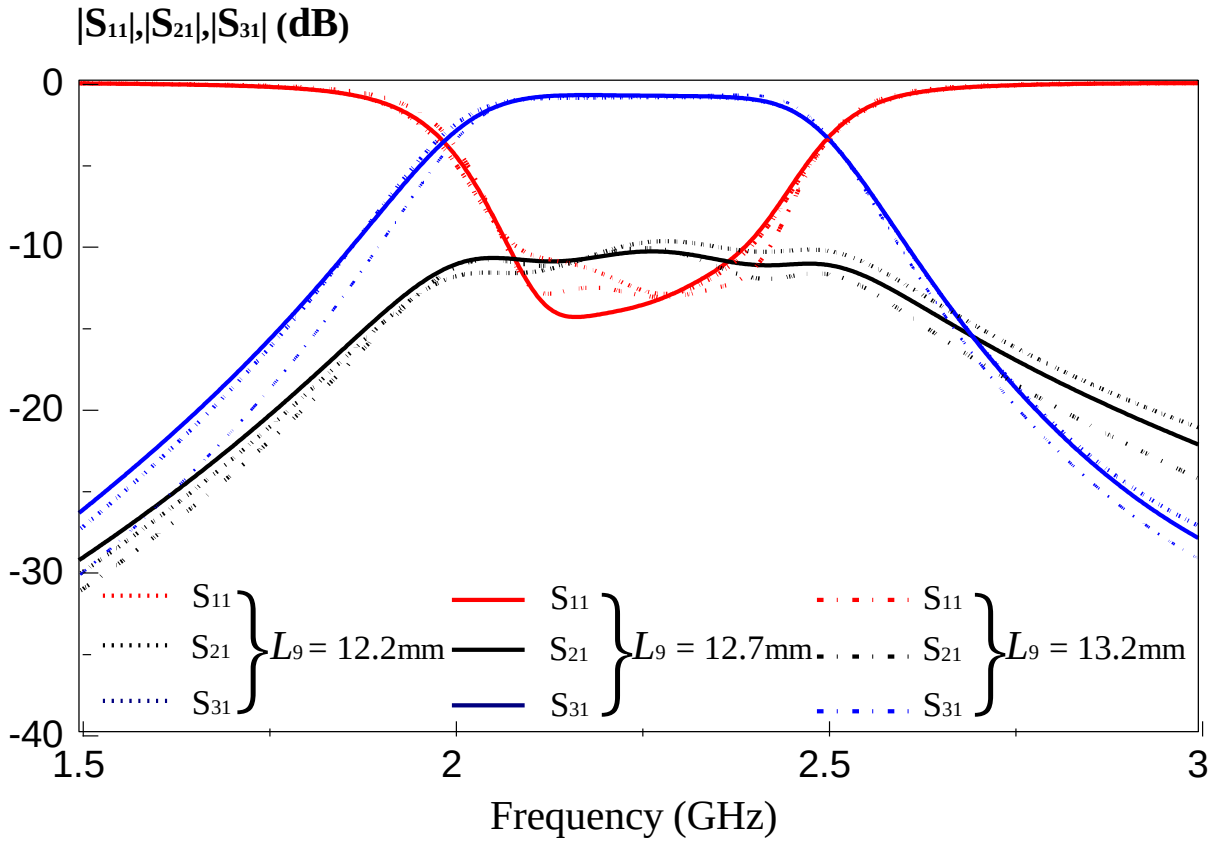

Figure 4.8 : Effect of Patch Length L_9

As shown in Figure 4.8, S21 is not flat across working frequency when L_9 is adjusted. Besides that, return loss of S11 is changing with L_9.

Analysis Parameter: L_{10}.

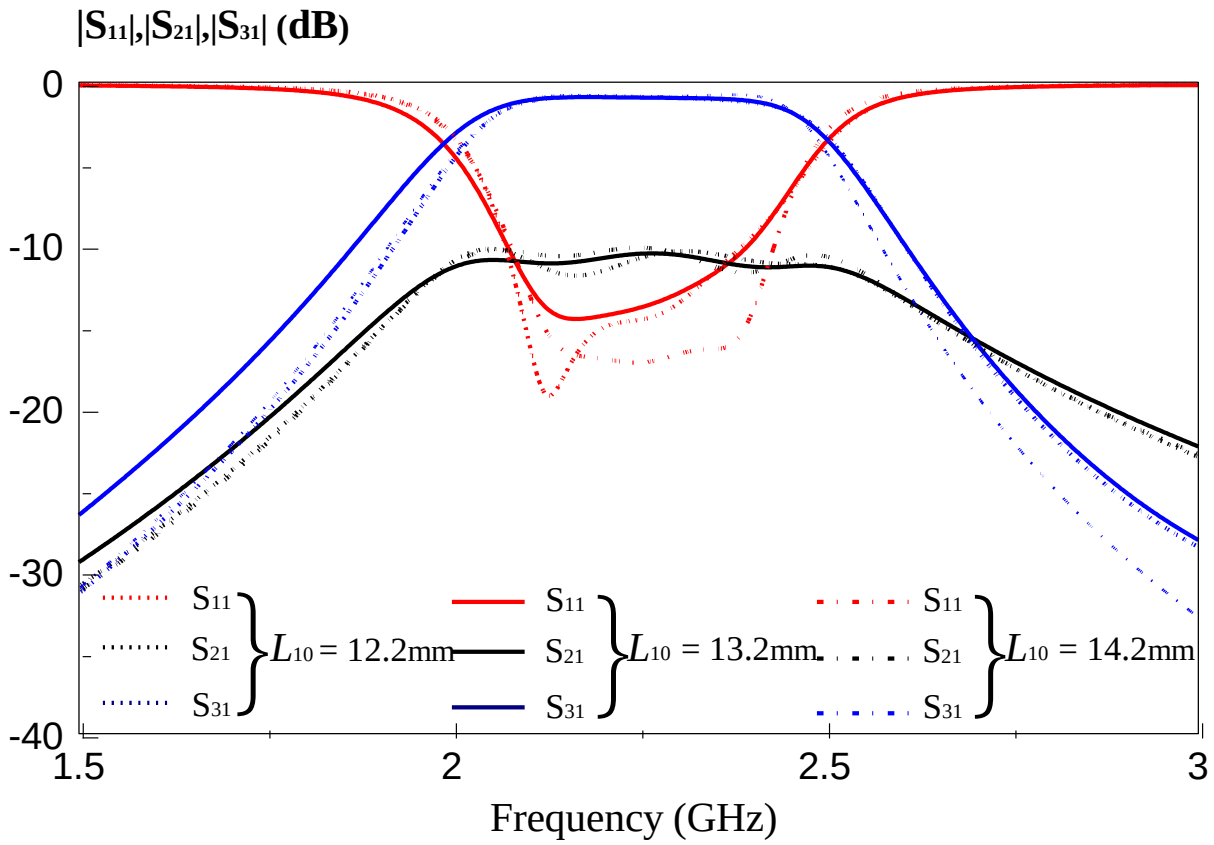

Figure 4.9 : Effect of Patch Length L_{10}

Figure 4.9 show the parametric analysis of the L_{10}. In Figure 4.9, when the L_{10} changed to 12.2mm or 14.2mm, it reduces the reflection loss but S21 is not flat across the operating frequency range.

Analysis Parameter: L_{11}

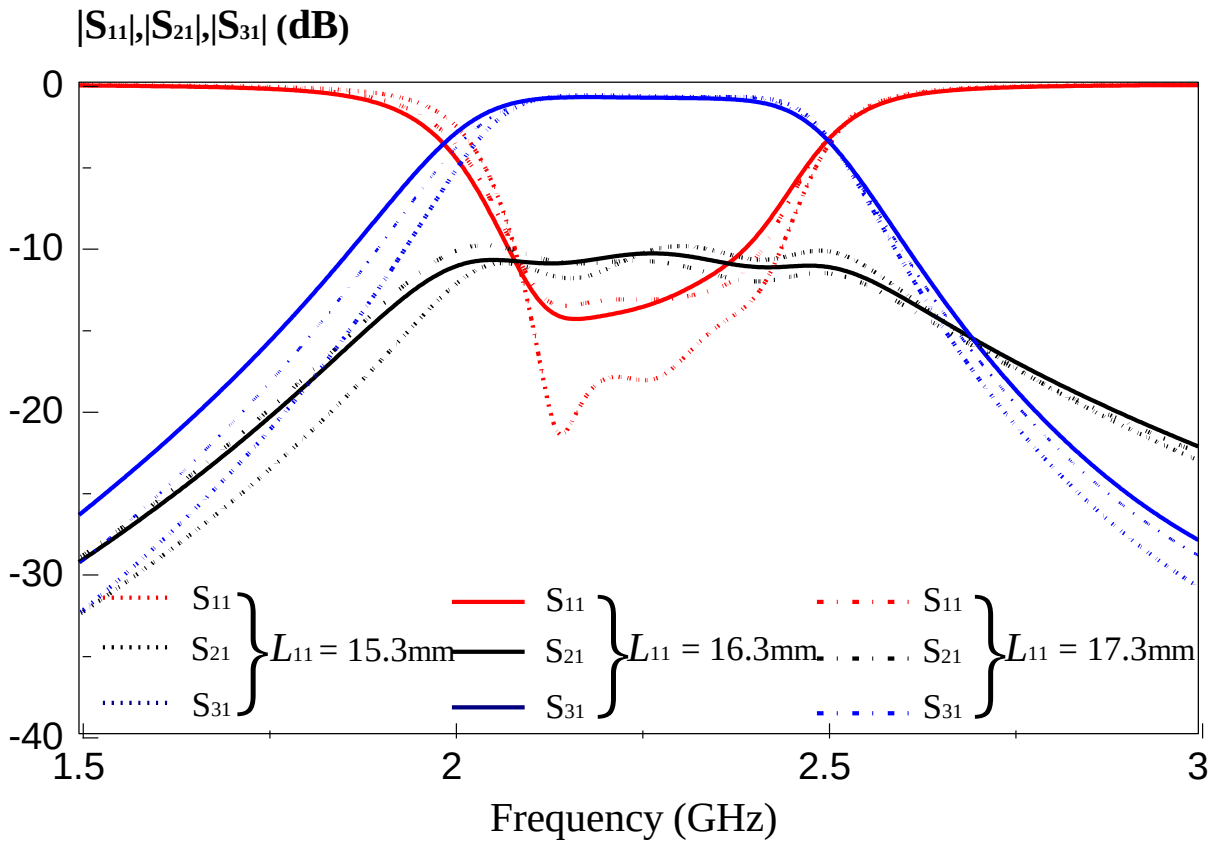

Figure 4.10 : Effect of Patch Length L_{11}

The return loss of two others lengths are better than proposed length. However, the 15.3mm and 17.33 L_{11} cannot provide flat amplitude across working frequency.

Analysis Parameter: L_{12}

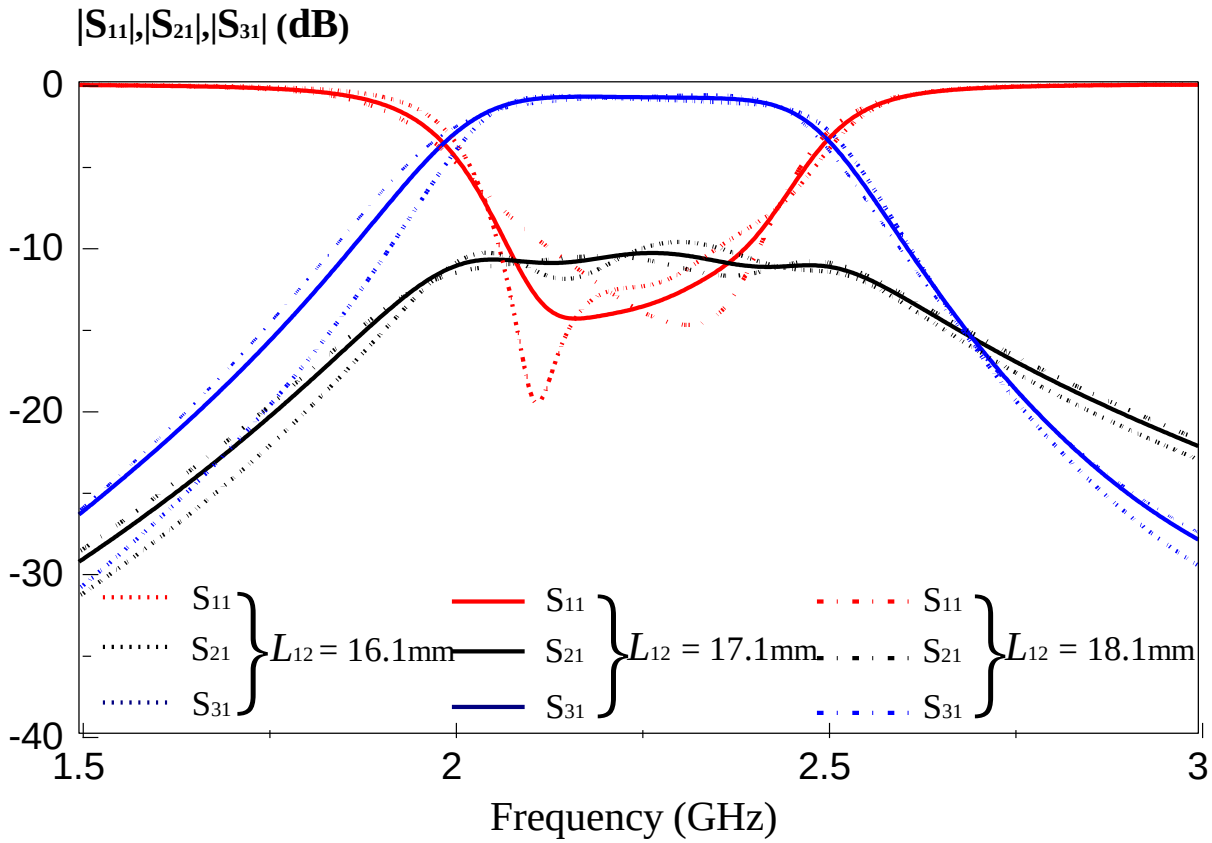

Figure 4.11: Effect of Patch Length L_{12}

From the Figure 4.11, it is obviously that the S21is not flat across the working frequency after substituting a 16.1mm or 18.1mm L12. Another significant change is the return loss; it shows that shorter L_{12} will reduce return loss.

4.2.2 Patch Width

Analysis Parameter: W_1, W_2 and W_3

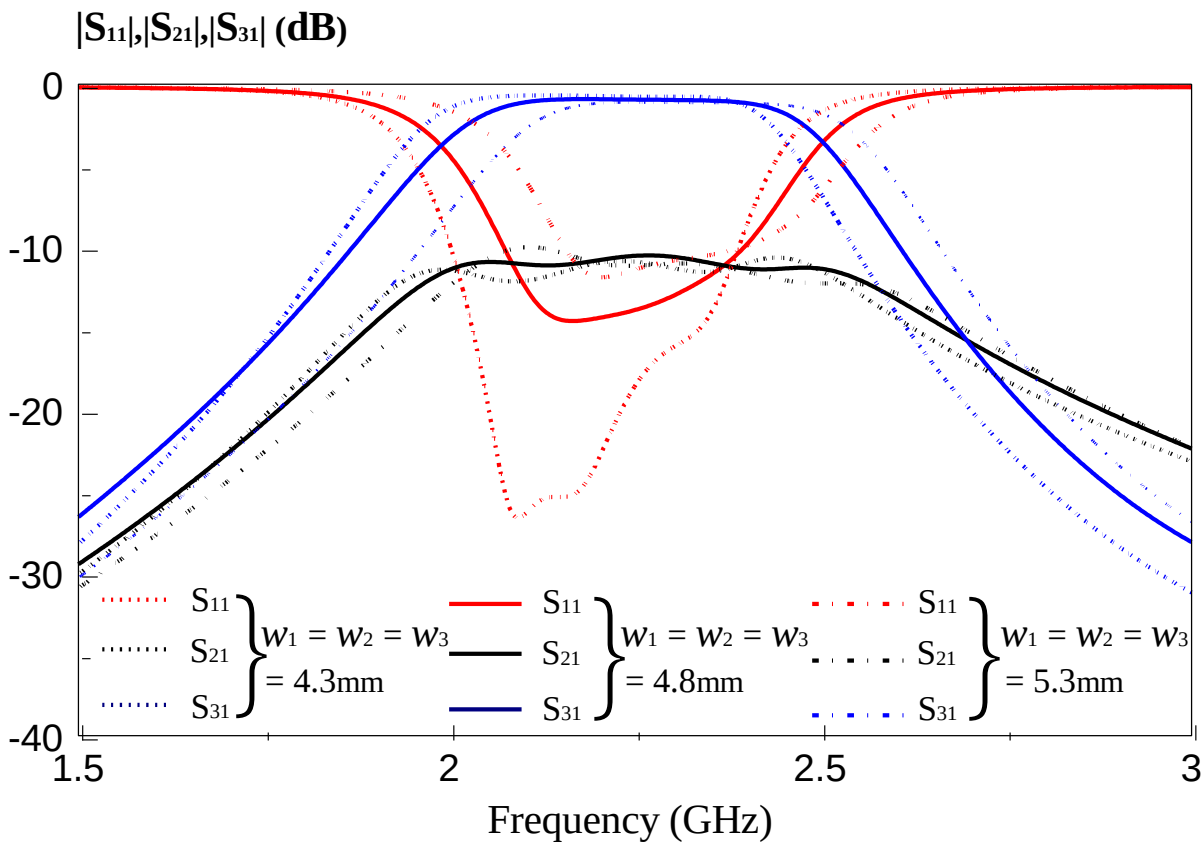

Figure 4.12 : Effect of Patch Width W_1, W_2 and W_3

The variation of the W_1, W_2 and W_3 parameters of the patch influence on the matching of this directional coupler. Meanwhile, it also influences operating frequency when W_1, W_2 and W_3 parameters is changing.

Analysis Parameter: W_4

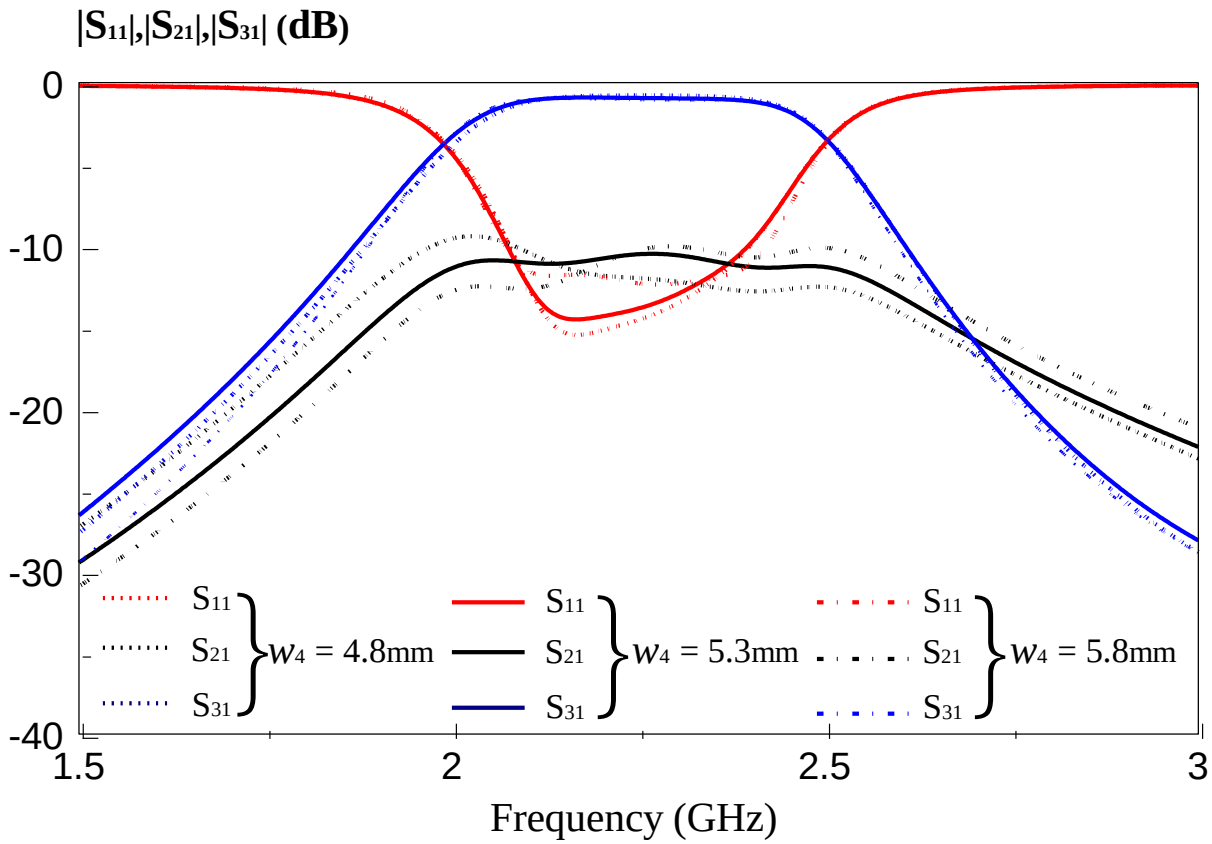

Figure 4.13 : Effect of Patch Width W_4

Shown in Figure 4.13 is the effect of W_4 which has the less significant change in S31.However, the S21 is flat across the operating frequency when W_4 is changed.

Analysis Parameter: W_5

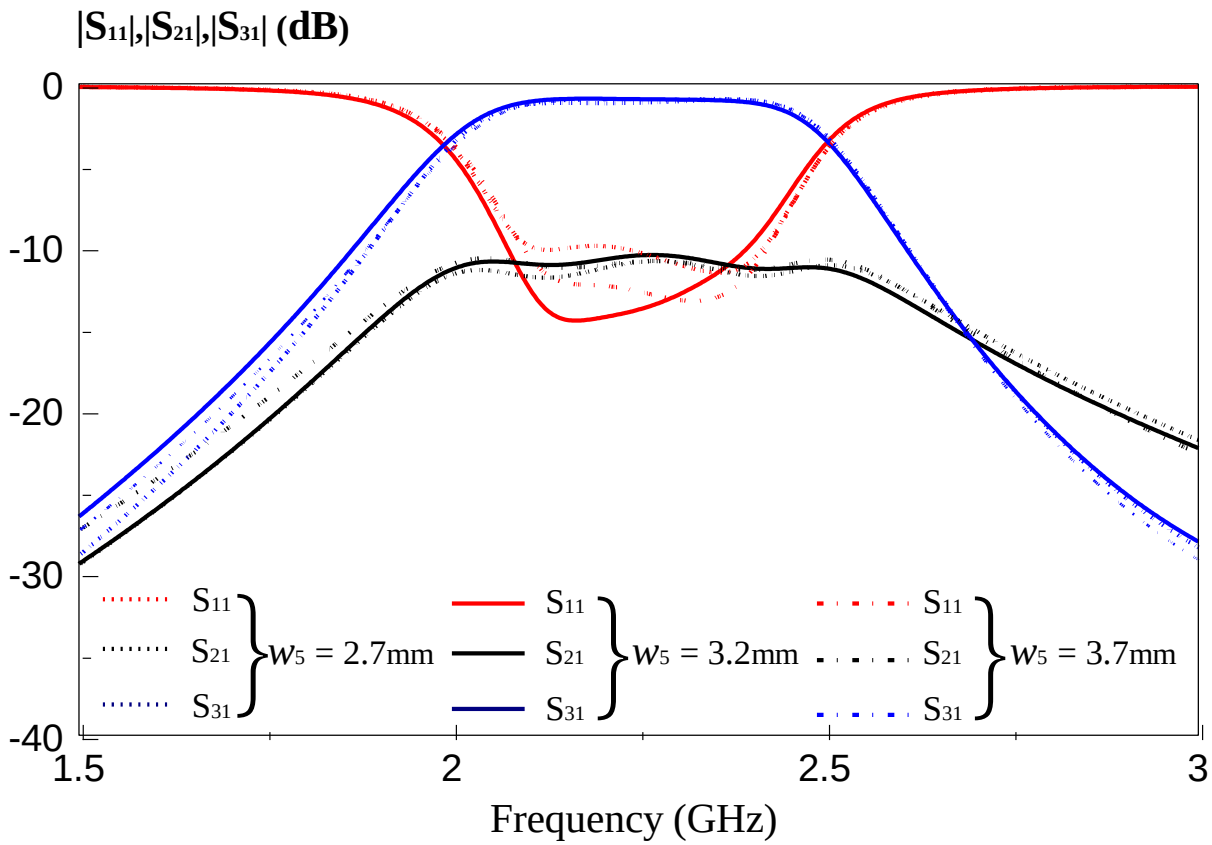

Figure 4.14 : Effect of Patch Width W_5

Shown in Figure 4.14 is the effect of W_5 which has the less significant change in S31 and S21. However, the return loss will increase when W_5 is changing.

Analysis Parameter: W_6

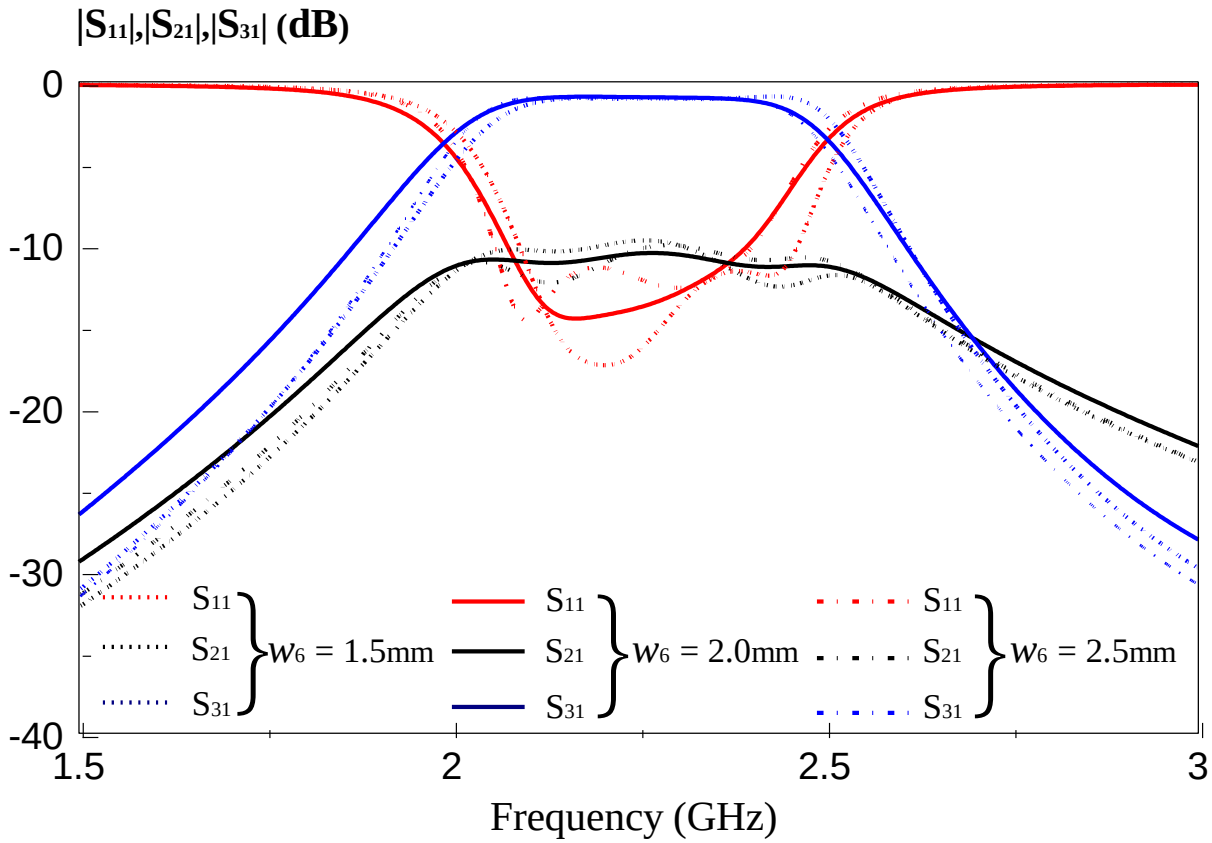

Figure 4.15 : Effect of Patch Width W_6

The Figure 4.15 shows the influence of the W_6 on the resonant frequency of the S21. Changing W_6 does not provide flat across resonant frequency. Beside, S11become 2 modes when W_6 is changing.

Analysis Parameter: W_7

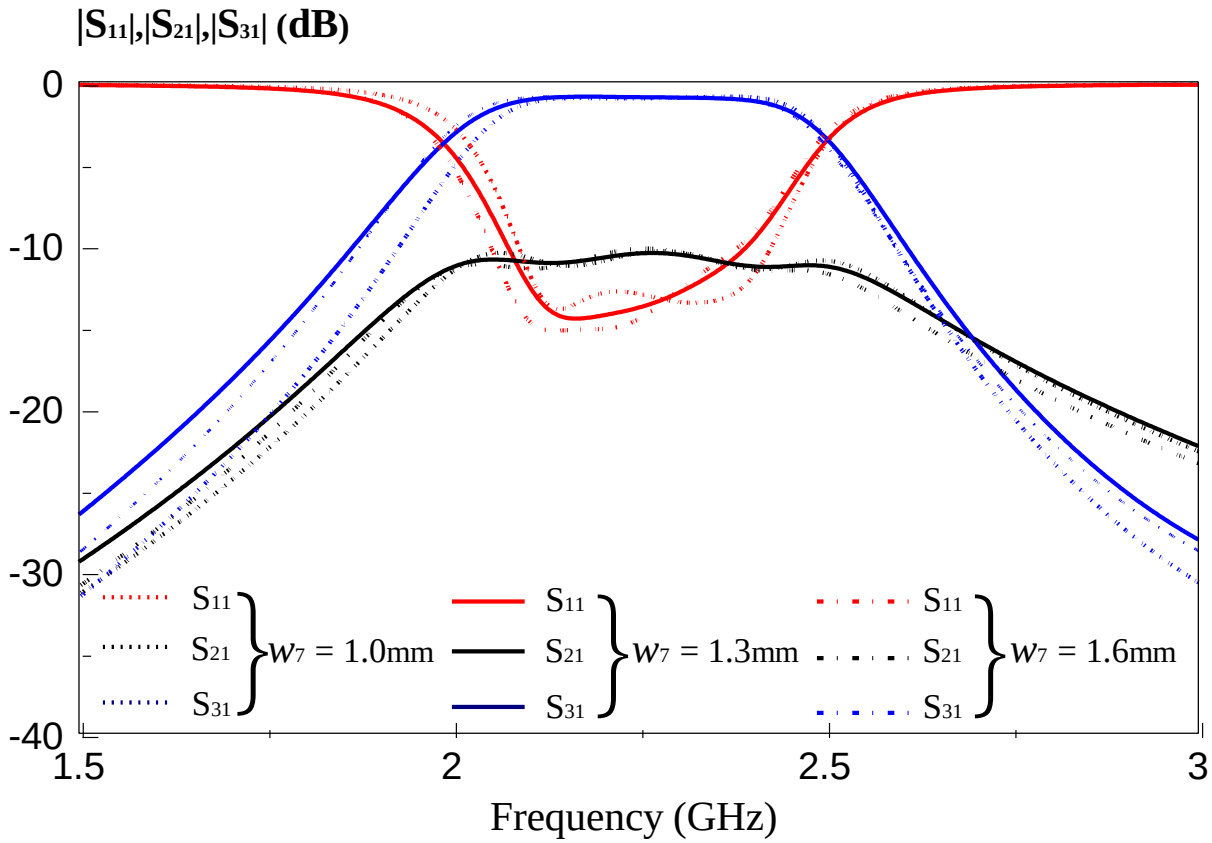

Figure 4.16 : Effect of Patch Width W_7

The simulation result is plotted in Figure 4.16. For the analysis purpose, 1.0mm and 1.6mm W_7 are using. There is not significant change for the 1.0mm and 1.6mm of W_7.

Analysis Parameter: W_8

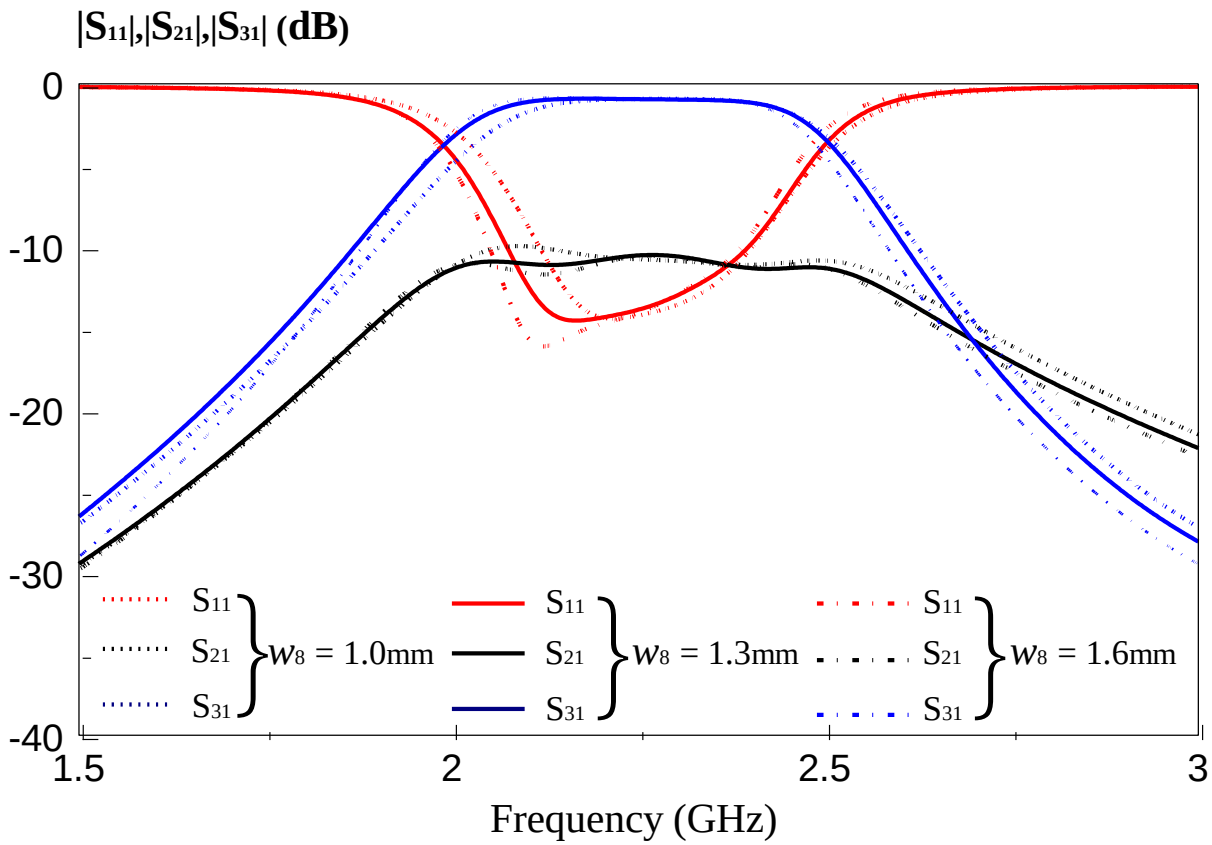

Figure 4.17 : Effect of Patch Width W_8

Figure 4.17 depicted the effect of patch width W_8.The change in W_8 leads to considerable changes in the operating frequency of the direction coupler.

Analysis Parameter: W_9

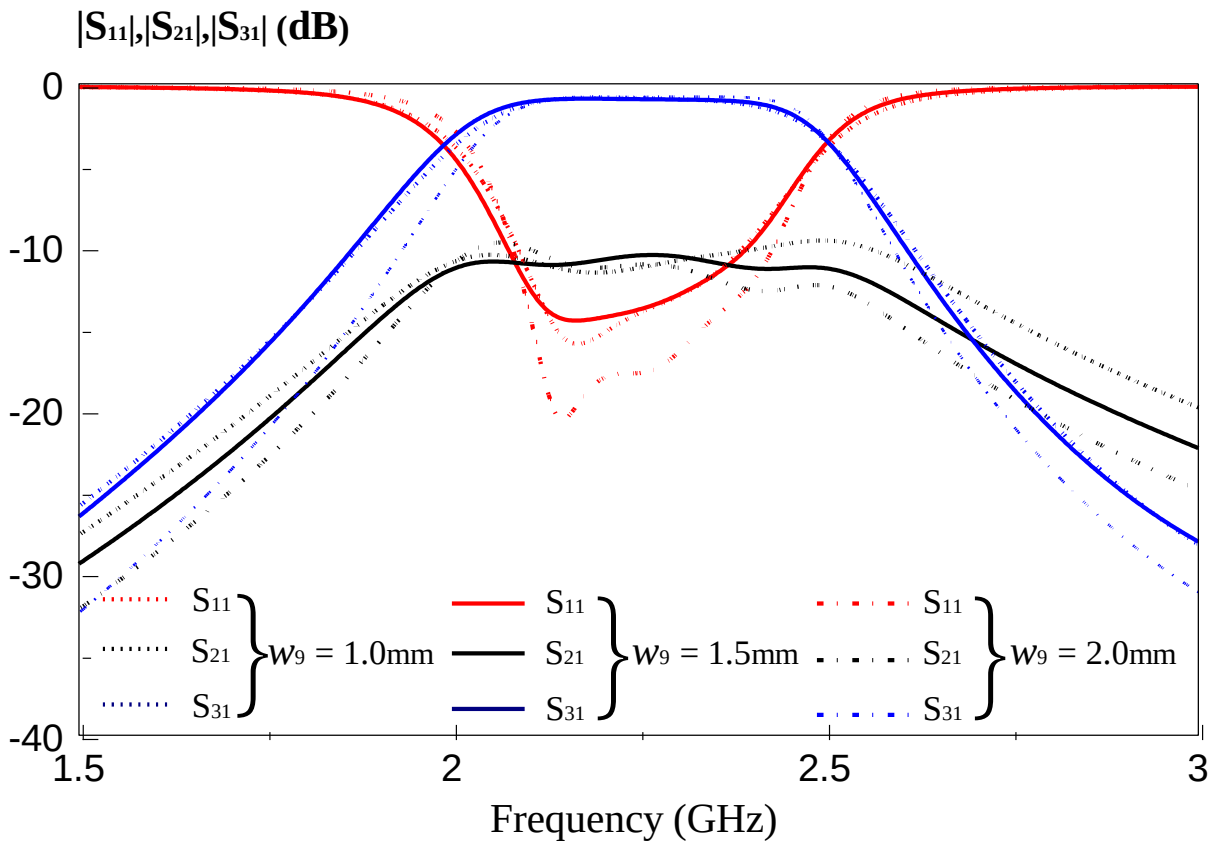

Figure 4.18 : Effect of Patch Width W_9

A better matching is expected to improve the whole performance of the directional coupler. The matching coefficient of the whole microstrip can be optimized by increase W_9.However, it provide no constant amplitude across the resonant frequency.

4.2.3 Gap

Analysis Parameter: G_1

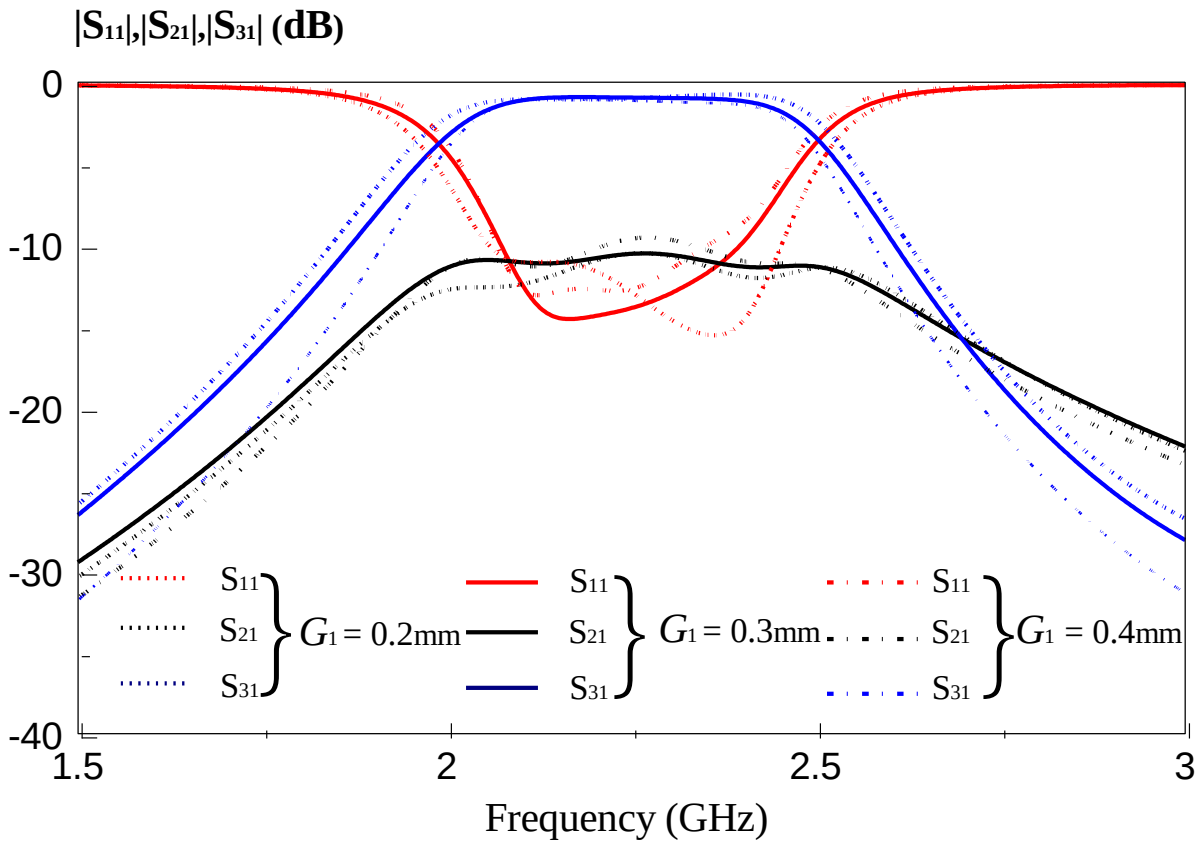

Figure 4.19 : Effect of Patch Gap G_1

Figure 4.19 shown the larger gap will provide a worst matching. Beside, the S21 is not flat across the operating frequency.

Analysis Parameter: G_2 and G_3

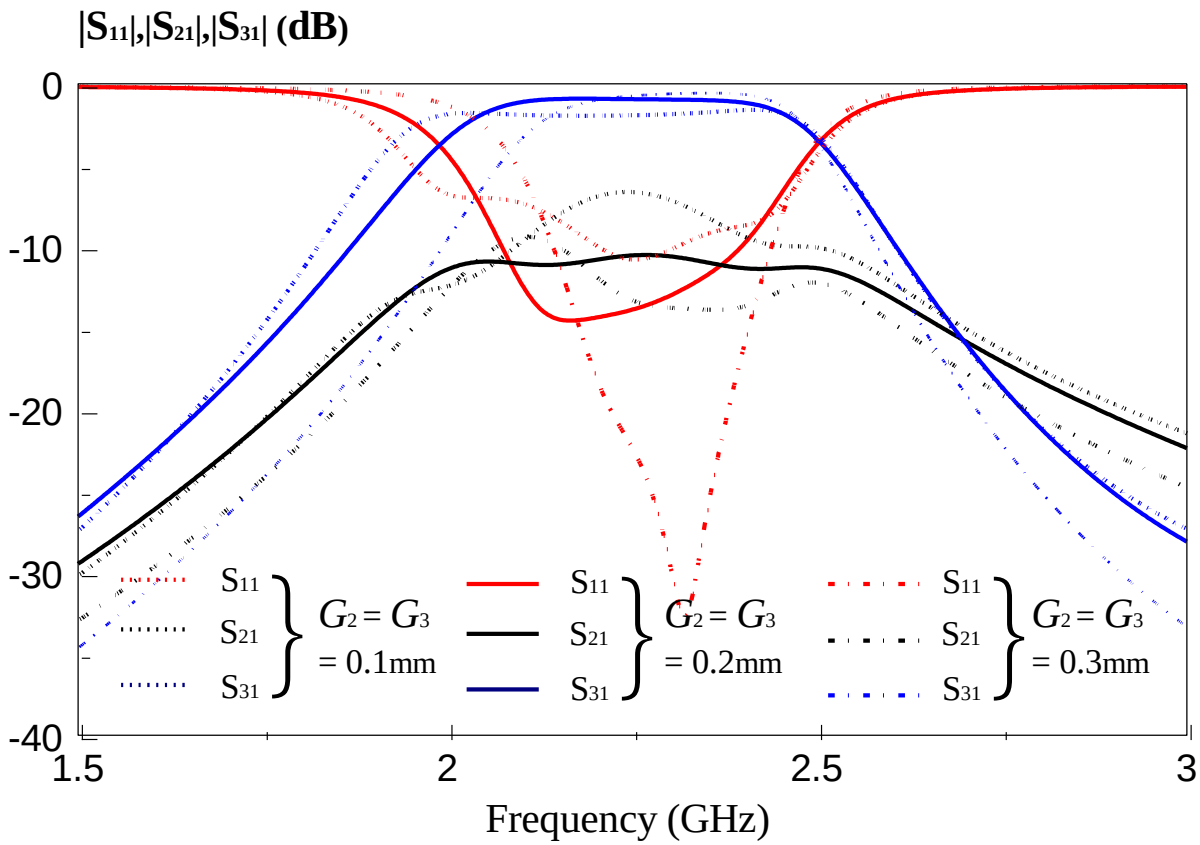

Figure 4.20 : Effect of Patch Gap G_2 and G_3

It can be observed that the bandwidth increases with decreasing gap between the patch and feeding line. However, 0.1mm gap cannot provide low return loss compare with 0.3mm gap.

Analysis Parameter: d_1

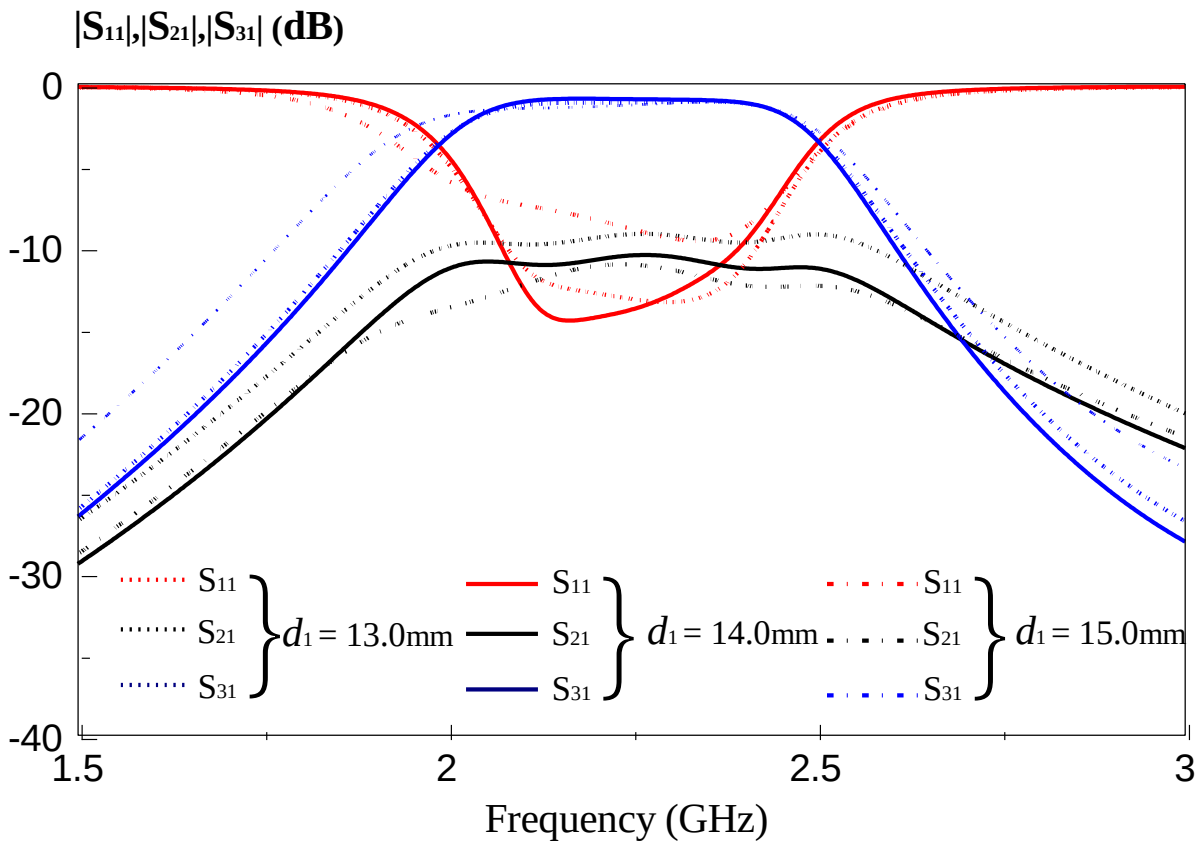

Figure 4.21: Effect of Patch Gap d_1

It is observed that decreasing the d_1 increases the S21 amplitude, while increasing the return loss. It is evident show that d_1 parameter is very important in filtering directional coupler.

Analysis Parameter: d_2

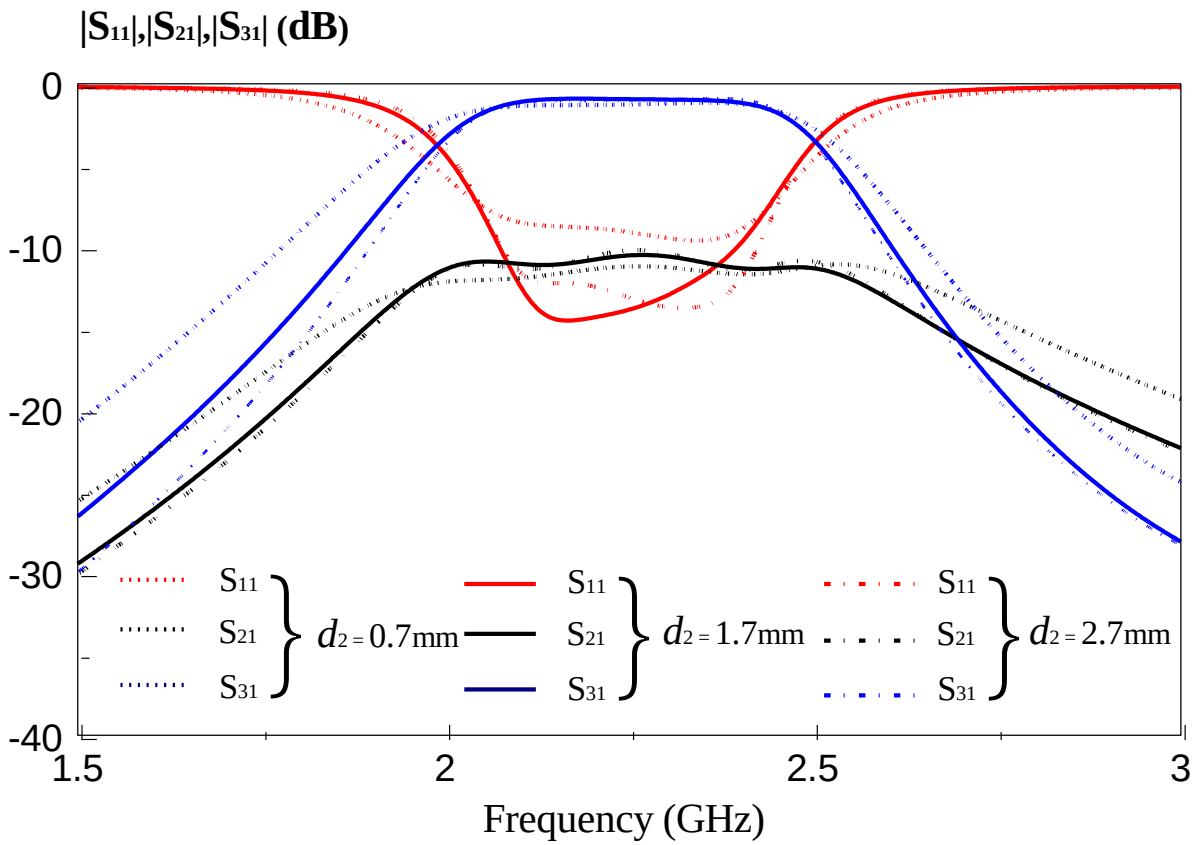

Figure 4.22 : Effect of Patch Gap d_2

When 0.7mm and 2.7mm gap are used, the return loss is higher than the 1.7mm gap. Therefore, 1.7mm d_2 are used to improve the directional coupler matching.

4.3 Discussion

It can be concluded from the above parametric analysis that the mutual coupling behaviors of microstrip are determined by d_1. It is evident show that d_1 will affect the magnitude of S21 in dB. Besides that, center frequency f_c, fractional bandwidth and error for both simulation and measurement result are calculated through the formulas shown in previous chapter. Hence, the measurement and simulation results was calculated and shown below.

	Result	
	Simulation	Experiment
f_l	2.074906	2.14794
f_h	2.397003	2.44569
fc	2.235955	2.296815
BW	14.41%	14.54%
Error		2.65%

Table 4-1: Comparison between the measurement and simulation.

Resonances from electric field pattern are observed in the step impendence "C" shape microstrip line. Each of the "C" shape patches has one standing wave. Moreover, the phase difference in between port 2 and port 3 is due to the four different "C" shapes of the electric field.

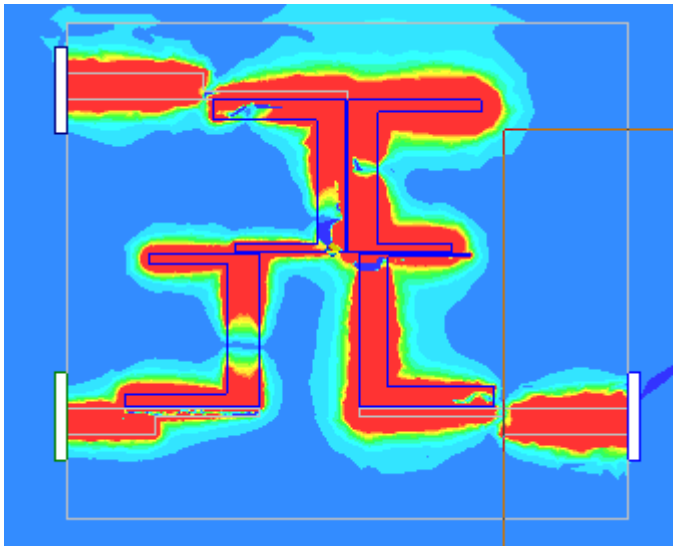

Figure 4.23: Electric field on centre frequency.

CHAPTER 5

CONCLUSION AND RECOMMENDATIONS

5.1 Achievements of the project

In this project, out-phase microstrip power divider and filtering directional coupler have been proposed and investigated. The design technique was investigated by modifying side-coupled bandpass filter to produce a high performance power divider and directional coupler. It has been shown that out of phase output is able to be produced from power divider with good power splitting; amplitude, phase balance, and outer band rejection are obtained. Moreover, out-phase microstrip power divider can generate transmission zero at S21 and S31.Hence,it improve the overall roll-off and provide a better reject skirt to the power divider. The filtering directional coupler able to be produced better matching, where the reflection loss is below -15db.Both of the design have a wide bandwidth where the fractional bandwidth more than 10%

5.2 Future Work

The fabricated out-phase microstrip power divider was a two-way power divider and it can only be used in limited application only. In future development, this design technique can have the opportunity to be developed three-way power divider. The new three-way divider design has to be proposed by adding the patch and feeding line. Meanwhile, the function is same with the two-way divider. The difference is only the number of outputs. However, S_{41} will be added into design consideration. There is a difficulty to optimized equal strength of output signals and out of phase between output ports.

In practical, coupling values found was 3, 6, 10, 20, 30, 40 & 50 dB. The fabricated filtering directional coupler has the 10dB coupling. In future development, various coupling value can be investigated .However, it will be much more challenging compare with the filtering directional coupler proposed because it will significant increase of return loss when the coupling values was increase.

5.3 Conclusion

As conclusion, the idea of out-phase microstrip power divider and filtering directional coupler has been designed. Experiments had been carried out and a reasonable and good agreement had been observed between the simulated and measured results. In this project, author was able to design filters or antennas based on HFSS simulation software and measured the results with VNA in laboratory .Beside, microwave engineering theory and concept had greatly improved after completing this project .Thus, the aim and objectives of this project had been achieved.

Reference

Dib, A. M. (2010). General Design of N-Way Multi-Frequency Unequal Split Wilkisson Power Divider Using Tranmission Line Transfomers. 115-129.

Gomez-Garcia, R., Alonso, J., & Amor-Martin, D. (2005). Sharp-rejection microwave planar filters using the branch-line directional coupler. *IEEE Xplore* .

Hong, J.-S. (2001). *Microstrip Filters for RF/Microwave Applications.* John Wiley & Sons, Inc.

Kejia Ding, D. S. (2011). A Novel Microstrip Line Three-way Power Divider. *IEEE Xplore* , 332-335.

M.Pozar, D. (1998). *Microwave Engineering.* New York: John Wiley & Sons,INC.
MECA Electronic,INC. (n.d.). Retrieved April 3, 2012, from MECA Electronic,INC: http://www.e-meca.com/tech_papers/directional-coupler-specs.php

microwaves101. (2012, February 18). Retrieved March 26, 2012, from microwaves101.: http://www.microwaves101.com/encyclopedia/microstrip.cfm
Nakajima, M., Yamashita, E., & Asa, M. (1990). New broad-band 5-section microstrip-line directional coupler. *IEEE Xplore* , 383-386.

Neuman, D. G. (2000, December). *madmadscientist*. Retrieved March 2012, 2012, from http://www.madmadscientist.com/html/Theory.htm#MicTheory

Stephane Avrillon, A. C. (2002). Dividing and filtering function integration for the development of a band-pass filtering power amplifier. *IEEE Xplore* , 1173-1176.